Title
Characterization of Spermatogenesis in the Planarian S. mediterranea

Author
Chretien, Jacqueline Hendries

Publication Date
2011

Peer reviewed|Thesis/dissertation

Characterization of Spermatogenesis in the Planarian *S. mediterranea*

By

Jacqueline Hendries Chretien

A dissertation submitted in partial satisfaction of the

requirements for the degree of

Doctor of Philosophy

in

Molecular and Cell Biology

in the

Graduate Division

of the

University of California, Berkeley

Committee in charge:

Professor Abby F. Dernburg, Chair
Professor W. Zacheus Cande
Professor David Weisblat
Professor Louise Glass

Spring 2011

Abstract

Characterization of Spermatogenesis in the Planarian *S. mediterranea*

by

Jacqueline Hendries Chretien

Doctor of Philosophy in Molecular and Cell Biology

University of California, Berkeley

Professor Abby F. Dernburg, Chair

Meiosis is a specialized reductional cell division by which sexual organisms produce gametes that can join to give rise to a euploid offspring. The mechanisms that enable the accurate segregation of homologous chromosomes in the first meiotic division have been studied in many organisms. Yet, a detailed molecular characterization of meiosis has not been carried out in any member of the lophotrochozoa, a large and diverse animal clade that includes molluscs, rotifers, annelid worms, and flatworms.

I have conducted an initial characterization of homolog pairing and recombination initiation in a novel model lophotrochozan, the freshwater planarian *Schmidtea mediterranea*. Like many species, these organisms form a telomere bouquet in early meiotic prophase. This bouquet normally persists throughout pachytene, and disruption of the telomere bouquet via depletion of the nuclear envelope protein Smed-SUN1 both disrupts homolog pairing and results in non-homologous synapsis.

This work has also revealed a telomere-proximal enrichment of double strand DNA breaks (DSBs), represented by Smed-RAD51 foci, and shown that DSB formation is dependent on the axial element protein Smed-HOP1. Depletion of HOP1 also disrupts progression through meiosis, and nuclei arrest in the bouquet stage without obvious homolog pairing or synaptonemal complex polymerization. Preliminary characterization of Smed-SMC3 suggests that partial loss of sister chromatid cohesion also disrupts homolog pairing, synapsis, and progression through meiosis.

This work introduces a number of novel tools and protocols for use in *S. mediterranea*, demonstrates that planarian spermatogenesis is a tractable model for the study of meiosis, and also suggests the existence of intriguing mechanisms that control homolog pairing, recombination and synapsis in this animal.

Dedication

To Eleanor Ruth — by far my favorite experiment in meiosis. (No offense to the planaria.)

Table of Contents

Acknowledgements

This work would not have been possible without the support of many, many people. In particular, I wish to thank Phil Newmark and Yuying Wang for supplying me with my first colony of *S. mediterranea* as well as for answering my many questions about planaria culture, techniques and tools; Jarrod Chapman and Dan Rohksar for sharing the centromere candidate repeats that they identified; and Pietr de Jong for kindly sharing fosmid clones (even though they didn't work). I would also like to thank Lena Hyatt and Margaux Bennett, whose work was extremely helpful in getting this project off the ground, Reena Zalpuri, for her EM expertise, and Youbin Xiang and Scott Hawley for being fantastic collaborators. Thanks also to the members of the Dernburg lab, past and present, for helpful discussions (and sitting through all my non-nematode group meetings), the members of my committee for their very useful suggestions and constructive criticism, and to Abby for always encouraging me to "just go for it."

And of course, so much gratitude to my partner and husband CJ, my sister Kara, and my mom. I could not have finished this without you!

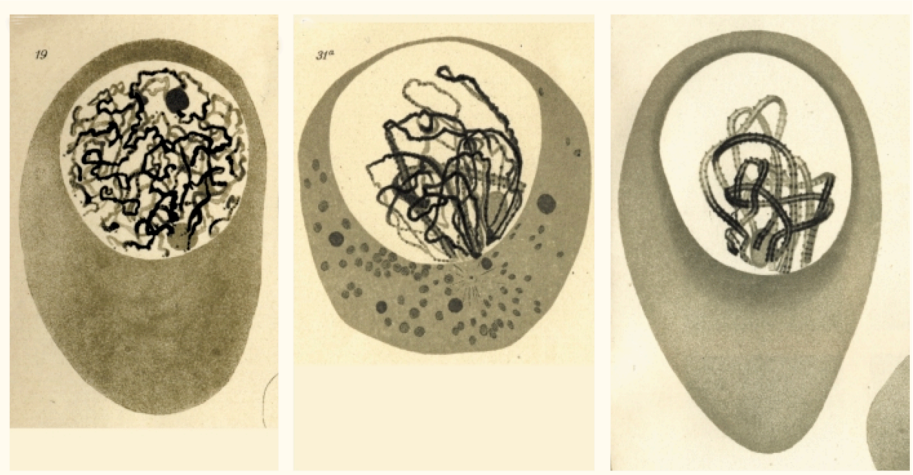

Progression through meiosis (leptotene, zygotene, and pachytene) in *Dendrocoelum lacteum*. Reproduced from Gelei, 1921.

Chapter I. Introduction

Meiosis is the specialized reductional cell division process by which sexually reproducing organisms generate gametes such as sperm, eggs, and pollen. This process is essential, as gametes with too many or too few chromosomes cannot create a zygote with the proper genetic complement at fertilization, leading to embryonic death or developmental anomalies.

In diploid organisms, the accurate halving of genetic material to yield haploid gametes is accomplished in two steps, with the segregation of homologous chromosomes in the first meiotic division followed by the segregation of sister chromatids in the second meiotic division. The segregation of homologous chromosomes in meiosis I presents a unique challenge for the cell, as it requires these chromosomes to recognize one another and maintain a physical association until they can be appropriately separated at anaphase I. While the specific mechanisms underlying homolog recognition and association remain somewhat mysterious, several key processes are known to enable accurate homolog segregation: (1) a reorganization of chromosomes within the nucleus, which enables pairing and alignment between homologous chromosomes; (2) the polymerization of the synaptonemal complex (SC), which stabilizes pairing between homologs; and (3) crossover recombination between homologs, which creates chiasmata that hold homologs together until anaphase I (Fig. 1). Recombination also generates genetic diversity through the exchange of genetic material. Although these processes and much of the associated molecular machinery is conserved across phyla, there is significant diversity in the meiotic program between species.

A brief review of meiotic prophase, with a focus on inter-species diversity in the meiotic program

In the first stage of meiotic prophase, *leptonema* (from the Greek for “thin threads”), chromosomes begin to condense. At the same time, a number of proteins are recruited to the chromosomes to form the chromosome axes, which later become the lateral elements of the synaptonemal complex. The axial element proteins that load during this stage are critical for all of the later events of meiosis. For example, subsets of these proteins help to establish and maintain chromosome condensation and sister chromatid cohesion, both of which are essential for accurate chromosome segregation in both mitosis and meiosis. Proper chromatin condensation and cohesion are also important for the normal assembly of other axial element and SC components, as well as the control of double strand DNA break (DSB) formation and subsequent crossover placement. Meiosis-specific cohesin subunits, such as Rec8 in *S. cerevisiae*, REC-8, COH-3 and COH-4 in *C. elegans*, and REC8 and SMC1β in mammals, also appear to have independent roles in promoting homolog pairing and SC assembly (recently

reviewed in Wood et al., 2010). Other axis components enable DSB formation and resolution (including the appropriate interhomolog vs. intersister repair bias), participate in checkpoint signaling, or form a physical scaffold for the assembly of the SC. Many axis proteins engage in more than one of these activities, either directly or indirectly. Additional roles for chromosome axis components may be appreciated as more of these proteins are identified; for example, the recently discovered cohesin subunit Rad21L has been suggested to help establish a "cohesin code" for homolog pairing and alignment in mice (Lee and Hirano, 2011; Ishiguro et al., 2011).

As meiosis progresses from leptonema to zygonema ("paired threads"), homologous chromosomes begin to pair and align with one another. This is frequently accompanied by a large-scale, cytoskeleton-driven rearrangement of the nucleus such that the chromosome ends are gathered in a "bouquet" at the nuclear envelope. However, many aspects of the bouquet, including its duration/persistence, degree of clustering, and even actin vs. microtubule dependence, vary across species. Mutant analyses also suggest potential differences in the function of the bouquet in different organisms. The classic view has been that this configuration provides a rough alignment of chromosomes that aids in homolog recognition and supports later events. Consistent with this, mutant strains of *S. pombe* that are defective in bouquet formation are delayed in homolog pairing and recombination, and bouquet mutants in *S. cerevisiae* exhibit defects in pairing, recombination, and SC formation (reviewed in Ding et al., 2010). Similarly, the *pam1* mutant in maize does not form a typical bouquet and exhibits incomplete and nonhomologous synapsis and unresolved chromosome interlocks (Golubovskaya et al., 2002). In mice and *Sordaria*, the bouquet stage is prolonged when recombination is perturbed, suggesting a link between these processes (Liebe et al., 2006; Storlazzi et al., 2010). In contrast, *C. elegans* does not form a classic telomere-mediated bouquet. Instead, connections between the microtubule cytoskeleton and regions at one end of each chromosome, called Pairing Centers, promote chromosome motion and are critical for timely pairing and appropriate SC assembly between homologs (Sato et al., 2009; Penkner et al., 2009). Thus, an emerging view is that chromosome movement is important for testing homology and licensing later steps of meiotic prophase, and that the clustering of chromosome ends may simply be a byproduct of cytoskeletal organization (Koszul and Kleckner, 2009; Sato et al., 2009; Wynne et al. submitted). Because the same factors likely mediate both cytoskeleton-based chromosome movement and telomere clustering, it has been challenging to separate these functions clearly. Meanwhile, the diversity of the phenotypes associated with loss of the bouquet suggests that this configuration may have a lesser or greater degree of importance in individual species. Interestingly, one aspect of the meiotic chromosome-cytoskeleton connection has been observed in all organisms investigated thus far: the involvement of SUN domain (Sad1/UNC-84 homology) proteins. These proteins reside in the inner nuclear envelope and, together with KASH domain partners in the outer nuclear envelope, act as a bridge between the chromosomes within the nucleus and the cytoskeleton outside it. However, the meiotic effects of disrupting SUN protein function vary across species (see Chapter IV).

Also during zygonema, programmed double strand DNA breaks (DSBs) are generated by the conserved endonuclease Spo11 (Cao et al., 1990; Keeney et al., 1997) and begin to recruit a number of components of the DNA repair machinery. A subset of these breaks go on to form crossovers, which is achieved when a break is repaired from the homologous chromosome with a particular topology (reviewed in Neale and Keeney, 2006; Yanowitz, 2010). The number of breaks that are generated is highly species and sex dependent and usually in several-fold excess of the number of crossovers formed, indicating that the formation of chiasmata is not the only function of the DNA repair machinery or specific repair intermediates in meiosis. The formation of recombination intermediates and/or presence of specific repair proteins is required for homologous pairing in many organisms, including yeast, plants, and mammals. Based on this data, it has been hypothesized that the homology search involved in the DSB repair process is important to maintain interhomolog associations at multiple loci (e.g., Cole et al., 2010). However, some organisms, including *C. elegans* and *Drosophila,* are able to achieve stable homolog pairing in the absence of DSB formation and repair, indicating that this is not always the case (Dernburg et al., 1998; McKim et al., 1998). Furthermore, while it is known that certain areas of the genome are more prone to break formation than others, the factors that control the extent and placement of DSB formation are only beginning to be characterized. Recent studies have suggested that DNA sequence, chromatin context and meiotic axis structure may all influence DSB placement (e.g., Kumar and de Massy, 2010; Kong et al., 2010; Mets and Meyer, 2009; Edlinger and Schlögelhofer, 2011; Grey et al., 2009).

Through zygonema and into pachynema ("thick threads"), homolog pairing is stabilized by the assembly of transverse filaments along these axes to form the proteinaceous synaptonemal complex (SC). The involvement of the SC in other meiotic processes varies considerably across species. As an extreme case, some fungi do not undergo synapsis (e.g., *S. pombe* and *A. nidulans*, shown by Bähler et al., 1993 and Egel-Mitani et al., 1982, respectively). In other organisms, SC polymerization is critical for the formation of late crossover intermediates (e.g., de Vries et al. 2005). In many cases, SC formation and DSB repair are interdependent; not only does recombination not occur normally in the absence of SC, but the SC does not form normally when DSB repair is disrupted (Roeder, 1997; Chua and Roeder 1998, Romanienko and Camerini-Otero, 2000; Baudat et al., 2000). The polymerization of the SC may also be important for stabilizing pairing independent of recombination. In *C. elegans*, for example, mutants that lack transverse filaments (e.g., *syp-1*) achieve initial homolog pairing in their pairing center regions but do not establish robust pairing at distal loci (MacQueen et al., 2002).

During pachynema, a subset of the DSBs that were made in earlier stages are processed as crossovers, leading to the exchange of genetic material, or recombination. In most organisms, the resulting chiasmata are required to maintain association between homologous chromosomes until anaphase I, although several organisms have evolved mechanisms that allow achiasmate segregation in one or both sexes (Dernburg et al., 1996; La Fuente et al., 2007; McKim et al., 1998, and reviewed in Bhalla and Dernburg, 2008). The number of crossovers per chromosome

is tightly controlled. In most species, each chromosome must receive at least one crossover (CO), but the formation of too many COs, or COs that are too close to one another or to centromeres or telomeres, can lead to non-disjunction. While CO site selection may be partially controlled by DSB placement, evidence of both CO homeostasis (the maintenance of normal levels of COs in the face of significantly reduced DSB formation) and CO interference (the suppression of COs in the vicinity of one another) has been found in *S. cerevisiae*, *C. elegans* and mammals (recently reviewed in Youds and Boulton, 2011), and evidence in several organisms suggests that DSBs are converted to COs at different rates in different regions of the genome. In particular, COs are often suppressed near centromeres, and may be enriched or suppressed near telomeres, depending on the species. The mechanisms that determine whether a particular break will be repaired as a crossover (CO) or non-crossover (NCO) are still not well understood, though the determination seems to be made relatively early in meiotic prophase. The CO vs. NCO decision is affected by chromatin structure, SC structure, and other factors, the relative influence of which also vary considerably across species (reviewed in Martinez-Perez and Colaiacovo, 2009). The dependence of CO formation on specific proteins also varies across species. For example, the Msh4, Msh5 and Mlh1 proteins have been found to be required for CO but not NCO formation in *S. cerevisiae*, while Msh4 and Msh5 seem to be involved in creating both COs and NCOs in mammalian systems (Lynn et al., 2007). Both of these proteins are entirely absent in *S. pombe* and *D. melanogaster*, although analagous complexes may eventually be found.

Once chiasmata have been established, the synaptonemal complex begins to disassemble at diplonema (“two threads”), allowing homologous chromosomes to separate except where crossovers have occurred. Chromosomes then condense dramatically at diakinesis, which is followed by metaphase and the first meiotic division. These processes are also regulated differently in different organisms, but will not be addressed in detail here.

Understandably, a major goal in the field of meiosis has been to determine how the regulation and interplay among meiotic processes have evolved differently along distinct lineages. Meiosis has been investigated in molecular detail in most of the common model organisms, including mice, insects, nematodes, fungi, *Arabidobsis*, maize, and several other crop plants. Although studies in “non-model” organisms are becoming less rare (e.g., Viera et al., 2009), the molecular basis of meiosis has still not been investigated in any of the lophotrochozoans, a large and diverse class of bilaterian animals that includes molluscs, rotifers, annelid worms, and flatworms.

The planarian as a model organism

The freshwater planarian has a long history as a laboratory organism. In the late 19th and early 20th centuries, biologists (including Ludwig von Graff, Libbie Henrietta Hyman, T.H. Morgan, C.M. Child, and many others; reviewed in Rieger, 1998) were drawn to planarian species due to their intriguing capacities for regeneration. A body of literature on planarian anatomy, identification, taxonomy, and ecology was published around the turn of the 20th century. Notably for the study of meiosis, the chromosomal bouquet was described in the planarian *Dendrocoelum lacteum* in 1921, the result of painstaking 3-D reconstructions of meiotic nuclei made by Josef Gelei. Amazingly, Gelei even pioneered micromanipulation experiments with meiotic chromosomes to demonstrate their strong connection to the nuclear envelope (Gelei, 1921a; 1921b, reviewed in Scherthan, 2001).

Although planarians fell out of favor as an experimental system in the later 20th century, as the genetic model presented by *Drosophila* drew many biologists in a different direction (for a compelling history of these parallel model organisms, see Mitman and Fausto-Sterling, 2006), several labs continued pioneering work in regenerative and developmental biology in planarian species. From the late 1930s to the mid-1980s, Mario Benazzi and Giuseppina Benazzi-Lentati and their colleagues conducted a number of cytogenetic studies to characterize the incredible diversity of planarian reproductive biology. This group's careful surveys of the karyotypes and "meiotic biotypes" of Europe's freshwater planarians demonstrated that these species employ one or more of several reproductive modes (asexual/fissiparous, parthenogenic, pseudoparthenogenic, or sexual), and revealed unique and variable achiasmate or semi-chiasmate meioses in a number of polyploid species (reviewed in Benazzi Lentati, 1976). In the 1980s, detailed ultrastructural and cytogenetic studies from Gareth Jones and colleagues described a correlation between SC length and chiasmata formation in *D. lacteum* (Jones and Croft, 1989), and unusual partially synaptic and achiasmate spermatogenesis and oogenesis in a rhabdocoel flatworm, *Mesostoma ehrenbergii ehrenbergii*[1] (Oakley, 1982; Oakley and Jones, 1982; Oakley, 1985; Croft and Jones, 1989). A number of ultrastructural studies of *Polycelis tenuis* from Theodore Lender's laboratory also contributed to a detailed picture of planarian spermatogenesis and other anatomy at the nanometer scale (Franquinet and Lender, 1972; 1973).

Beginning in the 1990s, increased interest in stem cell biology brought planarians back into the spotlight as model organisms (Newmark and Sánchez Alvarado, 2002). Today, molecular studies have been conducted in several species, notably *Dugesia japonica*, *Dugesia ryukuensis, Schmidtea mediterranea,* and *Schmidtea polychroa*, and the genome of *S. mediterranea* has been sequenced (Robb et al., 2007). The phylogenetic position of planarians within the animal kingdom has also been clarified relatively recently. For many years, it had been assumed that the

[1] The remarkable *M. e. ehrenbergii* segregates four of its seven chromosomes via unknown achiasmate mechanisms, while the other three chromosomes are undergo more traditional synapsis and recombination, carried out in special extensions of the nuclear envelope that form during meiotic prophase (Croft and Jones, 1989).

'simple' body plan of the flatworm indicated a basal position within the bilateria. More recently, molecular phylogenetic studies based on rDNA sequences have shown that this is not the case; rather, the platyhelminthes fall within the lophotrochozoa, a sister group of the ecdysozoa within the protostomes (Carranza et al., 1998; Adoutte et al., 2000). This reclassification has also been supported by detailed comparative anatomy studies (Carranza et al., 1997). The most recent analyses have placed the platyhelminthes as an early branching group within the lophotrochozoa (Philippe et al., 2005; Lartillot and Philippe, 2008; Nesnidal et al., 2010), although the animal phylogeny remains somewhat controversial (see Fig. 2).

Despite the intriguing studies conducted by Gelei, Benazzi, and Croft, and the increasing availability of modern molecular and cell biological tools, the molecular basis of meiosis has not yet been investigated in planarians, and it has been unclear to what extent homologs of meiotic proteins identified in other organisms have conserved functions in these organisms. Meanwhile, its phylogenetic position and the idiosyncratic reproductive biology observed across species make planaria an exciting system in which to investigate the roles of meiotic proteins, and the functional relationships among them, over evolutionary time.

Among the planarian species, *S. mediterranea* is particularly attractive for the study of meiosis. These animals are diploid and hermaphroditic, and both sexually-reproducing and asexual strains have been established in the laboratory. The small number of chromosomes (2n = 8), combined with abundant testes, facilitate cytological analyses. RNAi effectively disrupts protein expression and is relatively simple to perform (Sánchez Alvarado and Newmark, 1999; Newmark et al., 2003; Gurley et al., 2007). Comparative gene expression studies have identified a number of genes that are expressed in adult sexual *S. mediterranea* but not in juveniles or an asexual, germline-less strain (Zayas et al., 2005, Wang et al. 2010), providing candidate genes that are likely to be involved in reproduction. Similarly, the availability of a sequenced genome has allowed the identification of homologs of genes that are known to be involved in meiosis in other organisms (Robb et al., 2007). With respect to the reproductive diversity among planarians, the closely related species *S. polychroa* can live and reproduce as a diploid, a pseudoparthenogenic triploid, or a tetraploid (D'Souza et al., 2005; personal observations), and is beginning to be appreciated as a good model for the study of parthenogenesis (D'Souza and Michiels, 2009). Comparative studies of meiosis vs. pseudoparthenogenesis in these two species may help to illuminate how major changes in the regulation of meiosis can occur over a relatively short evolutionary period.

In this work, I have investigated meiosis in *S. mediterranea* spermatocytes for the first time at the molecular level (Chapter II). Based on the molecular information available at the outset of these studies, I chose to use a targeted screen approach, identifying a number of candidate meiotic genes through BLAST search and additional resources (as described above) and using RNAi to examine knockdown phenotypes. The resulting studies have touched on many

aspects of the meiotic program, providing a solid foundation for the further study of spermatogenesis in *S. mediterranea*. In particular, I identified and characterized two separate genes that encode proteins with key roles in meiotic prophase: the axial element protein Smed-HOP1, which is critical for recombination, homolog pairing, and synapsis (Chapter III), and the nuclear envelope protein Smed-SUN1, which is essential for bouquet formation and homolog pairing (Chapter IV). I will also describe the preliminary characterization of several other proteins with roles in meiosis (Chapter V) and provide a detailed discussion of the new cytological tools and strategies developed in this work (Chapter VI).

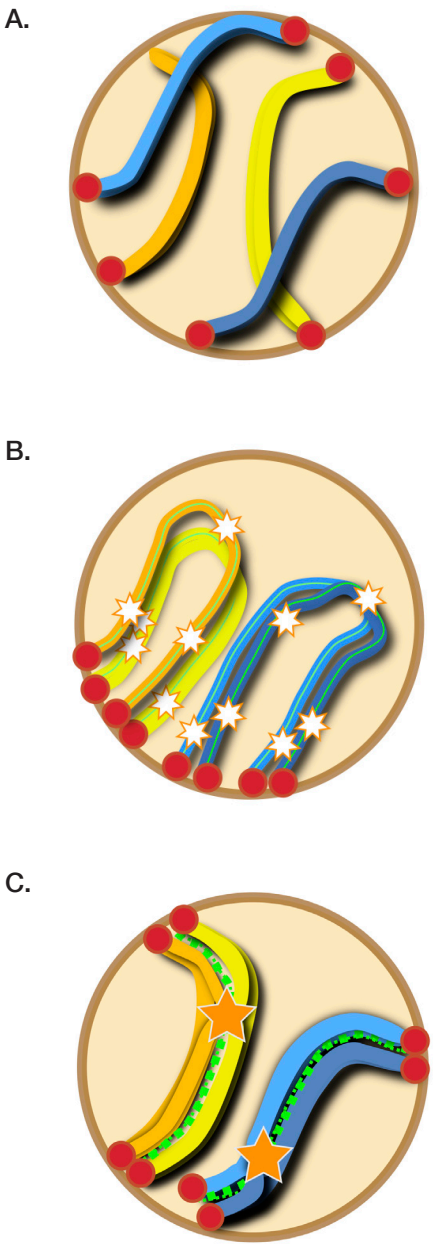

Figure 1. Cartoon model of the events of meiotic prophase.
(A) Chromosomes condense and telomeres (red) attach to the nuclear envelope early in meiotic prophase. **(B)** Telomeres cluster in the bouquet, axial elements (green) load, and double strand DNA breaks (stars) form slightly later in prophase. These events all contribute to the pairing and alignment of homologous chromosomes. **(C)** The central element of the synaptonemal complex (green) polymerizes between homologs. A subset of DNA breaks are repaired from the homolog as crossovers, which form chiasmata (orange stars) that hold homologous chromosomes together until separation at metaphase I.

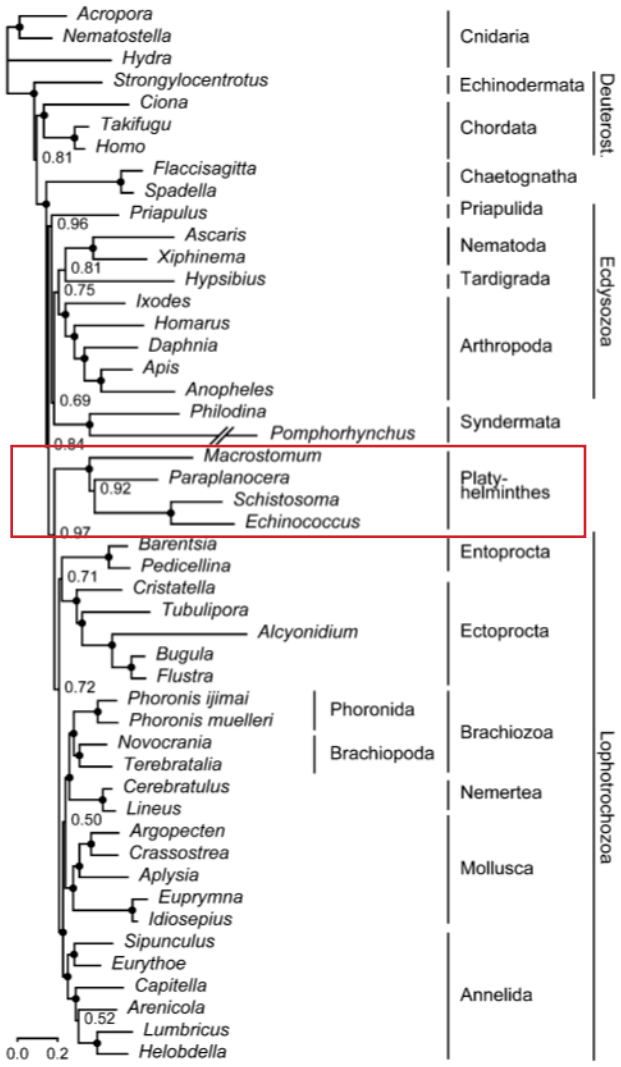

Figure 2. The platyhelminthes are within the lophotrochozoa or are a close outgroup.
The most recent phylogeny of all animal groups, based on ribosomal DNA sequences, places the platyhelminthes within the lophotrochozoa, or as a close outgroup to the lophotrochozoa. Reprinted from Nesnidal et al., 2010.

References

Adoutte, A., Balavoine, G., Lartillot, N., Lespinet, O., Prud'homme, B., and de Rosa, R. (2000). The new animal phylogeny: reliability and implications. Proc Natl Acad Sci USA *97*, 4453-4456.

Baudat, F., Manova, K., Yuen, J. P., Jasin, M., and Keeney, S. (2000). Chromosome synapsis defects and sexually dimorphic meiotic progression in mice lacking Spo11. Mol Cell *6*, 989-998.

Bähler, J., Wyler, T., Loidl, and Kohli, J. (1993). Unusual nuclear structures in meiotic prophase of fission yeast: a cytological analysis. J Cell Biol *121*, 241-256.

Benazzi Lentati, G. (1976). Gametogenesis and Egg Fertilization in Planarians. Platyhelminthes / by Mario Benazzi and Giuseppina Benazzi Lentati. In: *Animal cytogenetics; v. 1*. Berlin; Stuttgart: Bornträger.

Bhalla, N., and Dernburg, A. F. (2008). Prelude to a division. Annu Rev Cell Dev Biol *24*, 397-424.

Cao, L., Alani, E., and Kleckner, N. (1990). A pathway for generation and processing of double-strand breaks during meiotic recombination in S. cerevisiae. Cell *61*, 1089-1101.

Carranza, S., Littlewood, D. T., Clough, K. A., Ruiz-Trillo, I., Baguñà, J., and Riutort, M. (1998). A robust molecular phylogeny of the Tricladida (Platyhelminthes: Seriata) with a discussion on morphological synapomorphies. Proc Biol Sci *265*, 631-640.

Carranza, S., Baguna, J., and Riutort, M. (1997). Are the Platyhelminthes a monophyletic primitive group? An assessment using 18S rDNA sequences. Mol Biol Evol *14*, 485-497.

Chua, P.R., and Roeder, G.S. (1998). Zip2, a meiosis-specific protein required for the initiation of chromosome synapsis. Cell *93*, 349-59.

Cole, F., Keeney, S., and Jasin, M. (2010). Comprehensive, fine-scale dissection of homologous recombination outcomes at a hot spot in mouse meiosis. Mol Cell *39*, 700-710.

Croft, J. A., and Jones, G. H. (1989). Meiosis in Mesostoma ehrenbergii ehrenbergii. IV. Recombination nodules in spermatocytes and a test of the correspondence of late recombination nodules and chiasmata. Genetics *121*, 255-262.

D'Souza, T. G., and Michiels, N. K. (2009). Sex in Parthenogenetic Planarians: Phylogenetic Relic or Evolutionary Resurrection? In Lost Sex, I. Schön, K. Martens, and P. Dijk, eds. (Dordrecht: Springer Netherlands), p. 377-397.

D'Souza, T. G., Storhas, M., and Michiels, N. K. (2005). The effect of ploidy level on fitness in parthenogenetic flatworms. Biological Journal of the Linnean Society *85*, 191-198.

Dernburg, A. F., Sedat, J. W., and Hawley, R. S. (1996). Direct evidence of a role for heterochromatin in meiotic chromosome segregation. Cell *86*, 135-146.

Dernburg, A. F., McDonald, K., Moulder, G., Barstead, R., Dresser, M., and Villeneuve, A. M. (1998). Meiotic recombination in C. elegans initiates by a conserved mechanism and is dispensable for homologous chromosome synapsis. Cell *94*, 387-398.

de Vries, F.A., de Boer E., van den Bosch, M., Baarends, W.M., Ooms, M., Yuan, L., Liu, J.G., van Zeeland, A.A., Heyting, C., and Pastink, A. (2005). Mouse Sycp1 functions in synaptonemal complex assembly, meiotic recombination, and XY body formation. Genes Dev *11*, 1376-89.

Ding, D., Haraguchi, T., and Hiraoka, Y. (2010). From meiosis to postmeiotic events: alignment and recognition of homologous chromosomes in meiosis. FEBS J *277*, 565-570.

Edlinger, B., and Schlögelhofer, P. (2011). Have a break: determinants of meiotic DNA double strand break (DSB) formation and processing in plants. J. Exp. Bot. *62*, 1545-1563.

Egel-Mitani, M., Olson, L. W., and Egel, R. (1982). Meiosis in Aspergillus nidulans: another example for lacking synaptonemal complexes in the absence of crossover interference. Hereditas *97*, 179-187.

Franquinet, R., and Lender, T. (1972). [Ultrastructural aspects of spermiogenesis in Polycelis tenuis and Polycelis nigra (planarians)]. Zeitschrift für mikroskopisch-anatomische Forschung *86*, 481-495.

Franquinet, R., and Lender, T. (1973). [Ultrastructural study of testis of Polycelis tenuis and Polycelis nigra (Planarians). Evolution of male germ cells before spermatogenesis]. Zeitschrift für mikroskopisch-anatomische Forschung *87*, 4-22.

Gelei, J. (1921a). Weitere Studien über die Oogenese des Dendrocoelum lacteum. II. Die Längskonjugation der Chromosomen (Arch. Zellforsch).

Gelei, J. (1921b). Weitere Studien über die Oogenese des Dendrocoelum lacteum. III. Die Konjugation der Chromosomen in der Literatur und meine Befunde (Arch. Zellforsch).

Golubovskaya, I. N., Harper, L. C., Pawlowski, W. P., Schichnes, D., and Cande, W. Z. (2002). The pam1 gene is required for meiotic bouquet formation and efficient homologous synapsis in maize (Zea mays L.). Genetics 162, 1979-1993.

Grey, C., Baudat, F., and de Massy, B. (2009). Genome-wide control of the distribution of meiotic recombination. PLoS Biol *7*, e35.

Gurley, K., Rink, J., and Sánchez Alvarado, A. (2007). {beta}-Catenin Defines Head Versus Tail Identity During Planarian Regeneration and Homeostasis. Science.

Ishiguro, K., Kim, J., Fujiyama-Nakamura, S., Kato, S., and Watanabe, Y. (2011). A new meiosis-specific cohesin complex implicated in the cohesin code for homologous pairing. EMBO Rep *12*, 267-275.

Jones, G., and Croft, J. (1989). Chromosome-Pairing and Chiasma Formation in Spermatocytes and Oocytes of Dendrocoelum-Lacteum (Turbellaria, Tricladida) - a Cytogenetical and Ultrastructural-Study. Heredity *63*, 97-106.

Keeney, S., Giroux, C. N., and Kleckner, N. (1997). Meiosis-specific DNA double-strand breaks are catalyzed by Spo11, a member of a widely conserved protein family. Cell *88*, 375-384.

Kong, A., Thorleifsson, G., Gudbjartsson, D. F., Masson, G., Sigurdsson, A., Jonasdottir, A., Walters, G. B., Jonasdottir, A., Gylfason, A., Kristinsson, K. T., et al. (2010). Fine-scale recombination rate differences between sexes, populations and individuals. Nature *467*, 1099-1103.

Koszul, R., and Kleckner, N. (2009). Dynamic chromosome movements during meiosis: a way to eliminate unwanted connections? Trends Cell Biol *19*, 716-724.

Kumar, R., and de Massy, B. (2010). Initiation of Meiotic Recombination in Mammals. Genes *1*, 521-549.

La Fuente, de, Parra, Viera, Calvente, Gómez, Suja, Rufas, and Page (2007). Meiotic Pairing and Segregation of Achiasmate Sex Chromosomes in Eutherian Mammals: The Role of SYCP3 Protein. PLoS Genet *3*, e198.

Lartillot, N., and Philippe, H. (2008). Improvement of molecular phylogenetic inference and the phylogeny of Bilateria. Philos Trans R Soc Lond, B, Biol Sci *363*, 1463-1472.

Lee, J., and Hirano, T. (2011). RAD21L, a novel cohesin subunit implicated in linking homologous chromosomes in mammalian meiosis. J Cell Biol *192*, 263-276.

Liebe, B., Petukhova, G., Barchi, M., Bellani, M. A., Braselmann, H., Nakano, T., Pandita, T. K., Jasin, M., Fornace, A., Meistrich, M. L., et al. (2006). Mutations that affect meiosis in male mice influence the dynamics of the mid-preleptotene and bouquet stages. Exp Cell Res *312*, 3768-3781.

Lynn, A., Soucek, R., and Börner, G. V. (2007). ZMM proteins during meiosis: crossover artists at work. Chromosome Res *15*, 591-605.

MacQueen, A. J., Colaiacovo, M. P., McDonald, K., and Villeneuve, A. M. (2002). Synapsis-dependent and -independent mechanisms stabilize homolog pairing during meiotic prophase in C. elegans. Genes Dev *16*, 2428-2442.

Martinez-Perez, E., and Colaiacovo, M. P. (2009). Distribution of meiotic recombination events: talking to your neighbors. Curr Opin Genet Dev *19*, 105-112.

McKim, K. S., Green-Marroquin, B. L., Sekelsky, J. J., Chin, G., Steinberg, C., Khodosh, R., and Hawley, R. S. (1998). Meiotic synapsis in the absence of recombination. Science *279*, 876-878.

Mets, D. G., and Meyer, B. J. (2009). Condensins regulate meiotic DNA break distribution, thus crossover frequency, by controlling chromosome structure. Cell *139*, 73-86.

Mitman, G., and Fausto-Sterling, A. (2006). Whatever Happened To Planaria? C.M. Child and the Physiology of Inheritance. In: The Right Tool for the Job: At Work in 20th Century Life Sciences. Clarke, A. and J. Fujimura, eds. Princeton University Press.

Neale, M. J., and Keeney, S. (2006). Clarifying the mechanics of DNA strand exchange in meiotic recombination. Nature *442*, 153-158.

Nesnidal, M. P., Helmkampf, M., Bruchhaus, I., and Hausdorf, B. (2010). Compositional heterogeneity and phylogenomic inference of metazoan relationships. Mol Biol Evol *27*, 2095-2104.

Newmark, P. A., Reddien, P. W., Cebrià, F., and Sánchez Alvarado, A. (2003). Ingestion of bacterially expressed double-stranded RNA inhibits gene expression in planarians. Proc Natl Acad Sci USA *100 Suppl 1*, 11861-11865.

Newmark, P. A., and Sánchez Alvarado, A. (2002). Not your father's planarian: a classic model enters the era of functional genomics. Nat Rev Genet *3*, 210-219.

Oakley, H. A. (1982). Meiosis in Mesostoma-Ehrenbergii-Ehrenbergii (Turbellaria, Rhabdocoela). II. Synaptonemal Complexes, Chromosome-Pairing and Disjunction in Achiasmate Oogenesis. Chromosoma *87*, 133-147.

Oakley, H. A. (1985). Meiosis in Mesostoma ehrenbergii ehrenbergii (Turbellaria, Rhabdocoela). III. Univalent chromosome segregation during the first meiotic division in spermatocytes. Chromosoma *91*, 95-100.

Oakley, H. A., and Jones, G. (1982). Meiosis in Mesostoma-Ehrenbergii Ehrenbergii (Turbellaria, Rhabdocoela). I. Chromosome-Pairing, Synaptonemal Complexes and Chiasma Localization in Spermatogenesis. Chromosoma *85*, 311-322.

Penkner, A. M., Fridkin, A., Gloggnitzer, J., Baudrimont, A., Machacek, T., Woglar, A., Csaszar, E., Pasierbek, P., Ammerer, G., Gruenbaum, Y., et al. (2009). Meiotic chromosome homology search involves modifications of the nuclear envelope protein Matefin/SUN-1. Cell *139*, 920-933.

Philippe, H., Lartillot, N., and Brinkmann, H. (2005). Multigene analyses of bilaterian animals corroborate the monophyly of Ecdysozoa, Lophotrochozoa, and Protostomia. Mol Biol Evol *22*, 1246-1253.

Rieger, R. M. (1998). 100 Years of Research on "Turbellaria." Hydrobiologia *383*, 1-27.

Robb, S. M., Ross, and Sánchez Alvarado, A. (2007). SmedGD: the Schmidtea mediterranea genome database. Nucleic Acids Res.

Roeder, G. S. (1997). Meiotic chromosomes: it takes two to tango. Genes Dev *11*, 2600-2621.

Romanienko, P. J., and Camerini-Otero, R. D. (2000). The mouse Spo11 gene is required for meiotic chromosome synapsis. Mol Cell *6*, 975-987.

Sato, A., Isaac, B., Phillips, C. M., Rillo, R., Carlton, P. M., Wynne, D. J., Kasad, R. A., and Dernburg, A. F. (2009). Cytoskeletal forces span the nuclear envelope to coordinate meiotic chromosome pairing and synapsis. Cell *139*, 907-919.

Sánchez Alvarado, A., and Newmark, P. A. (1999). Double-stranded RNA specifically disrupts gene expression during planarian regeneration. Proc Natl Acad Sci USA *96*, 5049-5054.

Scherthan, H. (2001). A bouquet makes ends meet. Nat Rev Mol Cell Biol *2*, 621-627.

Storlazzi, A., Gargano, S., Ruprich-Robert, G., Falque, M., David, M., Kleckner, N., and Zickler, D. (2010). Recombination proteins mediate meiotic spatial chromosome organization and pairing. Cell *141*, 94-106.

Viera, A., Luis Santos, J., Teresa Parra, M., Calvente, A., Gómez, R., La Fuente, de, R., Angel Suja, J., Page, J., and Rufas, J. S. (2009). Cohesin axis maturation and presence of RAD51 during first meiotic prophase in a true bug. Chromosoma *118*, 575-589.

Wang, Y., Stary, J. M., Wilhelm, J. E., and Newmark, P. A. (2010). A functional genomic screen in planarians identifies novel regulators of germ cell development. Genes Dev *24*, 2081-2092.

Wood, A. J., Severson, A. F., and Meyer, B. J. (2010). Condensin and cohesin complexity: the expanding repertoire of functions. Nat Rev Genet *11*, 391-404.

Yanowitz, J. (2010). Meiosis: making a break for it. Curr Opin Cell Biol *22*, 744-751.

Youds, J. L., and Boulton, S. J. (2011). The choice in meiosis - defining the factors that influence crossover or non-crossover formation. J Cell Sci *124*, 501-513.

Zayas, R. M., Hernández, A., Habermann, B., Wang, Y., Stary, J. M., and Newmark, P. A. (2005). The planarian Schmidtea mediterranea as a model for epigenetic germ cell specification: analysis of ESTs from the hermaphroditic strain. Proc Natl Acad Sci USA *102*, 18491-18496.

Chapter II. Characterization of spermatogenesis in wild-type *S. mediterranea*

Introduction

As discussed at length in Chapter I, there is significant diversity in the meiotic program across species. Although cytogenetic studies have been conducted in several flatworm species over the past century, meiosis has not been described in molecular detail in any planarians. Thus, a major goal of my studies was to characterize wild-type meiosis in *S. mediterranea*. Below, I will describe the basic reproductive biology of these animals, as well as some key events of meiotic prophase that I have examined using modern cytological tools: changes in chromosome morphology throughout prophase (assayed by DAPI staining), bouquet formation (assayed by telomere FISH and immunofluorescence to Smed-SUN1), homolog pairing (assayed by chromosome-specific FISH), axial element dynamics (assayed by immunofluorescence to Smed-HOP1), and double strand DNA break dynamics (assayed by immunofluorescence to Smed-RAD51). The results of these studies reveal a number of intriguing phenomena in *S. mediterranea* spermatogenesis, including a persistent telomere bouquet and concomitant changes in nuclear envelope organization, a striking clustering of DSBs in telomere-proximal regions, and interesting axial element dynamics throughout meiotic prophase.

Results

The reproductive biology of Schmidtea mediterranea

Adult, sexual *S. mediterranea* (depicted in cartoon form in Figure 1A) range from approximately 1-2 cm in length and are obligate hermaphrodites. Mature sexual animals can be distinguished from juveniles by the presence of a gonopore on the ventral surface, approximately 2-4 mm from the tail tip, as well as by their size. In general, animals reach sexual maturity between two and three months after hatching or lateral amputation (to 2-3 mm pieces) and will continue to grow in size, albeit more slowly, for another several months. Animals begin mating when they reach sexual maturity but usually do not lay egg cases until they are 1.5 cm in length or larger, and the hatching rates of these cases is quite low. The basis of this poor fertility is not known, but may be related to the extensive inbreeding of the initial clonal line.

Mature sexual animals contain abundant testes lobes in the posterior 1/2 to 2/3 of the body, and ovaries can be found just behind the basal ganglia in the head region of the animal. Both testes and ovaries develop from pluripotent neoblasts as the animals grow in size upon development from hatchlings or regeneration from cut fragments and are resorbed when the animal degrows in response to starvation. Work in *Dugesia ryukyuensis* has described five stages of both planarian testis and ovarian development upon sexualization, which appear to be

paralleled in maturing *S. mediterranea* (Kobayashi and Hoshi, 2002; Wang et al., 2007). Of interest, several protein and hormone determinants of germ cell fate have been identified in *S. mediterranea* (Zayas et al., 2005; Wang et al., 2007; Handberg-Thorsager and Saló, 2007; Wang et al., 2010; Collins et al., 2010).

Planarian testis organization and nuclear morphology of spermatocytes

Mature testis lobes resemble mammalian seminiferous tubules, with mitotically dividing spermatogonia forming the outer layer of the lobe, meiotic spermatocytes organized in a loosely temporal progression from the outer layer in, and spermatids at various stages of maturity are found in the lumen of the testis lobe (Fig. 1B,C). Spermatocytes progress through meiosis in groups of eight nuclei that are derived from the same spermatogonial cell and produce 32 spermatids (as described in *Polycelis tenuis*; Franquinet and Lender, 1972; 1973). Due to the highly flexible nature of the planarians — both developmentally and mechanically — the exact dimensions of the testes are difficult to determine, but in general mature testes contain several hundred spermatocytes and occupy a volume of roughly 100 μm x 100 μm. The testes may continue to grow in volume and nucleus number as the individual planarian becomes larger, but fully mature spermatids are observed in the smaller testes of animals that have just reached sexual maturity. Throughout this work, I have mainly studied small mature animals, both to save time in culture and because smaller animals are more amenable to preparation for cytology.

A number of distinct stages of meiotic prophase can be identified based on the morphology of DAPI-stained chromosomes in well-fixed tissue cryosections (Fig. 1D-L). It is generally possible to distinguish leptotene/zygotene nuclei (Fig. 1E, F), which contain partially condensed chromosomes, from pachytene-like nuclei (Fig. 1G), which appear to have a fully polymerized synaptonemal complex (SC) between homologs, as reflected by clearly parallel DAPI-staining tracks. As shown in Figure 1L, quantification of these stages showed that approximately 40% of all non-spermatid testis nuclei can be classified as leptotene/zygotene, and about 22% of all nuclei exhibit pachytene (synapsed) morphology, with some variation between testis lobes (n=767 nuclei; two independent testes sections in each of four animals). Transmission electron microscopy of thin sections (Fig. 1N; Fig. 6) revealed a similar proportion of non-spermatid nuclei with visible synaptonemal complex structures (9/51; 18%), indicating that pachytene chromosome morphology as assessed by DAPI staining can be considered a reliable proxy for SC formation. Occasionally, groups of enlarged diplotene-like nuclei or compact, diakinesis-like nuclei can be observed in some testes (Fig. 1H, I); their low abundance suggests that these stages may be quite transient. The fact that certain stages of spermatogenesis are not found in all testes also suggests that, like mammalian seminiferous tubules, planarian testes may each contain distinct groupings of germ cells at particular stages of development (for a review of mammalian spermatogenesis, see Hermo et al., 2010).

Formation of the telomere bouquet and concomitant redistribution of Smed-SUN1

One key event described in the meiotic prophase of nearly all organisms is the *de novo* attachment of chromosome ends to the nuclear envelope and their clustering within a limited region of the nucleus (bouquet formation). As described in Chapter I, a classical bouquet has been previously characterized in cytogenetic and mechanical detail in the planarian *Dendrocoelum lacteum*, but bouquet formation has not been investigated specifically in *S. mediterranea*. In order to observe bouquet formation, I developed DNA FISH techniques (described in more detail in Chapter VI) and synthesized a probe that hybridizes to the planarian telomere sequence (TTAGGG; identified in *Polycelis tenuis*, Joffe et al., 1998) in order to examine telomere localization in spermatocytes. Telomere FISH to tissue cryosections showed that the majority of prophase nuclei (80.9%) are organized in an obvious bouquet, with telomeres clustering together at the nuclear envelope (Fig. 2A,F). Interestingly, the bouquet conformation persists in nearly all pachytene nuclei. This is in striking contrast to other organisms, in which the bouquet is relatively transient (e.g., only 0.3-0.6% of spermatocytes in mouse; (Liebe et al., 2006) and 5-10% of meiocytes in *Sordaria;* Storlazzi et al., 2010) or at least dispersed upon entrance to pachytene (reviewed in Scherthan, 2007).

Although telomere FISH is a robust assay for bouquet formation, I was also interested in developing other markers for the bouquet. In many organisms, nuclear envelope proteins containing a SUN (Sad1/UNC-84 homology) domain associate intimately with chromosome ends (i.e., telomeres or Pairing Centers) during meiosis and are involved in meiotic chromosome reorganization (reviewed in Fridkin et al., 2008 and Hiraoka and Dernburg, 2009). I identified several candidate genes in *S. mediterranea* by searching the genome for regions with homology to a consensus SUN domain. Three genes were identified (mk4.001469.07.01, mk4.001275.01.01, and mk4.003039.01.01) and designated Smed-SUN1, SUN2, and SUN3, respectively. We generated an antibody specific to the protein with the greatest homology to *C. elegans* SUN1 (Smed-SUN1) and I investigated its localization by immunofluorescence in tissue cryosections. These experiments revealed that SUN1 is widely expressed and localizes throughout the nuclear envelope in many cell types (see Chapter IV, Figure 1). In spermatocytes, SUN1 concentrates dramatically at a limited region of the nuclear envelope. Immunostaining combined with FISH demonstrated that this region corresponds to the cluster of telomeres in the bouquet (Fig. 2B). This localized SUN1 staining persists throughout pachytene, similar to the bouquet, and SUN1 can therefore be used as a marker for the bouquet as an alternative to telomere FISH. Notably, the region of the nuclear envelope occupied by SUN1 in *S. mediterranea* spermatocytes is somewhat broader than has been observed in other organisms, where the SUN domain proteins that are involved in the movement of meiotic chromosomes often co-localize very tightly with chromosome ends. Strong SUN1 staining can also be observed throughout the nuclear envelope (i.e., not concentrated in one domain) in immature spermatids.

Stable pairing of homologous chromosomes occurs late in the meiotic program

The stable pairing and alignment of homologous chromosomes is perhaps the most critical event of meiotic prophase, but also one of the most challenging to investigate. I examined homolog pairing dynamics using chromosome-specific FISH in tissue cryosections. I synthesized two chromosome-specific probes, one that recognizes a centromeric region of Chromosome II (CEN-2; 5'-GCT ATC ATG TAG AGA ATC AAA-3') and one that recognizes the rDNA locus at one end of Chr. II, and examined their localization in spermatocytes and also metaphase chromosome spreads (described in more detail in Chapter VI). I found that the rDNA probe is not ideal for assaying pairing, at least in the context of the telomere bouquet, as it is located in a subtelomeric region and its signal is sometimes quite diffuse in spermatocyte nuclei. The CEN-2 probe, on the other hand, is distant from telomeres, and thus a more useful tool for assaying homolog pairing (Fig. 2C,D). Although the CEN-2 probe shows some hybridization to the centromeric region of Chr. III as well as to Chr. II in metaphase chromosome spreads, the weak signals from Chr. III that can be seen in some spermatocyte nuclei are easily distinguished from the brighter foci on Chr. II, and this does not usually present a significant hurdle to assaying homologous chromosome pairing with this probe.

Hybridization with the CEN-2 probe indicated that, despite the early clustering of telomeres in a bouquet conformation, homolog pairing does not occur until relatively late in the meiotic program, at least at this locus. CEN-2 foci remain well separated in leptotene and zyogtene stage spermatocytes (Fig. 2C), even though most of these nuclei exhibit telomere clustering. When I measured the distance between FISH foci in three classes of nuclei (pre-meiotic, leptotene/zygotene, pachytene), I observed a similar distribution of distances in pre-meiotic nuclei and leptotene/zygotene spermatocytes (2.34 ± 1.07 μm vs. 2.09 ± 0.99 μm; $p=0.462$). There was no obvious class of zygotene nuclei with paired CEN-2 signals. Extensive pairing at this locus was achieved only in pachytene nuclei, which appear to have essentially complete SC formation (1.10 ± 0.77 μm; $p<0.001$ compared to earlier stages) (Fig. 2D,E). This observation may suggest that synapsis occurs relatively quickly after pairing is accomplished, or perhaps that SC polymerization is required to stabilize pairing, as in *C. elegans* (MacQueen et al., 2002). This observation would also be consistent with particularly late pairing of centromeres (i.e., relative to other loci), as has been observed in many organisms. Although I have not observed any indications of pre-meiotic association of centromeres or other special behavior for centromeric regions, it is certainly possible that centromeres exhibit their own unique pairing dynamics. Nevertheless, these data indicate that chromosomes are likely not fully paired for an extended amount of time prior to synapsis.

The axial element component HOP1 loads early in prophase and persists through pachytene

Another marker of progression through meiosis is the formation of meiotic axes. We generated an antibody to the axial element protein Smed-HOP1 (mk4.001053.00.01), which was identified by a homology search of the *S. mediterranea* genome with the *S. cerevisiae* Hop1 protein sequence, and examined its localization in cryosections. As shown in Figure 3B, foci of HOP1 appear on meiotic chromosomes very early in MI prophase (probably at leptotene). Nuclei with weak HOP1 staining and dispersed telomeres are observed occasionally, but are much less abundant than nuclei with both HOP1 staining and telomere clustering, showing that HOP1 loading occurs approximately concomitant with or slightly before bouquet formation. This early loading also makes HOP1 a good marker for distinguishing between spermatocytes and pre-meiotic spermatogonia.

Several other aspects of HOP1 staining may be useful for identifying substages of meiotic prophase. In particular, HOP1 staining appears weaker near the bouquet in some zygotene nuclei (Fig. 3C), which may be indicative of a distinct event in or substage of zygotene. It is often possible to observe a cluster of nuclei that all exhibit this pattern (e.g., Fig. 3A, lower right), further indicating that this phenomenon has a biological basis and is not simply artifactual. It is not clear whether this weakened staining represents a temporary removal of the HOP1 protein or perhaps a modification of the protein or its local environment that masks its antigen availability. Several recent studies of Hormad1 and Hormad2, the mouse homologs of HOP1, have shown that these proteins are depleted from chromosome axes after Sycp1 loading (Wojtasz et al., 2009; Fukuda et al., 2010). However, in *S. mediterranea*, HOP1 staining generally appears to be strong and essentially contiguous on all chromosomes in pachytene nuclei, indicating that it is not permanently removed from axes upon synapsis (Fig. 3D). An alternative possibility is that HOP1 is transiently masked upon SC loading; epitope masking upon synapsis has been observed for ASY1 in *Z. mays* (Golubovskaya et al., 2006). In well-stained sections, the stronger staining and increased spatial separation of distinct HOP1 stretches in pachytene can also be used to help distinguish pachytene nuclei from zygotene nuclei.

Double strand DNA breaks (DSBs) appear in zygotene, peak and resolve during pachytene, and are concentrated near the bouquet

The programmed formation of double strand DNA breaks (DSB) during meiosis is essential for crossover recombination. Because the number and timing of DSB formation varies widely between sexes and across organisms, we were especially interested in characterizing DSB dynamics in *S. mediterranea*. In collaboration with Youbin Xiang at the Hawley lab (manuscript in preparation), we investigated DSB formation using immunofluorescence to Smed-RAD51 in testis cryosections. This highly conserved protein localizes to resected DSBs, where it promotes

the formation of DNA strand invasion intermediates that are crucial for subsequent break repair. RAD51 foci are frequently used as a proxy for the presence of DSBs.

Co-staining with RAD51 and SUN1 reveals clusters of RAD51 foci at/near the bouquet in leptotene/zygotene nuclei and some pachytene nuclei (Fig. 4A). The clustered nature of meiotic DSBs is also highly likely to be the product of a regulated biological process, as X-irradiation (10 Gy, at 1.0 Gy/min) resulted in an increased number of RAD51 foci that were distributed more evenly throughout the nucleus, in spermatocytes at all stages of meiotic prophase (Fig. 4B). In non-irradiated animals, focus formation appears to begin in zygotene (Fig. 4D) and peak around 20-30 clustered foci in pachytene (Fig. 4E), although some pachytene nuclei exhibit somewhat fewer and more dispersed (non-clustered) RAD51 foci (Fig. 4F). Quantification of RAD51 foci per nucleus in these different stages is shown in Figure 4G. Notably, RAD51 foci are generally observed at one end of a stretch of HOP1 and usually do not coincide with HOP1 staining.

TUNEL staining reveals low baseline levels of germline apoptosis and significant programmed DNA breaks in maturing spermatids

In many metazoans, DNA damage or the failure of synapsis during meiosis trigger distinct surveillance mechanisms that lead to the apoptosis of the affected cells (Bhalla and Dernburg, 2005). In order to examine the baseline level of germline apoptosis in *S. mediterranea*, I conducted TUNEL to cryosectioned animals. TUNEL enzymatically detects broken DNA and therefore strongly labels the nuclei of apoptotic cells that have initiated programmed DNA degradation (Gold et al., 1994; Negoescu et al., 1996). In *S. mediterranea*, apoptosis is strongly upregulated at the cut site within 4-8 hours after amputation (Pellettieri et al., 2009), which I was able to take advantage of as a positive control for these experiments.

As shown in Figure 5, TUNEL to 30 µm longitudinal sections of wild-type animals indicates a low level of germline apoptosis, with one or more TUNEL-positive spermatocytes observed in only about 10% of all testis sections (~0.1-0.3% of testis nuclei). Interestingly, considerable numbers of TUNEL-positive spermatids can be observed in the lumen of 10-26% of testes in some wild-type animals (Fig. 5D). The same phenomenon is observed in mice and humans due to DNA breaks that are necessary for chromatin remodeling and sperm nucleus packaging and are made by Topoisomerase II during stages IX-XII of the seminiferous epithelium cycle (Marcon and Boissonneault, 2004; Leduc et al., 2008). This presents a challenge to the unambiguous identification of apoptotic nuclei, as it is difficult to distinguish apoptotic spermatocytes from immature spermatids that may be undergoing chromatin remodeling, which could lead to under- or overcounting of apoptotic cells. The relatively small number of TUNEL-positive spermatocytes in each testis, in combination with the variable sizes of testes in wild-type animals (due to normal differences in development, size, feeding habits,

etc.) also complicates the precise quantification of number of apoptotic events per round of spermatogenesis. Furthermore, feeding habits can affect the level of apoptosis in *S. mediterranea*; in asexual animals, the number of apoptotic nuclei distributed throughout the animal doubles between 1 and 2 weeks after the last feeding (Pellettieri et al., 2009). Increased apoptosis is likely to be part of the mechanism by which the reproductive organs regress in response to starvation, and could thus also present difficulties for the quantitation of germline apoptosis in this animal.

Despite these challenges, the results of TUNEL in wild-type testis sections are consistent with a low baseline level of germline apoptosis. The large number of TUNEL-positive spermatids in some testes, likely representing chromatin remodeling during sperm nucleus packaging, also reveals another parallel between spermatogenesis in *S. mediterranea* and mammalian systems.

Discussion

Several features of meiosis in *S. mediterranea* stand out as especially unique and interesting. Strikingly, the telomere bouquet is formed early in meiotic prophase and persists through the pachytene stage, while homolog pairing occurs relatively late and apparently almost concurrently with synapsis. The duration of the bouquet stage varies considerably between species, and the factors that determine the length of the bouquet stage relative to other stages of meiotic prophase are not well understood. In *S. cerevisiae,* maize, and mice, bouquet dissolution is linked to the progression of recombination through the ATM kinase, and the bouquet stage is extended when recombination or ATM signaling is disrupted (Pandita et al., 1999; Scherthan et al., 2000; Harper et al., 2004; Liebe et al., 2006); bouquet dissolution is also connected to the resolution of specific recombination intermediates in *Sordaria* (Storlazzi et al., 2010). In *C. elegans*, exit from the "transition zone" seems to be contingent on the satisfaction of some homolog pairing surveillance mechanism and/or completion of synapsis (e.g., Carlton et al., 2006; MacQueen et al., 2002). Thus, the dynamics of nuclear organization during meiosis may be regulated by different mechanisms in different species. The particularly long-lived bouquet in *S. mediterranea* may indicate that bouquet exit in this organism is connected with a later stage of recombination, for example, or that recombination progresses relatively slowly in this organism. Alternatively, it may be evidence of a continued requirement for chromosome motion after synapsis, for example, to resolve chromosome interlocks, as has been suggested in several species (e.g., Golubovskaya et al. 2002, Sheehan and Pawlowski, 2009; Koszul and Kleckner, 2009). In the future, identification of genes for which knockdown causes premature bouquet exit in *S. mediterranea* could lead to a better understanding of the factors that regulate nuclear organization during meiotic prophase.

It has also been suggested that genome content and structure may heavily influence bouquet and homolog pairing dynamics (Koszul and Kleckner, 2009; Bozza and Pawlowski, 2008). Some features of the *S. mediterranea* genome, most notably its very high repeat content (approximately 46%; Jurka et al., 2005; SmedGD v. 3.1 release notes), could generate significant ectopic pairing and thus present a challenge for homolog recognition. In this situation, a particularly long-lived homology search in the context of the bouquet, and/or long period of cytoskeleton-based chromosome movement, might be required in order to achieve proper pairing and recombination initiation. The relative lack of zygotene nuclei with fully paired homologs (i.e., paired CEN-2 foci) is also consistent with this hypothesis. However, this is not sufficient to explain why the bouquet conformation persists through pachytene.

Telomere-proximal regions may play a special role in DSB formation and recombination

Another particularly interesting observation from this study is that RAD51 foci cluster dramatically near the bouquet, implying that telomere-proximal regions of the genome may act as hotspots for DNA break formation. This idea is not unprecedented; DSB mapping studies in *S. cerevisiae* using ChIP have shown that breaks are suppressed within ~20 kB of telomeres but elevated between 50 and 100 kB from chromosome ends (Blitzblau et al., 2007; Buhler et al., 2007), and suggested that an enrichment of DSBs near telomeres would help ensure that all chromosomes, even very short ones, could receive at least one crossover. Studies in many plant species (summarized in Phillips et al., 2010) indicate that recombination occurs most frequently at distal regions of chromosomes. Cytogenetic studies in *D. lacteum* and *M. e. ehrenbergii* also suggest that chiasma distribution is skewed toward chromosome ends in spermatocytes in several flatworm species (Jones and Croft, 1989; Oakley and Jones, 1982). Nevertheless, the pronounced clustering of RAD51 foci in *S. mediterranea* is a novel finding and thus far unique among animal species. The relative absence of DSBs at interstitial loci in most nuclei may also have interesting implications for the role of telomere-proximal recombination intermediates in mediating homolog pairing and alignment. Recently, Corredor and colleagues showed that subtelomeric regions, but not other regions of the chromosome, are involved in homology assessment and synapsis initiation in wheat, and suggest that restricting the homology search to a small portion of each chromosome may protect against inappropriate recombination and pairing of homeologous loci in allodiploid organisms (Corredor et al., 2007). Given the variable ploidy levels observed throughout the planaria, it is tempting to speculate that a similar mechanism might be active in *S. mediterranea*.

The factors that determine DSB placement within the genome are still not well understood. They appear to include sequence motifs, which vary widely from species to species, chromatin state, which can be affected by transcriptional activity as well as specific chromatin modifications, and chromatin loop/axis structure. In particular, gene-rich regions are known to be prone to DSBs, relative to heterochromatic regions (e.g., Blitzblau et al. 2007). While the gene

structure of *S. mediterranea* is not known, chromosome banding studies indicate that there may be some heterochromatin enrichment at the telomeres and around centromeres (Canovai et al. 2004). This would be somewhat inconsistent with an enrichment of coding regions in subtelomeric regions, at least for some chromosomes. In any case, it is clear that the observed DSB clustering in *S. mediterranea* is generated by a specific biological activity, as irradiation does not produce the same pattern of RAD51 distribution. With this in mind, it will be very interesting to identify the factors that promote DSB (and potentially crossover) formation specifically in this region.

HOP1 also appears to be particularly dynamic near the bouquet, with weaker staining in a subset of zygotene nuclei. Given that HOP1 is required to generate DSBs in *S. mediterranea* (shown in Chapter IV), it is reasonable to hypothesize that this phenomenon may be related to the DSB clustering in this region. For example, this change in staining might reflect a difference in chromatin or axis structure that specifically permits or encourages DSB formation and masks the HOP1 epitope (possibly related to SC loading, as observed in maize and *Arabidopsis*; Golubovskaya et al. 2006), or some local modification of the HOP1 protein related to its DSB promoting activity that alters antigen availability. An alternative, though not mutually exclusive, possibility is that this weaker staining reflects a temporary removal of the HOP1 protein upon the initiation of central element loading. In mice, the HOP1 homologs HORMAD1 and -2 are removed from axes in a PCH2/TRIP13-dependent manner upon central element polymerization, which may be important for the function of the synapsis surveillance mechanism and/or normal completion of crossovers (Wojtasz et al., 2009; Roig et al., 2010); a similar Pch2-dependent depletion of Hop1 from synapsed axes occurs in *S. cerevisiae* (Börner et al., 2008). Consistent with this, telomere-proximal loci have been suggested to serve as synapsis initiation sites in several organisms, including the planarian *D. lacteum* (Jones and Croft, 1989), and sites of recombination have also been suggested to initiate central element loading in many organisms. Based on chromosome morphology alone, it is difficult to discern whether the regions of zygotene chromosomes in *S. mediterranea* that do not stain with HOP1 have synapsed or not, but this will be interesting to investigate as the appropriate reagents are developed.

Conclusions

The intriguing clustering of double strand breaks and HOP1 dynamics observed near telomeres will make *S. mediterranea* a particularly interesting organism in which to study the role of telomeres and telomere-proximal regions in initiating meiotic recombination and synapsis. The persistent bouquet may also offer an opportunity to investigate the specific role of telomere clustering in other meiotic processes, as well as factors that regulate nuclear organization during meiosis. In addition, spermatogenesis in *S. mediterranea* resembles mammalian spermatogenesis in terms of testis organization and some aspects of sperm maturation, and may be an accessible model for mammalian spermatogenesis.

Materials and methods - see Chapter VI.

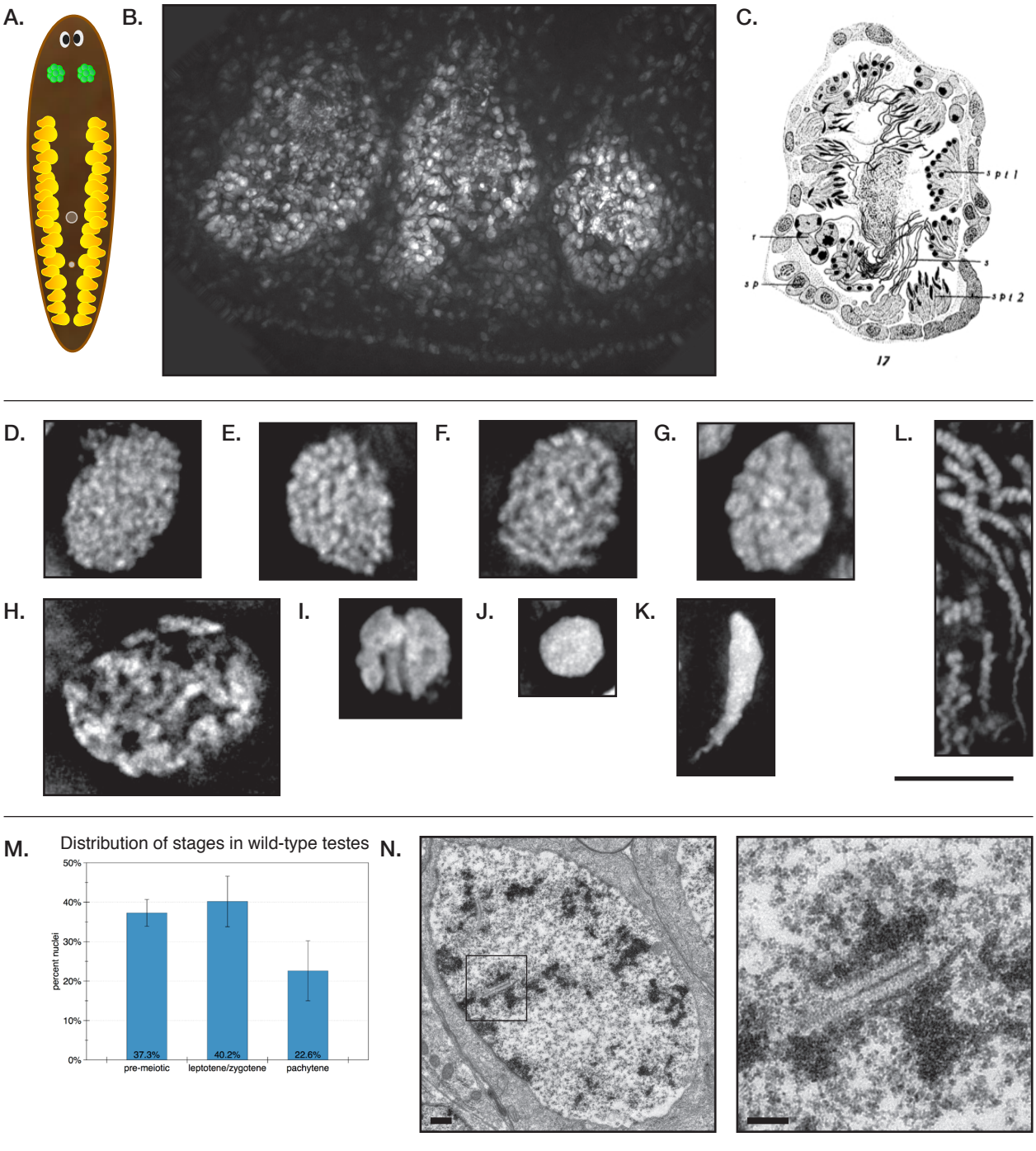

Figure 1. Basic reproductive anatomy of *S. mediterranea* and stages of meiotic prophase in spermatocytes. **(A)** Cartoon depiction of an adult hermaphrodite animal. Testes are shown in yellow and ovaries are shown in green. The two spots on the ventral midline correspond to the pharyngeal pore (upper) and gonopore (lower), respectively. **(B)** DAPI stained partial cross-section through a posterior portion of the animal. Three DAPI-bright testes lobes can be seen as in the ventral half of the section. **(C)** Schematic of planarian testis lobe organization, reproduced from Hyman, 1925. **(D-K)** Examples of meiotic stages that can be distinguished based on DAPI morphology: pre-meiotic (D), leptotene (E), zygotene (F), pachytene (G), diplotene (H), diakinesis (I), immature spermatid (J), elongating spermatid (K), mature spermatids (L). Scale bar = 5µm. **(M)** Distribution of testis nuclei at specific stages. n=767 nuclei from two sections in each of four animals. **(N)** Electron microscopy of a pachytene spermatocyte demonstrating synaptonemal complex structure at two levels of magnification. Scale bars: 0.5µm (left), 0.2µm (right).

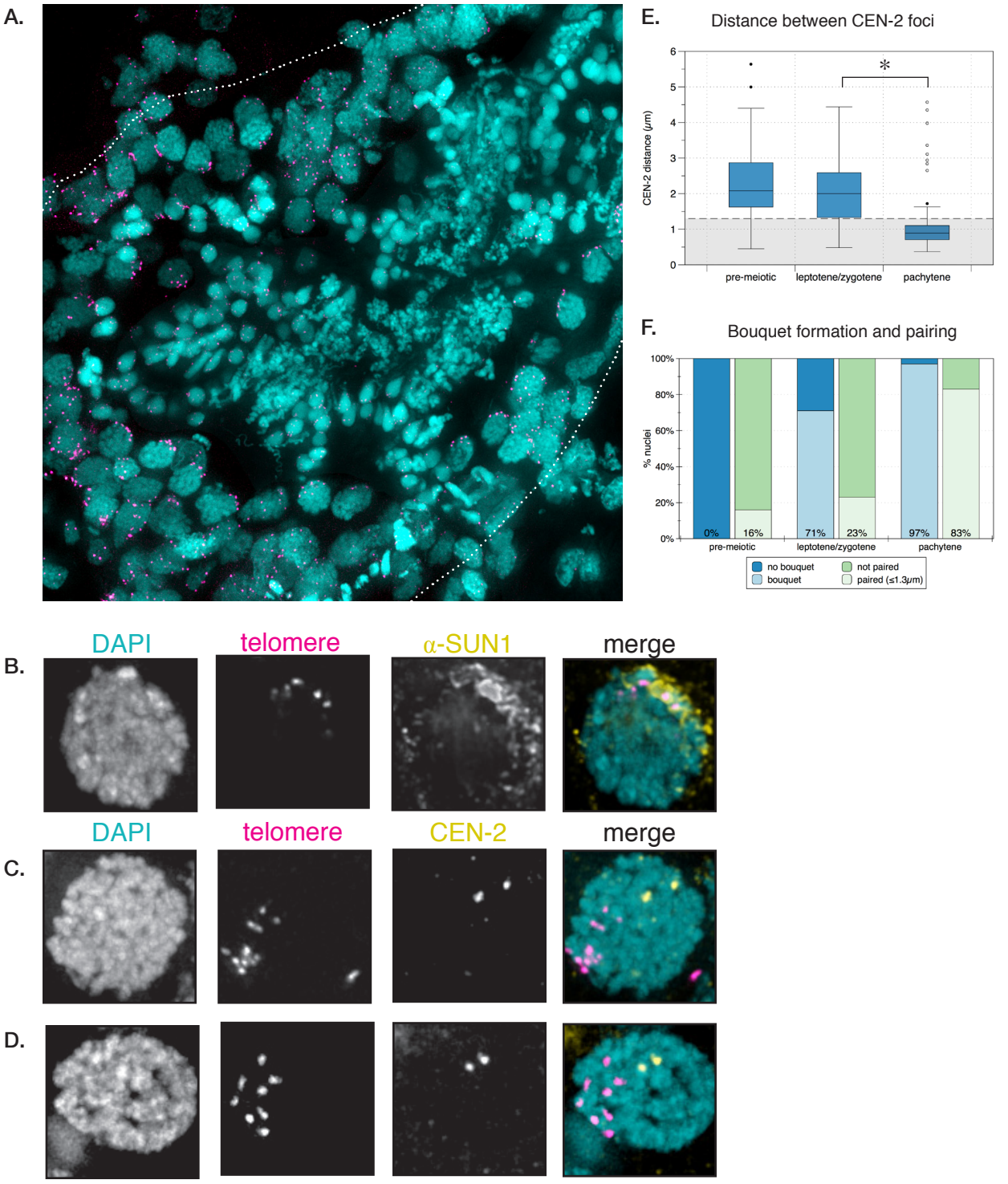

Figure 2. Bouquet formation and homolog pairing in wild-type *S. mediterranea* spermatocytes.
(A) Whole testis, showing that most spermatocyte nuclei exhibit pronounced telomere clustering. Pink, telomere FISH; blue, DAPI. **(B)** Smed-SUN1 co-localizes with telomere FISH signals at the bouquet region of the nucleus. **(C-D)** Homologous chromosomes, marked by a FISH probe to the centromeric region of Chromosome II (CEN-2), are generally unpaired in zygotene (C) and paired in pachytene (D). **(E)** Quantification of distances between CEN-2 foci in pre-meiotic, leptotene/zygotene, and pachytene nuclei. n=234 nuclei from three animals. *p<0.001. **(F)** Quantification of bouquet frequency and pairing frequency in pre-meiotic, leptotene/zygotene, and pachytene nuclei.

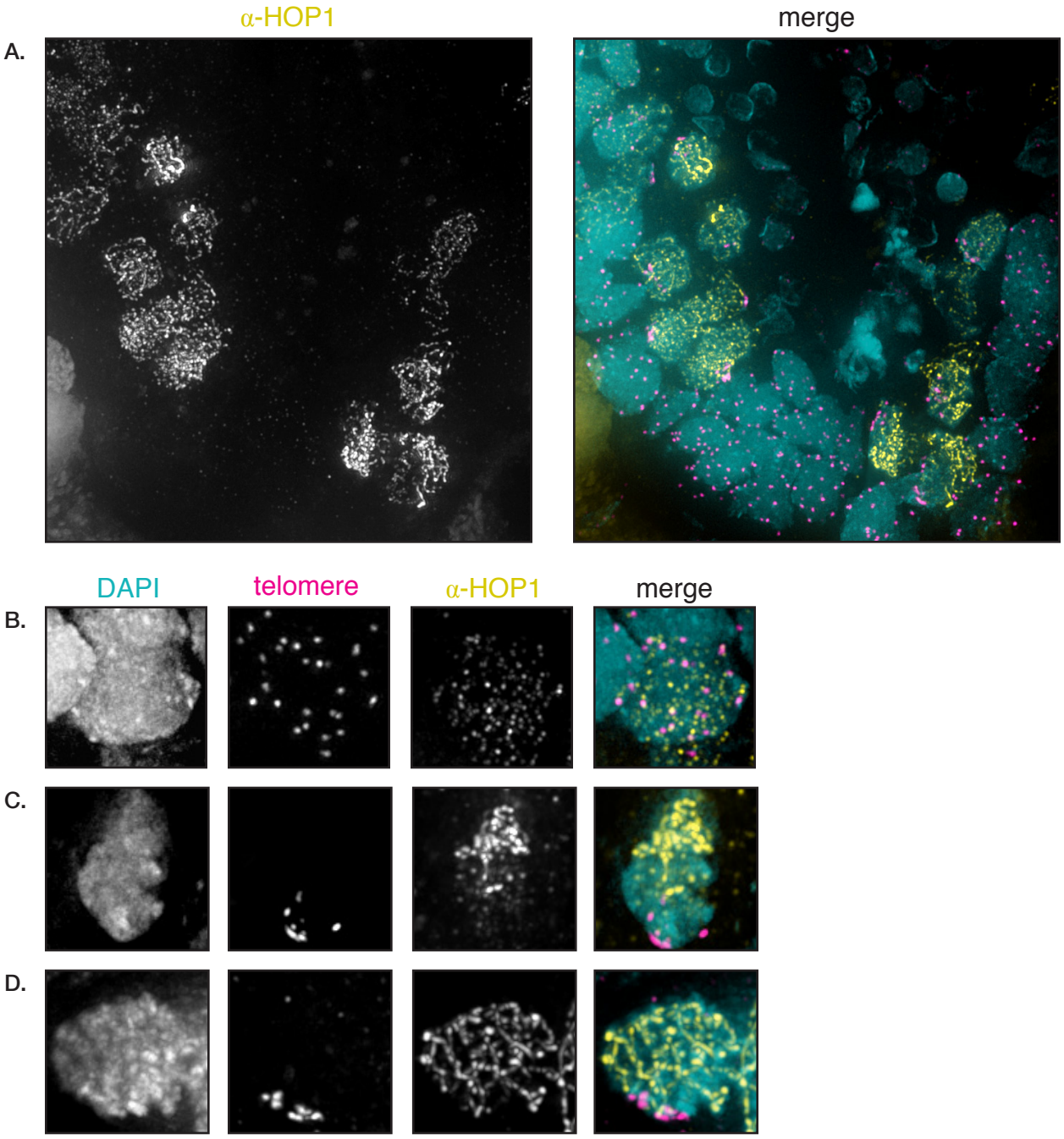

Figure 3. Localization of Smed-HOP1 in wild-type spermatids.
(A) Immunofluorescent staining of a testis section with α-HOP1 antibody. Yellow, α-HOP1; pink, telomere FISH; blue, DAPI. **(B)** Weak HOP1 staining can be observed in some nuclei prior to bouquet formation. **(C)** HOP1 staining is diminished near the bouquet in a subset of zygotene nuclei. **(D)** Strong HOP1 staining is observed in most pachytene nuclei.

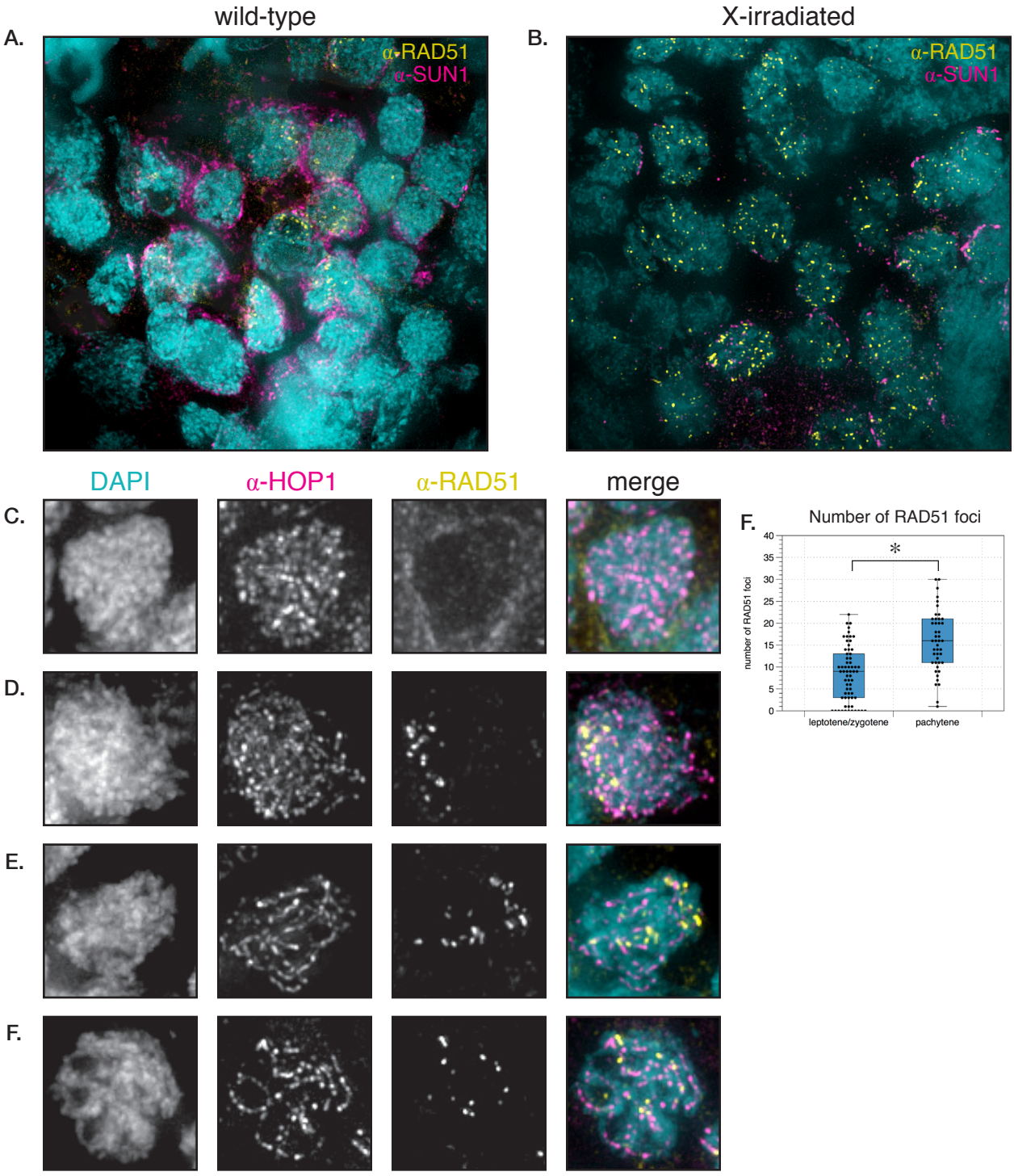

Figure 4. Localization of Smed-RAD51 in wild-type spermatids.
(A) Immunofluorescent staining of a testis section with α-SUN1 and α-RAD51 antibodies shows clusters of RAD51 foci that localize near the bouquet. yellow, α-RAD51; pink, α-SUN1; blue, DAPI. **(B)** Irradiation (10 Gy) produces a non-clustered pattern of RAD51 foci. **(C)** Few or no RAD51 foci are observed in early prophase. **(D)** Clusters of RAD51 foci can be observed in zygotene nuclei. **(E)** Clusters of large numbers of RAD51 foci are observed in some pachytene nuclei. **(F)** Fewer and more dispersed RAD51 foci are observed in a subset of pachytene nuclei. (Datasets courtesy Youbin Xiang, Stowers Institute). **(G)** Quantification of RAD51 foci in wild-type. *p<0.000; n=110 nuclei.

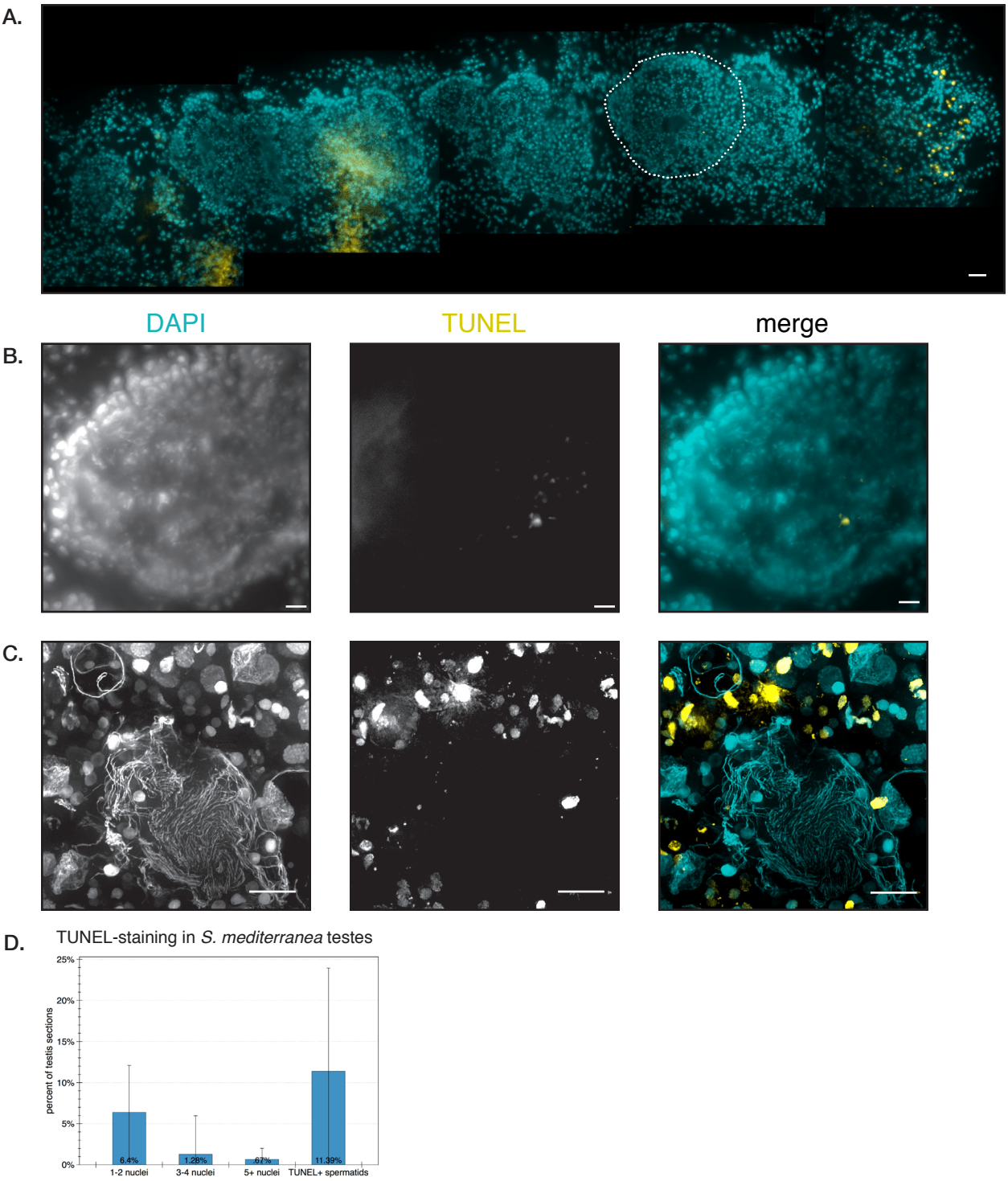

Figure 5. TUNEL staining of apoptosis in wild-type *S. mediterranea* sections
(A) TUNEL staining of a longitudinal section of *S. mediterranea*. The TUNEL-positive nuclei at the amputation site (far right) serve as a positive control. A single testis is outlined in white as an example. Blue, DAPI; yellow, TUNEL. Scale bar = 50µm. **(B)** Small numbers of TUNEL-positive spermatocytes can be observed in some testes. Scale bar = 10µm. **(C)** Significant numbers of TUNEL-positive spermatids are observed in approximately 10-26% of testes in some animals. Scale bar = 10µm. **(D)** Quantification of TUNEL staining in wild-type demonstrates significant variability from animal to animal. n=422 testis sections taken in four animals.

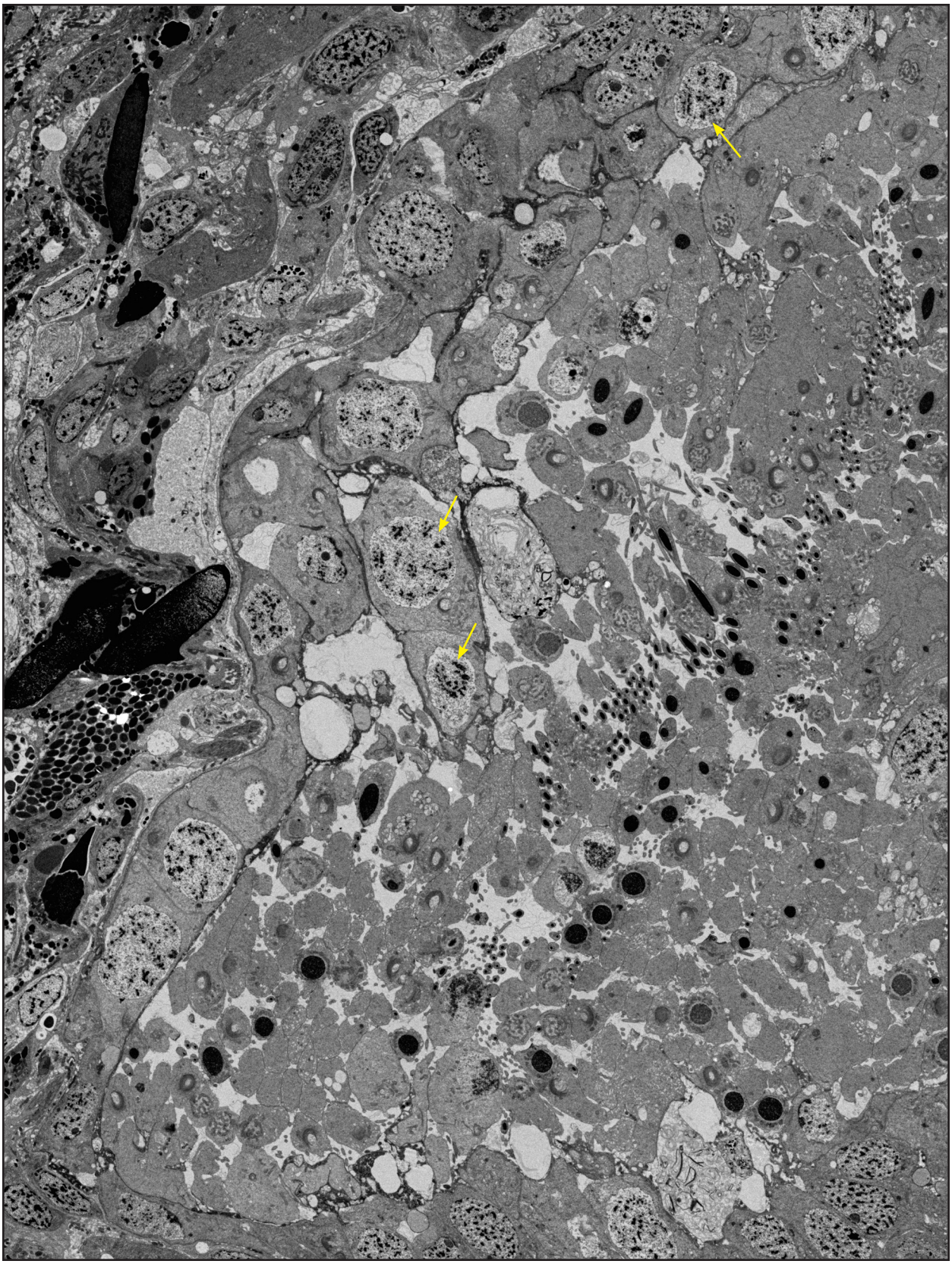

Figure 6. Transmission electron microscopy through a testis cross-section.
Pachytene nuclei that contain examples of SC figures are indicated with yellow arrows.

References

Bhalla, N., and Dernburg, A. F. (2005). A conserved checkpoint monitors meiotic chromosome synapsis in Caenorhabditis elegans. Science *310*, 1683-1686.

Blitzblau, H. G., Bell, G. W., Rodriguez, J., Bell, S. P., and Hochwagen, A. (2007). Mapping of meiotic single-stranded DNA reveals double-stranded-break hotspots near centromeres and telomeres. Curr Biol *17*, 2003-2012.

Bozza, C. G., and Pawlowski, W. P. (2008). The cytogenetics of homologous chromosome pairing in meiosis in plants. Cytogenet Genome Res *120*, 313-319.

Börner, G. V., Barot, A., and Kleckner, N. (2008). Yeast Pch2 promotes domainal axis organization, timely recombination progression, and arrest of defective recombinosomes during meiosis. Proceedings of the National Academy of Sciences *105*, 3327-3332.

Buhler, C., Borde, V., and Lichten, M. (2007). Mapping meiotic single-strand DNA reveals a new landscape of DNA double-strand breaks in Saccharomyces cerevisiae. PLoS Biol *5*, e324.

Canovai, R., Stocchino, G., Privitera, I., Alberti, A., Pala, M., and Galleni, L. (2004). Chromosome bands in freshwater triclads. Hydrobiologia 305, 85-90.

Carlton, P. M., Farruggio, A. P., and Dernburg, A. F. (2006). A link between meiotic prophase progression and crossover control. PLoS Genet *2*, e12.

Collins, J. J., Hou, X., Romanova, E. V., Lambrus, B. G., Miller, C. M., Saberi, A., Sweedler, J. V., and Newmark, P. A. (2010). Genome-wide analyses reveal a role for peptide hormones in planarian germline development. PLoS Biol *8*, e1000509.

Corredor, E., Lukaszewski, A. J., Pachón, P., Allen, D. C., and Naranjo, T. (2007). Terminal regions of wheat chromosomes select their pairing partners in meiosis. Genetics *177*, 699-706.

Franquinet, R., and Lender, T. (1972). [Ultrastructural aspects of spermiogenesis in Polycelis tenuis and Polycelis nigra (planarians)]. Zeitschrift für mikroskopisch-anatomische Forschung *86*, 481-495.

Franquinet, R., and Lender, T. (1973). [Ultrastructural study of testis of Polycelis tenuis and Polycelis nigra (Planarians). Evolution of male germ cells before spermatogenesis]. Zeitschrift für mikroskopisch-anatomische Forschung *87*, 4-22.

Fridkin, A., Penkner, A., Jantsch, V., and Gruenbaum, Y. (2008). SUN-domain and KASH-domain proteins during development, meiosis and disease. Cell Mol Life Sci.

Fukuda, T., Daniel, K., Wojtasz, L., Toth, A., and Höög, C. (2010). A novel mammalian HORMA domain-containing protein, HORMAD1, preferentially associates with unsynapsed meiotic chromosomes. Exp Cell Res *316*, 158-171.

Gold, R., Schmied, M., Giegerich, G., Breitschopf, H., Hartung, H. P., Toyka, K. V., and Lassmann, H. (1994). Differentiation between cellular apoptosis and necrosis by the combined use of in situ tailing and nick translation techniques. Lab. Invest. *71*, 219-225.

Golubovskaya, I. N., Harper, L. C., Pawlowski, W. P., Schichnes, D., and Cande, W. Z. (2002). The pam1 gene is required for meiotic bouquet formation and efficient homologous synapsis in maize (Zea mays L.). Genetics 162, 1979-1993.

Golubovskaya, I. N., Hamant, O., Timofejeva, L., Wang, C. R., Braun, D., Meeley, R., and Cande, W. Z. (2006). Alleles of afd1 dissect REC8 functions during meiotic prophase I. J Cell Sci 119, 3306-3315.

Handberg-Thorsager, M., and Saló, E. (2007). The planarian nanos-like gene Smednos is expressed in germline and eye precursor cells during development and regeneration. Dev Genes Evol *217*, 403-411.

Harper, L., Golubovskaya, I. N., and Cande, W. (2004). A bouquet of chromosomes. J Cell Sci *117*, 4025-4032.

Hermo, L., Pelletier, R., Cyr, D. G., and Smith, C. E. (2010). Surfing the wave, cycle, life history, and genes/proteins expressed by testicular germ cells. Part 1: background to spermatogenesis, spermatogonia, and spermatocytes. Microsc. Res. Tech. *73*, 241-278.

Hiraoka, Y., and Dernburg, A. F. (2009). The SUN rises on meiotic chromosome dynamics. Dev Cell *17*, 598-605.

Hyman, L. (1925). The Reproductive System and Other Characters of Planaria dorotocephala Woodworth. Trans. Amer. Micr. Soc.

Joffe, B. I., Solovei, I. V., and Macgregor, H. C. (1998). Ordered arrangement and rearrangement of chromosomes during spermatogenesis in two species of planarians (Plathelminthes). Chromosoma *107*, 173-183.

Jones, G., and Croft, J. (1989). Chromosome-Pairing and Chiasma Formation in Spermatocytes and Oocytes of Dendrocoelum-Lacteum (Turbellaria, Tricladida). A Cytogenetical and Ultrastructural Study. Heredity *63*, 97-106.

Jurka, J., Kapitonov, V. V., Pavlicek, A., Klonowski, P., Kohany, O., and Walichiewicz, J. (2005). Repbase Update, a database of eukaryotic repetitive elements. Cytogenet Genome Res *110*, 462-467.

Kobayashi, K., and Hoshi, M. (2002). Switching from asexual to sexual reproduction in the planarian Dugesia ryukyuensis: change of the fissiparous capacity along with the sexualizing process. Zool Sci *19*, 661-666.

Koszul, R., and Kleckner, N. (2009). Dynamic chromosome movements during meiosis: a way to eliminate unwanted connections? Trends Cell Biol *19*, 716-724.

Leduc, F., Maquennehan, V., Nkoma, G. B., and Boissonneault, G. (2008). DNA damage response during chromatin remodeling in elongating spermatids of mice. Biol Reprod *78*, 324-332.

Liebe, B., Petukhova, G., Barchi, M., Bellani, M. A., Braselmann, H., Nakano, T., Pandita, T. K., Jasin, M., Fornace, A., Meistrich, M. L., et al. (2006). Mutations that affect meiosis in male mice influence the dynamics of the mid-preleptotene and bouquet stages. Exp Cell Res *312*, 3768-3781.

MacQueen, A. J., Colaiacovo, M. P., McDonald, K., and Villeneuve, A. M. (2002). Synapsis-dependent and -independent mechanisms stabilize homolog pairing during meiotic prophase in C. elegans. Genes Dev *16*, 2428-2442.

Marcon, L., and Boissonneault, G. (2004). Transient DNA strand breaks during mouse and human spermiogenesis new insights in stage specificity and link to chromatin remodeling. Biol Reprod *70*, 910-918.

Negoescu, A., Lorimier, P., and Labat-Moleur, F. (1996). In situ apoptotic cell labeling by the TUNEL method: improvement and evaluation on cell preparations. J Histochem Cytochem. *44*, 959-68.

Oakley, H.A., and Jones, G. (1982). Meiosis in Mesostoma-Ehrenbergii Ehrenbergii (Turbellaria, Rhabdocoela). I. Chromosome-Pairing, Synaptonemal Complexes and Chiasma Localization in Spermatogenesis. Chromosoma *85*, 311-322.

Pandita, T. K., Westphal, C. H., Anger, M., Sawant, S. G., Geard, C. R., Pandita, R. K., and Scherthan, H. (1999). Atm inactivation results in aberrant telomere clustering during meiotic prophase. Mol Cell Biol *19*, 5096-5105.

Pellettieri, J., Fitzgerald, P., Watanabe, S., Mancuso, J., Green, D., and Sánchez Alvarado, A. (2009). Cell death and tissue remodeling in planarian regeneration. Dev Biol.

Phillips, D., Nibau, C., Ramsay, L., Waugh, R., and Jenkins, G. (2010). Development of a Molecular Cytogenetic Recombination Assay for Barley. Cytogenet Genome Res *129*, 154-161.

Roig, I., Dowdle, J. A., Toth, A., de Rooij, D. G., Jasin, M., and Keeney, S. (2010). Mouse TRIP13/PCH2 is required for recombination and normal higher-order chromosome structure during meiosis. PLoS Genet *6*.

S. mediterranea genome assembly 3.1 release notes (2006). Available at http://genome.wustl.edu/pub/organism/Invertebrates/Schmidtea_mediterannea/assembly/Schmidtea_mediterranea-3.1/ASSEMBLY.

Scherthan, H. (2007). Telomere attachment and clustering during meiosis. Cell Mol Life Sci *64*, 117-124.

Scherthan, H., Jerratsch, M., Dhar, S., Wang, Y. A., Goff, S. P., and Pandita, T. K. (2000). Meiotic telomere distribution and Sertoli cell nuclear architecture are altered in Atm- and Atm-p53-deficient mice. Mol Cell Biol *20*, 7773-7783.

Sheehan, M. J., and Pawlowski, W. P. (2009). Live imaging of rapid chromosome movements in meiotic prophase I in maize. Proceedings of the National Academy of Sciences *106*, 20989-20994.

Storlazzi, A., Gargano, S., Ruprich-Robert, G., Falque, M., David, M., Kleckner, N., and Zickler, D. (2010). Recombination proteins mediate meiotic spatial chromosome organization and pairing. Cell *141*, 94-106.

Wang, Y., Stary, J. M., Wilhelm, J. E., and Newmark, P. A. (2010). A functional genomic screen in planarians identifies novel regulators of germ cell development. Genes Dev *24*, 2081-2092.

Wang, Y., Zayas, R. M., Guo, T., and Newmark, P. A. (2007). nanos function is essential for development and regeneration of planarian germ cells. Proc Natl Acad Sci USA *104*, 5901-5906.

Wojtasz, L., Daniel, K., Roig, I., Bolcun-Filas, E., Xu, H., Boonsanay, V., Eckmann, C. R., Cooke, H. J., Jasin, M., Keeney, S., et al. (2009). Mouse HORMAD1 and HORMAD2, two conserved meiotic chromosomal proteins, are depleted from synapsed chromosome axes with the help of TRIP13 AAA-ATPase. PLoS Genet *5*, e1000702.

Zayas, R. M., Hernández, A., Habermann, B., Wang, Y., Stary, J. M., and Newmark, P. A. (2005). The planarian Schmidtea mediterranea as a model for epigenetic germ cell specification: analysis of ESTs from the hermaphroditic strain. Proc Natl Acad Sci USA *102*, 18491-18496.

Chapter III. Smed-HOP1 is required for double strand break formation, homolog pairing, synapsis, and progression through meiosis

Introduction

The axial element Hop1 was first identified in *S. cerevisiae* in a screen for mutants defective in homolog pairing (Hollingsworth and Byers, 1989). Subsequent work on Hop1 in yeast has shown that it loads onto chromosome axes early in meiosis and is required for the appropriate pairing, recombination, synapsis, and segregation of homologous chromosomes (Hollingsworth and Byers, 1989; Hollingsworth et al., 1990). In 1998, it was appreciated that Hop1 shared a region of significant homology with the DNA polymerase ζ subunit Rev7 and the spindle assembly checkpoint protein Mad2 (mitotic arrest deficient 2). These proteins all play roles in linking DNA damage recognition with subsequent checkpoint signaling, suggesting that the HORMA domain (Hop1, Rev7, Mad2) might be specifically involved in these processes (reviewed in (Aravind and Koonin, 1998)).

Meiotic homologs of Hop1 have been identified in *Arabidopsis* and maize (ASY1), *C. elegans* (HIM-3, HTP-1 -2, and -3), and mammals (HORMAD1, HORMAD2). These proteins all localize to chromosome axes but have distinct effects on other events in meiosis. For example, in *C. elegans,* disruption of *him-3* or *htp-3* causes failure in chromosome clustering, pairing, and synapsis, while conversely, disruption of the paralogous *htp-1* results in inappropriate synapsis between non-homologous chromosomes (reviewed in Colaiacovo, 2006; Goodyer et al., 2008). Furthermore, a pair of recent studies in mice have shown that *hormad1* is required to achieve wild-type levels of double strand break and crossover formation, and that *Hormad1* has independent roles in facilitating normal homolog alignment and SC formation and meiotic checkpoint signaling (Shin et al., 2010; Daniel et al., 2011). Therefore, I was interested in exploring the functions of HOP1 in *S. mediterranea*.

Results

Smed-HOP1 loads early in prophase and persists through pachytene

As discussed in Chapter II, I identified the HORMA domain-containing protein Smed-HOP1 (mk4.001053.01) by a BLAST search of the *S. mediterranea* genome with the *S. cerevisiae* Hop1 protein sequence (alignment shown in Figure 1). We generated an antibody to this protein, and I examined its localization in cryosections.

As shown in Figure 1B, HOP1 appears on meiotic chromosomes very early in MI prophase, approximately concomitant with or slightly before bouquet formation. Interestingly,

HOP1 staining appears weaker near the bouquet in some zygotene nuclei. This may suggest that the HOP1 protein in this region of the nucleus is temporarily removed from axes. However, Smed-HOP1 appears to be stronger and more contiguous on all chromosomes in pachytene nuclei, indicating that it is not permanently removed from axes upon synapsis (in contrast to Hormad1 and Hormad2 in mouse; Wojtasz et al., 2009; Fukuda et al., 2010). Alternatively, HOP1 may be transiently modified in a way that alters its antigen availability, or that the local environment of the axis may be modified for a short period during meiotic prophase such that our HOP1 epitope is masked (e.g., Golubovskaya et al. 2006).

RNAi of Smed-hop1 disrupts homolog pairing, synapsis, and DSB formation

Based on the diverse roles that Hop1 homologs play in homolog pairing, programmed DNA double strand break formation, SC formation, and meiotic checkpoint signaling, I was interested in studying the effect of HOP1 depletion in *S. mediterranea*. Strikingly, *hop1(RNAi)* caused a dramatic shift in the proportion of nuclei in each stage of meiotic prophase, and mature spermatids were not observed (Fig. 2A). In wild-type testes, approximately 22% of all nuclei displayed a pachytene-like (synapsed) chromosome morphology. This was never observed in *hop1(RNAi)* testes ($p<0.001$), indicating a complete failure of synapsis (Fig. 2A,D). Probably as a direct consequence, the proportion of nuclei with leptotene/zygotene morphology was greatly elevated (70% of all nuclei vs. 40% in wild type; $p<0.001$, Fig. 2D). These results indicate that HOP1 is required for SC loading and progression through meiosis, and that the absence of HOP1 leads to meiotic arrest and the accumulation of nuclei in early prophase.

Bouquet formation and the accompanying redistribution of SUN1 were not affected by HOP1 knockdown (Fig. 2B), indicating that HOP1 is unlikely to be required for chromosome attachment to the nuclear envelope or for reorganization, and also that axes must be at least somewhat functional in *hop1(RNAi*), in contrast to what has been described for other components of meiotic chromosome axes (Liebe et al., 2004; Golubovskaya et al., 2006). Indeed, telomere bouquets sometimes appeared more tightly clustered in *hop1(RNAi)* animals. However, homolog pairing at centromeric loci was not observed in animals lacking *hop1* function. FISH experiments showed that CEN-2 foci remain separated in most spermatocytes, even those with a telomere bouquet (Fig. 2C). This indicates that HOP1 is required to achieve stable homolog pairing in *S. mediterranea*. The distances between CEN-2 foci are somewhat larger in *hop1(RNAi)* than in wild-type (2.58 ± 1.3 μm vs. 2.09 ± 0.99 μm; $p=0.004$, Fig. 2E), indicating that although the bouquet appears to form normally, distal loci may be slightly more dispersed in *hop1(RNAi)*. This may be similar to the alignment defects observed in *Hormad1-/-* mice (Daniel et al., 2011).

HOP1 knockdown also disrupted normal DSB dynamics. Few or no RAD51 foci were observed in *hop1(RNAi)* spermatocytes (Fig. 3A). However, abundant RAD51 foci were detected following irradiation of *hop1(RNAi)* animals (Fig. 3B), indicating that RAD51 can still be

recruited to DSBs even when HOP1 is not present on axes. Together, these results strongly indicate that HOP1 is required for DSB formation in *S. mediterranea*. (These experiments were performed by Youbin Xiang and analyzed jointly; manuscript in preparation).

Mature spermatids are not produced, but apoptosis is not obviously elevated, in hop1(RNAi)

Consistent with the apparent arrest of meiosis prior to synapsis, mature spermatids were never observed in *hop1(RNAi)* testes. DAPI-bright bodies resembling immature spermatids were sometimes observed, but were less abundant than in wild type. This suggests the presence of some culling mechanism, possibly induced by the presence of axes lacking SC, that prevents cells with inappropriately synapsed nuclei from developing into mature spermatids and removes them from the testes. I attempted to quantify apoptosis in the testes of these animals using TUNEL (Fig. 4). Analyses of 640 testis sections in seven animals revealed one or more apoptotic nuclei in roughly 10% of testes lobes, but never any massive or widespread TUNEL staining of spermatocytes. Due to the variable sizes/stages of testes in *S. mediterranea*, as well as the variable numbers of TUNEL-positive nuclei observed from animal to animal in wild-type, it is not possible to quantitatively compare the level of apoptosis in *hop1(RNAi)* to that in wild-type testes, but the data do not suggest a gross elevation of apoptosis in *hop1(RNAi)*. These data also show that apoptosis is not blocked in *hop1(RNAi)*.

Discussion

Studies in many systems suggest that HORMA domain-containing axial element proteins have three critical and at least partly independent functions in meiosis. First, they promote double strand break formation (and possibly other early steps in recombination), second, they facilitate SC central element loading and polymerization, and third, they contribute to checkpoint mechanisms that inhibit progression through meiosis in the presence of errors. The absence of DSB formation, failure of homolog pairing, and failure of SC loading and progression through meiosis seen in *Smed-hop1(RNAi)* suggest that these functions are conserved in *S. mediterranea*.

One interesting aspect of the *Smed-hop1(RNAi)* phenotype is the moderately increased distance between CEN-2 foci in *hop1(RNAi)* compared to similarly staged wild-type spermatocytes, showing a failure of homolog pairing and alignment despite the robust and persistent formation of the bouquet. This might be partly attributed to defects in DSB formation, since recombination intermediates are known to facilitate the homology search and alignment of homologs in many organisms. However, given that RAD51 foci concentrate near the bouquet in wild-type, it is unclear to what degree recombination intermediates promote alignment further away from telomeres. Another attractive possibility is that HOP1 is required to initiate or propagate the polymerization of the synaptonemal complex, and that this is required to stabilize

homolog pairing at interstitial loci, as in *C. elegans*. Although the chromosome axes in *hop1 (RNAi)* are at least somewhat functional, as they allow progression through the bouquet stage, it is quite plausible that the depletion of HOP1 could cause general axis assembly defects. Any such failure to recruit or properly organize axis components could potentially affect chromosome pairing and alignment and/or SC loading in a DSB-independent manner.

In general, it is not clear whether the primary defect in *hop1(RNAi)* is its failure to generate DSBs or whether HOP1 has independent roles in homolog pairing and alignment, SC formation, or meiotic progression. Daniel and colleagues (Daniel et al., 2011) recently demonstrated that defects in SC formation and γH2AX accumulation on unsynapsed chromosomes were more severe in a *Hormad1 -/- Spo11-/-* double mutant than in a *Spo11-/-* single mutant (which completely lacks DSBs), suggesting that Hormad1 promotes SC formation independent of its role in DSB formation. In the future, it would be interesting to see whether ectopic DSB generation can at least partially rescue any of the defects that are observed in *hop1 (RNAi)*. No increase in homolog pairing or progression through meiosis were observed in our X-irradiation experiments, but it is possible that rescue might be seen at different dosages or recovery times.

Conclusions

This analysis demonstrates a critical role for Smed-HOP1 in DSB formation and subsequent homolog pairing, alignment and meiotic progression (i.e., synapsis). Future studies may uncouple these roles or demonstrate that DSBs are specifically required for alignment and synapsis in *S. mediterranea.*

Materials and methods - see Chapter VI.

A.

```
ScHop1/1-263          1 MSNKQLVKPKTE--------TKTEITTE-QSQKLLQTMLTMSFGCLAFLRGLFPDDIFVDQRFVPEKVEKNYNKQ 66
SmHop1/1-269          1 MPVALLTKEKTW-----SKMFPTIFTTEQQSLVFMKKLFAVAISNIVYIRSIFPEYAFFDKHL---------- 58
HsHORMAD1/1-240       1 MATAQLQRTPMS-----ALVFPNKISTEHQSLVLVKRLLAVSVSCITYLRGIFPECAYGTRYL---------- 58
MmHormad1/1-241       1 MATMQLQRTASL----SALVFPNKISTEHQSLMFVKRLLAVSVSCITYLRGIFPERAYGTRYL---------- 59
HsHORMAD2/1-248       1 MATAQLSHCITIHKASKETVFPSQITNEHESLKMVKKLFATSISCITYLRGLFPESSYGERHL---------- 63
MmHormad2/1-246       1 MATAQLSHNTRTLKASKNTIFPSQVTNEHESLVVVKKLFATCISCITYLRGLFPESSYRDRRL---------- 63

ScHop1/1-263         67 NTSQNNSIKIKTLIRGKSAQADL-LLDWLEKGVFKSIRLKCLKALSLGIF--LEDPTDLLENYIFSFDYDEENNV 138
SmHop1/1-269         59 -----EGIKLKILREDSKCPGASKVINWVR-GCFDALDRHYLKAVVIGFYTDIKDPDTVIESYSFKFTYGQD--- 124
HsHORMAD1/1-240      59 -----DDLCVKILREDKNCPGSTQLVKWML-GCYDALQKKYLRMVVLAVYTNPEDPQTISECYQFKFKYTNN--- 124
MmHormad1/1-241      60 -----DDLCVKILKEDKNCPGSSQLVKWML-GCYDALQKKYLRMIILAVYTNPGDPQTISECYQFKFKYTKN--- 125
HsHORMAD2/1-248      64 -----DDLSLKILREDKKCPGSLHIIRWIQ-GCFDALEKRYLRMAVLTLYTDPMGSEKVTEMYQFKFKYTKE--- 129
MmHormad2/1-246      64 -----DDLSLKILREDKKCPGSLHIIKWIQ-GCFDALEKRYLHMAVLTLYTNPKEPEKVTEIYQFRFKYTKK--- 129

ScHop1/1-263         139 NINVNLSGNKKGS----------KNADPENETISLLD----SRRMVQQLMRRFIIITQSLEPLPQKKFLTMRLMF 199
SmHop1/1-269         125 SVSVKLDNTSKTELVLKIRTNYYSYSSGLEAVIKNDDAPETIKKSTLSLLRTLILAGNTQDPLPEKVFVTMKLLY 199
HsHORMAD1/1-240      125 GPLMDFI--SKNQ----------SNESSMLS-----TD-----TKKASILLIRKIYILMQNLGPLPNDVCLTMKLFY 179
MmHormad1/1-241      126 GPIMDFI--SKNQ----------NNKSSTTS-----AD-----TKKASILLIRKIYVLMQNLGPLPNDVCLTMKLFY 180
HsHORMAD2/1-248      130 GATMDFDSHSSST----------SFESGTNN-----ED-----IKKASVLLIRKLYILMQDLEPLPNNVVLTMKLHY 186
MmHormad2/1-246      130 GTTMDFD--SSST----------SFESGTDS-----ED-----IKKACSLLIRQLYILMQNLGPLPNDVILTMKLHY 184

ScHop1/1-263         200 NDNVD-EDYQPELFKDATFDKR-ATLKVPTNLDNDAIDVGTLNTKHHKVA---------LSVLSAATSSMEKAGN 263
SmHop1/1-269         200 YDEITPDDYEPNGFRTCDYAGF-RHETETINA-----KLGHVETPEFEKENETPVLNETRKITPNCSRTCSEEEF 268
HsHORMAD1/1-240      180 YDEVTPPDYQPPGFKDGDCEGV-IFEGEPMYL-----NVGEVSTPFHIFK---------VKVTTERERMENIDST 239
MmHormad1/1-241      181 YDEVTPPDYQPPGFKDGDCEGV-IFDGDPTYL-----NVGEVPTPFHTFR---------LKVTTEKERMENIDST 240
HsHORMAD2/1-248      187 YNAVTPHDYQPLGFKEGVNSHFLLFDKEPINV-----QVGFVSTGFHSMK---------VKVMTEATKVIDLENN 247
MmHormad2/1-246      185 YNSVTPHDYQPPGFKEAVNSHFLLFEGEPVSL-----RMGSVSSGFHSMK---------VKVTTEATRMLDGENS 245
```

B.

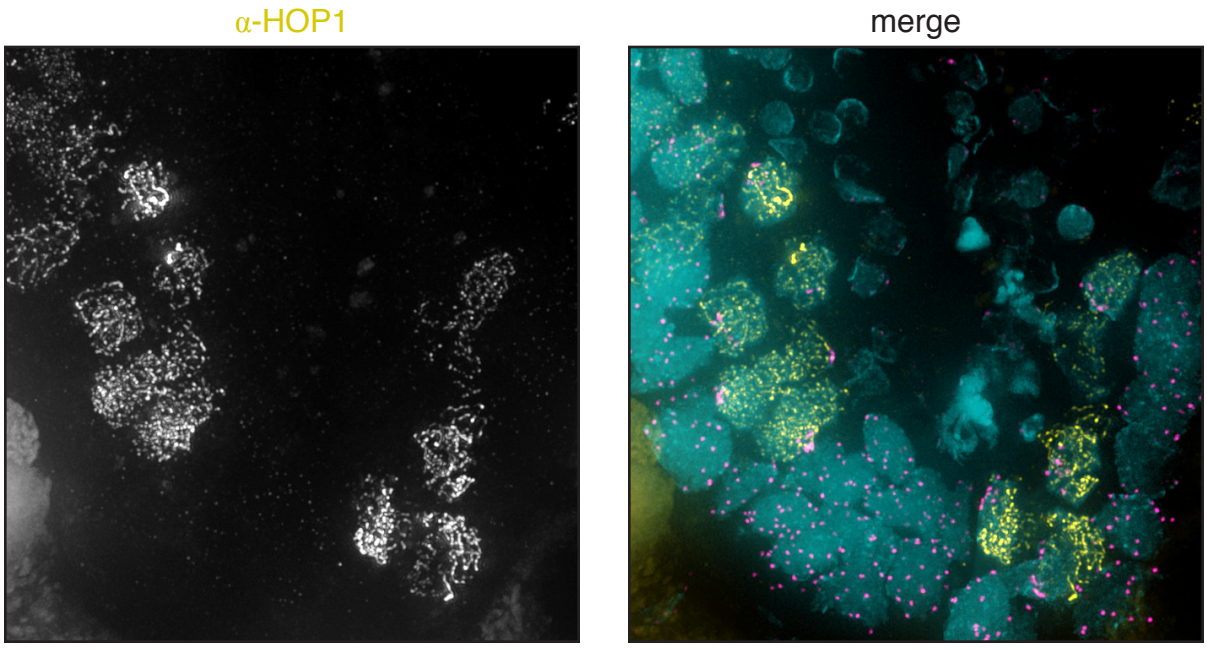

Figure 1. Identification of Smed-HOP1 and its localization in spermatocytes.
(A) CLUSTALW alignment of the HORMA domains of the *S. mediterranea* HOP1 protein with *S. cerevisiae* Hop1 and the mouse and human HORMAD proteins. **(B)** HOP1 localizes to chromosome axes in spermatocytes, prior to the formation of the bouquet. α-HOP1 staining is weaker near the telomeres in a subset of zygotene spermatocytes but remains localized to axes in pachytene nuclei. Yellow, α-HOP1; pink, telomere FISH; blue, DAPI. (More examples of α-HOP1 staining in spermatocytes are shown in Figure 3 of Chapter II.)

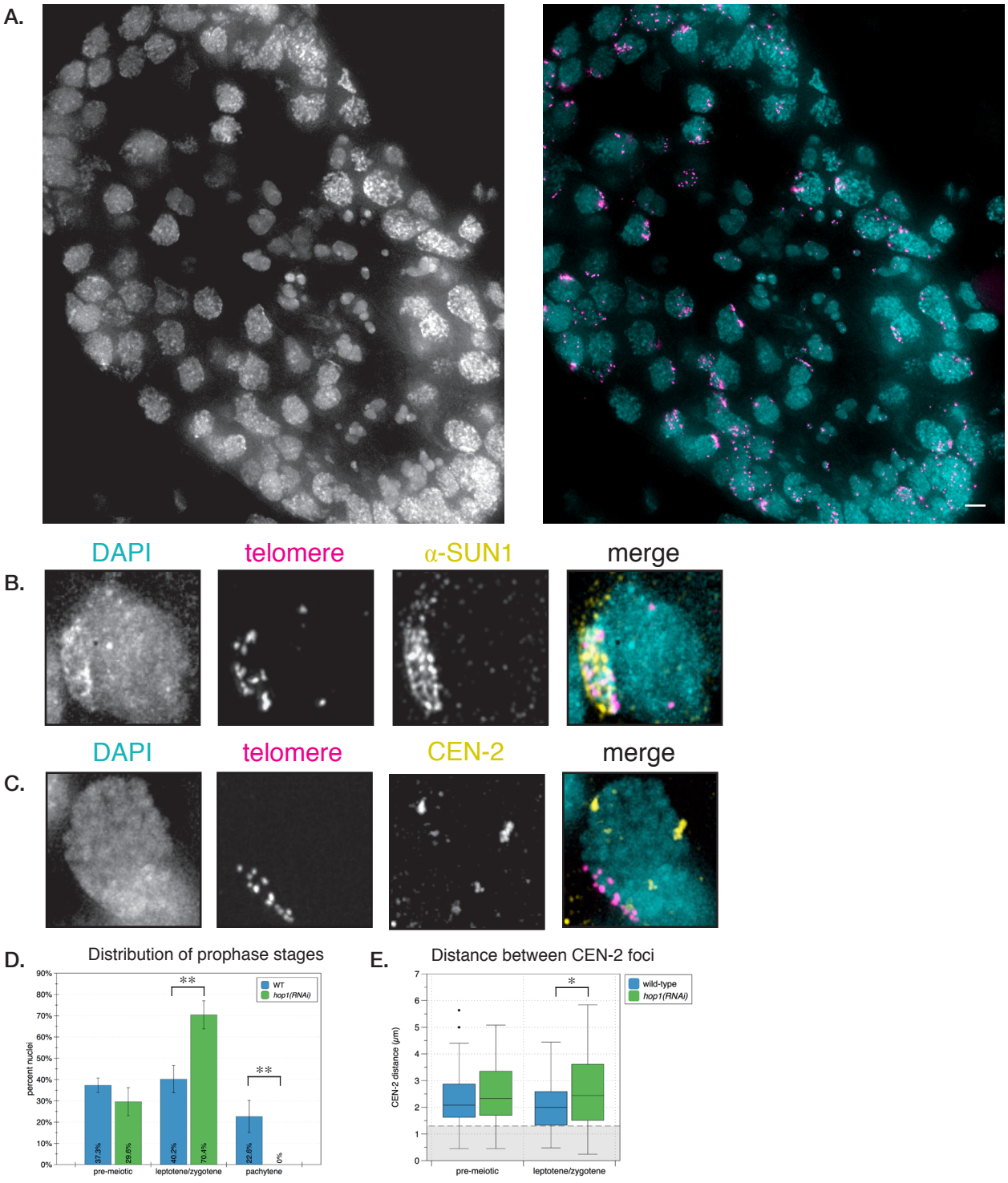

Figure 2. RNAi of *Smed-hop1* disrupts homolog pairing and causes arrest prior to synapsis.
(A) Testis section showing the absence of pachytene-stage nuclei and mature spermatids in *hop1(RNAi)* testes. Pink, telomere FISH; blue, DAPI. Scale bar = 5μm. **(B)** Bouquet formation and SUN1 protein localization are normal in *hop1(RNAi)*. **(C)** Homologous chromosomes do not pair in *hop1(RNAi)*. CEN-2 loci remain well-separated in zygotene nuclei. **(D)** Distribution of prophase stages in WT vs. *hop1(RNAi)*, suggesting meiotic arrest prior to pachytene (i.e., SC formation). **p<0.001. **(E)** Measurement of the distances between CEN-2 foci shows that these loci remain well separated in *hop1(RNAi)* and may be less closely juxtaposed than in wild-type leptotene/zygotene stage spermatocytes. *p≤0.005.

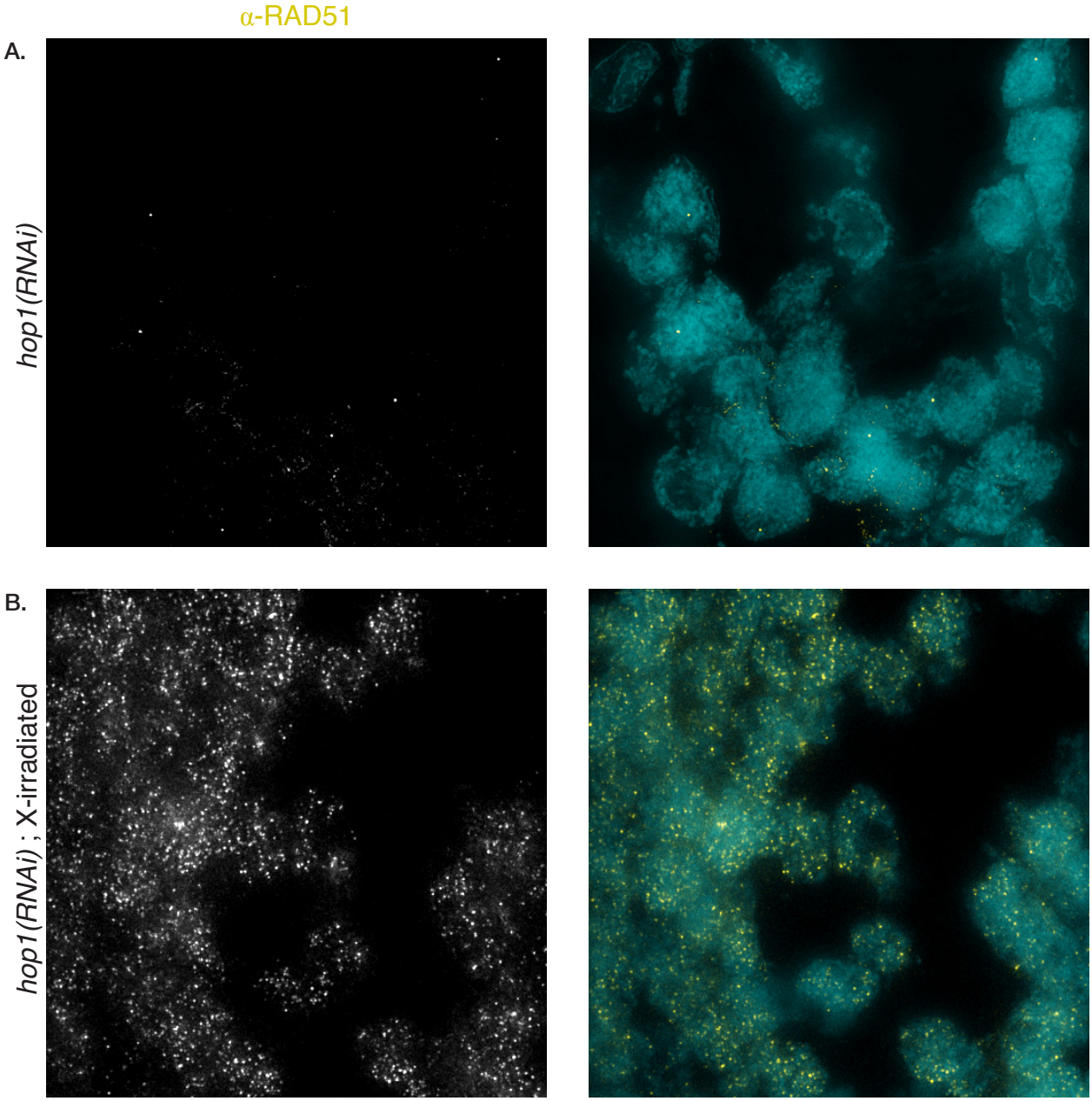

Figure 3. Smed-HOP1 is required for double strand break formation.
(A) Testis section showing the absence of RAD51 foci in *hop1(RNAi)* spermatocytes. **(B)** Testis section showing that RAD51 focus formation in *hop1(RNAi)* spermatocytes is rescued by X irradiation (10 Gy). Datasets courtesy of Youbin Xiang, Stowers Institute.

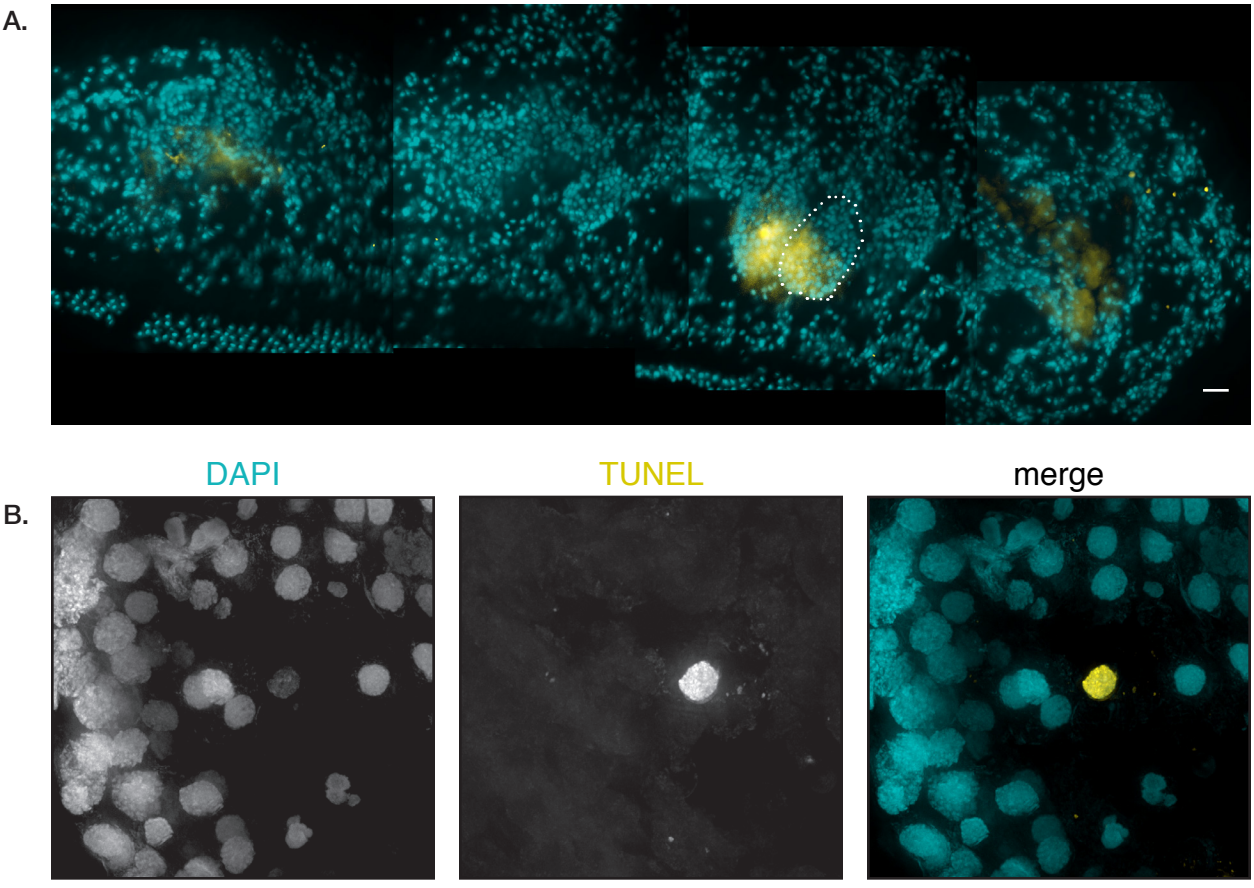

Figure 4. TUNEL staining of apoptosis in *hop1(RNAi)* testes.
(A) TUNEL staining of a longitudinal section of a *hop1(RNAi)* animal. The TUNEL-positive nuclei at the amputation site (far right) serve as a positive control. A single testis is outlined in white. Blue, DAPI; yellow, TUNEL. Scale bar = 50µm. **(B)** TUNEL-positive spermatocytes can be observed in some *hop1(RNAi)* testes. Scale bar = 5µm. **(C)** Quantification of TUNEL staining in wild-type demonstrates variability from animal to animal, and shows that germline apoptosis is not grossly elevated in *hop1(RNAi)*. n=620 testis sections from 7 animals.

References

Aravind, L., and Koonin, E. V. (1998). The HORMA domain: a common structural denominator in mitotic checkpoints, chromosome synapsis and DNA repair. Trends Biochem Sci *23*, 284-286.

Colaiacovo, M. P. (2006). The many facets of SC function during C. elegans meiosis. Chromosoma *115*, 195-211.

Daniel, K., Lange, J., Hached, K., Fu, J., Anastassiadis, K., Roig, I., Cooke, H. J., Stewart, A. F., Wassmann, K., Jasin, M., et al. (2011). Meiotic homologue alignment and its quality surveillance are controlled by mouse HORMAD1. Nat Cell Biol.

Fukuda, T., Daniel, K., Wojtasz, L., Toth, A., and Höög, C. (2010). A novel mammalian HORMA domain-containing protein, HORMAD1, preferentially associates with unsynapsed meiotic chromosomes. Exp Cell Res *316*, 158-171.

Golubovskaya, I. N., Hamant, O., Timofejeva, L., Wang, C. R., Braun, D., Meeley, R., and Cande, W. Z. (2006). Alleles of afd1 dissect REC8 functions during meiotic prophase I. J Cell Sci *119*, 3306-3315.

Goodyer, W., Kaitna, S., Couteau, F., Ward, J. D., Boulton, S. J., and Zetka, M. (2008). HTP-3 links DSB formation with homolog pairing and crossing over during C. elegans meiosis. Dev Cell *14*, 263-274.

Hollingsworth, N. M., Goetsch, L., and Byers, B. (1990). The HOP1 gene encodes a meiosis-specific component of yeast chromosomes. Cell *61*, 73-84.

Hollingsworth, N. M., and Byers, B. (1989). HOP1: a yeast meiotic pairing gene. Genetics *121*, 445-462.

Liebe, B., Alsheimer, M., Höög, C., Benavente, R., and Scherthan, H. (2004). Telomere attachment, meiotic chromosome condensation, pairing, and bouquet stage duration are modified in spermatocytes lacking axial elements. Mol Biol Cell *15*, 827-837.

Shin, Y., Choi, Y., Erdin, S. U., Yatsenko, S. A., Kloc, M., Yang, F., Wang, P. J., Meistrich, M. L., and Rajkovic, A. (2010). Hormad1 mutation disrupts synaptonemal complex formation, recombination, and chromosome segregation in mammalian meiosis. PLoS Genet *6*, e1001190.

Wojtasz, L., Daniel, K., Roig, I., Bolcun-Filas, E., Xu, H., Boonsanay, V., Eckmann, C. R., Cooke, H. J., Jasin, M., Keeney, S., et al. (2009). Mouse HORMAD1 and HORMAD2, two conserved meiotic chromosomal proteins, are depleted from synapsed chromosome axes with the help of TRIP13 AAA-ATPase. PLoS Genet *5*, e1000702.

Chapter IV. Smed-SUN1 is required for bouquet formation, homolog pairing, and homologous synapsis

Introduction

One event of meiotic prophase that is conserved across nearly all organisms is the connection of chromosome ends inside the nucleus to the cytoskeleton through factors within the nuclear envelope. This attachment is important for the subsequent reorganization of chromosomes within the nucleus, which in turn promotes homolog pairing, recombination, synapsis, and successful completion of meiotic prophase. In many organisms, including *S. mediterranea,* chromosomes adopt a stereotypical bouquet conformation with telomeres clustered together near the centrosome/SPB at one region of the nuclear envelope (Scherthan, 2007), but the function of this arrangement remains enigmatic. It has long been assumed that the bouquet facilitates the chromosome homology search by bringing chromosomes into a rough alignment. However, another emerging view is that the bouquet conformation may simply be a byproduct of cytoskeletal organization, and that chromosome movement is the key factor that enables homolog alignment and other events of meiotic prophase (Bhalla and Dernburg, 2008; Koszul and Kleckner, 2009).

SUN domain (Sad1/UNC-84 homology) proteins, which reside in the inner nuclear envelope, have been implicated in meiotic chromosome dynamics in many organisms, but the effects of SUN protein deletion or knockdown vary across species. In *S. cerevisiae*, Mps3 is essential for for spindle pole body (SPB) function during mitosis, and therefore for viability. However, a deletion within the N-terminal nucleoplasmic domain that supports mitotic division but disrupts Mps3 binding to the meiosis-specific telomere binding protein Ndj1 results in failure of meiotic bouquet formation, delays in homolog pairing and synapsis, and modest defects in recombination and chromosome segregation (Conrad et al., 2007). Similarly, Sad1 in *S. pombe* is essential for SPB function, but the disruption of meiosis-specific Sad1-telomere interactions by mutation of the meiosis-specific proteins Bqt1 or Bqt2 abrogates the characteristic “horsetail” movement of the chromosomes during meiotic prophase. This leads to delays in homolog pairing and recombination as well as to an increase in ectopic recombination (Tang et al. 2006, Chikashige et al., 2006; Davis and Smith, 2006). In *C. elegans,* Pairing Centers remain associated with the nuclear envelope in a *sun-1* null background, but the loss of SUN-1 function leads to inappropriate pairing and synapsis between non-homologous chromosomes, elevated apoptosis, and the production of aneuploid gametes (Penkner et al., 2007; Sato et al., 2009; Penkner et al., 2009). In *Sun1-/-* mice, telomeres are disconnected from the nuclear envelope, leading to the failure of homolog pairing and recombination, incomplete loading of the central element protein SYCP1, and extensive apoptosis (Ding et al., 2007). A second SUN domain protein, Sun2, is also redistributed to sites of chromosome attachment to the nuclear envelope

during meiosis in mice (Schmitt et al., 2007), although the roles of Sun2 in chromosome tethering and/or motility have not been tested directly.

Based on these observations, the current model for SUN protein function in meiosis in all systems is that these proteins mediate the attachment of telomeres to the cytoskeleton through the nuclear envelope, and that the resulting transduction of force from the cytoskeleton to the chromosomes is important for normal chromosome dynamics, homolog pairing, SC polymerization, and recombination (reviewed in Hiraoka and Dernburg, 2009). However, the variability of meiotic phenotypes observed upon SUN protein disruption suggests that these proteins may play somewhat different roles in different systems.

Results

The identification of SUN domain proteins in S. mediterranea

Based on the known involvement of SUN proteins in meiotic chromosome dynamics in other organisms, I wanted to determine whether SUN domain-containing proteins might play a role in bouquet formation and chromosome pairing in *S. mediterranea*. As described in Chapter II, I conducted a BLAST search in SmedGD with a consensus SUN domain and retrieved three genes (mk4.001469.07.01, mk4.001275.01.01, and mk4.003039.01.01), designated as *Smed-sun1, Smed-sun2*, and *Smed-sun3*, respectively. An alignment of these proteins with the SUN domain from the *M. musculus* Sun1 protein and an unrooted tree showing the relationships between SUN domains from several organisms are shown in Figure 1A and 1B. I initially chose to focus on *Smed-sun1* because it was the best annotated of the three SUN domain containing genes and also had the strongest homology to the *C. elegans* SUN-1 protein.

We generated an antibody specific to Smed-SUN1. Immunofluorescence to tissue cryosections showed that it is widely expressed in many cell types. In epidermal cells and mesenchymal cells, for example, SUN1 staining could be seen throughout the nuclear envelope (Fig. 1C). In spermatocytes, however, SUN1 concentrates dramatically within one region of the nuclear envelope, corresponding to the bouquet (Fig. 1D). Unlike other SUN proteins that have been implicated in chromosome attachment to the nuclear envelope during meiosis, Smed-SUN1 did not co-localize exclusively with chromosome ends. However, its clear enrichment in a domain surrounding the telomeres strongly suggests a role in meiotic chromosome dynamics.

RNAi of Smed-sun1 disrupts bouquet formation and homolog pairing and results in non-homologous synapsis

RNAi targeting *Smed-SUN1* completely disrupted both bouquet formation and homolog pairing (Fig. 2A). Nevertheless, telomeres remained localized to the nuclear envelope in the absence of detectable SUN1 protein, even after several months of RNAi feeding. RNAi targeting the other two SUN domain-containing genes did not have any obvious effects on meiosis or in somatic tissues, nor were the defects observed in *sun1(RNAi)* enhanced or rescued in *sun1;sun2 (RNAi)*, *sun1;sun3(RNAi)* or even *sun1;sun2;sun3(RNAi)* animals (data not shown).

Despite the disruption of the bouquet, SC formation still occurred in *sun1(RNAi)* spermatocytes. HOP1 staining appeared normal, indicating that axial element loading occurs independently of SUN1 function (Fig. 2B). Nuclei with pachytene-like chromosome morphology and unpaired homologs were frequently observed in *sun1(RNAi)* testes (Fig. 2C,D). In wild-type animals, the average distance between FISH signals corresponding to the centromeric locus on Chromosome II (CEN-2) was markedly lower in pachytene than in earlier stages, but in *sun1 (RNAi),* the average distance between CEN-2 foci was actually slightly greater in pachytene-like nuclei (2.87 ± 1.18 μm vs. 2.24 ± 1.05 μm in leptotene/zygotene; p=0.017, Fig. 2F). CEN-2 signals were paired (≤1.3 μm apart) in only 3% of these nuclei (1/38), indicating widespread non-homologous synapsis. Independent DNA FISH experiments with a probe that recognizes the rDNA locus at one end of Chr. II also showed two well-separated foci in 96% of pachytene stage nuclei (31/33), further indicating inappropriate SC loading between non-homologs (Fig. 2D).

I observed a slightly elevated proportion of spermatocyte nuclei with leptotene/zygotene-like chromosome morphology in *sun1(RNAi)* animals (48% vs. 40% in wild type, p=0.039, Fig. 2G), suggesting that synapsis may be slightly delayed in the absence of homolog pairing and bouquet formation. However, a significant proportion of spermatocyte nuclei in *sun1(RNAi)* animals displayed pachytene-like morphology (20% vs. 22% in wild type, p=0.706, Fig. 2G), indicating that SC formation was not abrogated. To confirm this observation, I also assessed SC formation by transmission electron microscopy in thin sections from wild-type and *sun1(RNAi)* animals (>2 months from first feeding). Synaptonemal complexes were clearly observed in the spermatocytes of both animals (Fig. 2E), reinforcing the conclusions based on fluorescence imaging. Taken together, these results indicate that extensive non-homologous synapsis occurs in *sun1(RNAi)* spermatocytes.

It is not clear whether this aberrant central element loading occurs between sister chromatids, between non-homologous chromosomes (e.g., Chr. I synapsing with Chr. II) or between folded over chromosomes. I observed greater numbers of distinct telomere FISH foci in *sun1(RNAi)* pachytene nuclei compared to wild-type (Fig. 2H; 13.8 ± 1.7 vs. 8.4 ± 0.7; p<0.0001), which does not confirm or rule out any of the possibilities presented above, but does indicate that if SC is formed between non-homologous or folded over chromosomes they cannot be fully aligned from end to end. Meanwhile, the observation of synapsed chromosomes with a

CEN-2 or rDNA focus on one side of the SC but not the other (e.g., Fig. 2C) and the comparable widths of pachytene chromosomes in wild-type and *sun1(RNAi)* argues against inter-sister synapsis.

Co-depletion of HOP1 and SUN1 disrupts bouquet formation, pairing, and synapsis

As described above, the loss of SUN1 function resulted in promiscuous synapsis between nonhomologous chromosomes. In *C. elegans*, it has been suggested that the nonhomologous synapsis seen in *sun-1* mutants may be evidence that SUN-1 or SUN-1 dependent chromosome motion is important for inhibiting SC loading between inappropriate partners (Sato et al., 2009). To better characterize the possible role of SUN1 in monitoring pairing and/or licensing synapsis in *S. mediterranea*, I investigated the consequences of depleting SUN1 in a *hop1(RNAi)* background, in which synapsis does not occur (see Chapter III).

The spermatocytes in *sun1(RNA);hop1(RNAi)* animals exhibited a combination of the defects observed following individual knockdowns. Bouquet formation and chromosome pairing were disrupted, as in *sun1(RNAi)* animals, and no nuclei with pachytene-like morphology were observed, as in *hop1(RNAi)* (Fig. 3). Distances between CEN-2 foci were similar in leptotene/zygotene stage nuclei in *sun1(RNAi)* and *sun1;hop1(RNAi)*. This indicates that SUN1 function is not required to prevent SC loading in the absence of recombination and pairing in *hop1(RNAi)*. Conversely, this result also suggests that recombination intermediates or other HOP1 dependent structures are required for the non-homologous synapsis observed in *sun1(RNAi)*.

Maverick chromosomes are occasionally observed in sun1(RNAi) *spermatocytes*

The disruption of the bouquet and homolog pairing in *sun1(RNAi)* spermatocytes is occasionally accompanied by the appearance of “maverick” chromosomes, which seem to be pulled out of the nucleus (Fig. 4). A telomere FISH signal is always observed at the end of these chromosomes, indicating that the mavericks are telomere-led. Similar events have been seen transiently in live imaging of budding yeast, maize, and *C. elegans,* where they have been shown to be cytoskeleton-dependent (Koszul et al., 2008; Sheehan and Pawlowski, 2009, Wynne et al. submitted). Interestingly, it is sometimes possible to observe >1 chromosome/telomere within the same maverick (Fig. 4B).

Mavericks tend to co-occur in multiple spermatocytes in the same animal and are only observed in animals fixed after short periods of RNAi feeding (~2 weeks from first feeding). This suggests that they probably occur within a specific window of *sun1* knockdown, when SUN1 protein has been depleted to a certain level but is not completely absent. Thus, it seems likely that the mavericks represent a dysregulation of the pulling force that is normally exerted on chromosome ends during prophase. Unfortunately, SUN1 depletion via RNAi cannot be

controlled finely enough to confirm this hypothesis, and the difficulty of reliably reproducing the conditions necessary for maverick formation has precluded their further investigation.

Mature spermatids are not produced in sun1(RNAi) testes

Despite the apparent progression of meiosis through at least pachytene, mature spermatids were never observed in *sun1(RNAi)* testes, and immature spermatids were also less abundant than in wild type. This suggests the presence of some culling mechanism, possibly induced by unresolved DNA damage, that prevents cells with inappropriately synapsed nuclei from developing into mature spermatids and removes them from the testes. I attempted to quantify apoptosis in the testes of these animals using TUNEL (Fig. 5). Analyses of 140 testis sections in two animals revealed one or more apoptotic nuclei in roughly 20% of testes lobes, but I did not observe massive or widespread TUNEL staining, as is seen in *Sun1-/-* mice. Due to the small numbers of apoptotic nuclei relative to the total number of spermatocytes, as well as the variable sizes (and possibly stages) of testes in *S. mediterranea*, I was unable to quantitatively compare the level of apoptosis in *sun1(RNAi)* to that in wild-type testes. However, the limited analysis that was possible did show that apoptosis is not blocked and is consistent with a slight elevation of programmed cell death in *sun1(RNAi)*. Similar levels of apoptosis were seen in *sun1;hop1(RNAi)*, suggesting that if apoptosis is increased, it is likely not dependent on DSB formation and/or the presence of HOP1.

Discussion

The role of *Smed-sun1* in meiosis seems to be analogous to that of SUN proteins in other organisms, in that it is required for normal chromosome dynamics during meiotic prophase. However, it is interesting that its localization in prophase spermatocytes is relatively diffuse. SUN proteins colocalize tightly with telomeres in *S. pombe*, *S. cerevisiae*, and *M. musculus*, and with chromosome Pairing Centers in *C. elegans*. In contrast, Smed-SUN1 appears to localize not only to telomeres but also to a broad region surrounding the bouquet. Furthermore, telomeres appear to remain localized to the nuclear envelope in *sun1(RNAi)* spermatocytes. This suggests that the depletion of SUN1 by RNAi does not completely disrupt telomere attachment to the nuclear envelope, and that this attachment (mediated by a different, as-yet unidentified factor) is not sufficient for bouquet formation. Thus, Smed-SUN1 may have a specific function in connecting meiotic chromosomes to the cytoskeleton and organizing them within the nuclear envelope. This would be similar to the apparent meiotic roles of SUN-1 in *C. elegans*, Mps3 in *S. cerevisiae*, and Sad1 in *S. pombe*, but distinct from Sun1 in mouse. My observation of maverick chromosomes in some *sun1(RNAi)* spermatocytes after short RNAi feedings are consistent with a model in which a high level of SUN1 protein, perhaps the critical concentration required for

SUN1 aggregation, is necessary for chromosome organization in the bouquet, but that a somewhat lower level of SUN1 protein is sufficient to maintain an association between the chromosome and the cytoskeleton; this association generates mavericks in the absence of stabilizing SUN1 aggregation.

Despite the disruption of bouquet formation and homolog pairing in *sun1(RNAi)* animals, synapsis is not abrogated, although it may be somewhat delayed. The observation of nuclei with pachytene-like morphology and clearly unpaired centromeric and rDNA loci indicates that *sun1 (RNAi)* causes non-homologous synapsis, similar to what is seen in *C. elegans*, rather than simply reducing or delaying the appropriate inter-homolog interactions, as is observed in *S. cerevisiae* and in mice. It is unclear whether this aberrant synapsis represents foldover synapsis, SC loading between sister chromatids, or synapsis of non-homologous chromosomes, although the average of ~14 distinct telomere foci observed in *sun1(RNAi)* pachytene nuclei indicates that if the central element loads between folded over or non-homologous chromosomes, these chromosomes cannot be fully aligned from end to end. It should also be pointed out that, as SC formation cannot yet be directly visualized with fluorescence microscopy, it is possible that nuclei I presume to be completely synapsed based on chromosome morphology may actually lack SC at some loci; this should be clarified in future work. Nonetheless, this result indicates that homolog pairing is not absolutely required for SC formation or, alternatively, that *sun1* is required for the function of some barrier to SC loading between unpaired chromosomes in addition to its role in mediating bouquet formation and pairing. However, *sun1* does not seem to be required for the pre-synaptic arrest observed in *hop1(RNAi)* spermatocytes, as *hop1 (RNAi);sun1(RNAi)* spermatocytes still arrest in leptotene/zygotene. Conversely, the absence of SC in *hop1(RNAi);sun1(RNAi)* supports the hypothesis that HOP1 or recombination intermediates may be required to initiate central element loading in both homologous and non-homologous situations.

Given the crucial roles of SUN proteins in other organisms and the broad expression of SUN1 in *S. mediterranea,* it is somewhat unexpected that *sun1(RNAi)* does not affect viability or cause major somatic defects. These animals appear to be completely normal apart from the observed meiotic phenotypes, although I did not attempt to find subtle effects on nucleus positioning or other aspects of cell biology. Additionally, knockdown of the other two putative SUN domain genes in the *S. mediterranea* genome does not lead to obvious somatic or meiotic phenotypes. This is especially surprising given that the *Smed-sun2* gene is known to be upregulated and strongly expressed in germ cells (Wang et al., 2010). The absence of an observable phenotype cannot be attributed entirely to functional redundancy in these genes, nor to low turnover of these proteins, as neither double knockdowns nor even the triple knockdown seem to have any somatic effects even after several months of RNAi feeding (as a caveat, the effectiveness of RNAi knockdown cannot be confirmed absolutely). Given the state of the *S. mediterranea* genome assembly, it is certainly possible that there are additional SUN domain

proteins that have yet to be identified; alternatively, the essential functions performed by SUN proteins in other organisms could be carried out by different factors in *S. mediterranea*.

Conclusions

This analysis demonstrates a key role for Smed-SUN1 in the attachment of chromosomes to the cytoskeleton and bouquet formation in meiosis, similar to its roles in other organisms. The persistent attachment of telomeres in *sun1(RNAi)* indicates that factors other than SUN1 are responsible for connecting meiotic chromosomes to the nuclear envelope; this might be an interesting area for future investigation. Finally, the synapsis observed in *sun1(RNAi)* despite failure to pair and align homologs, similar to what is seen in the *C. elegans sun-1* null, reveals that synapsis can not only extend, but also initiate, between non-homologous chromosomes. The absence of synapsis in *sun1(RNAi);hop1(RNAi)* animals confirms that synapsis initiation is dependent on HOP1.

Materials and methods - see Chapter VI.

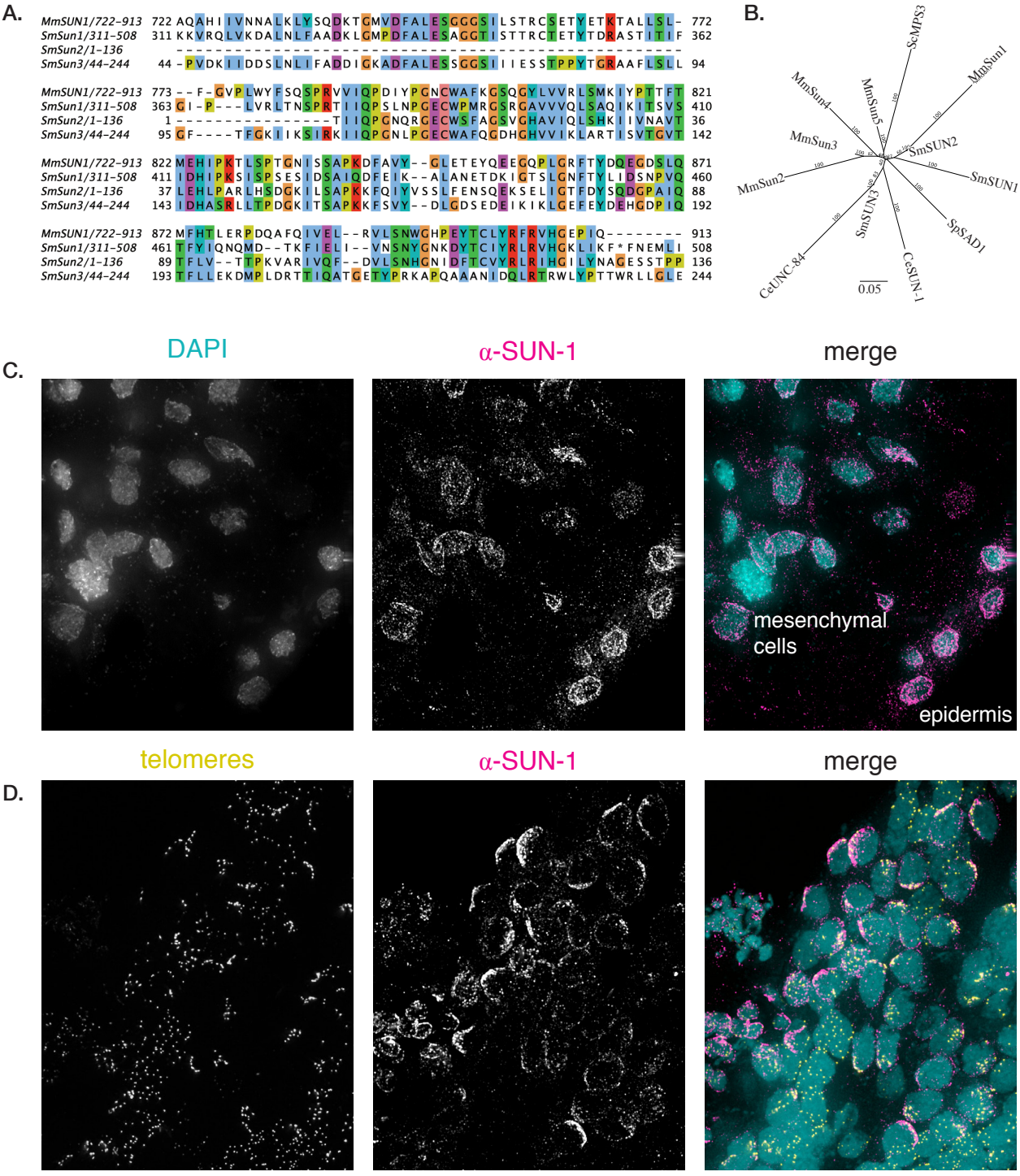

Figure 1. Identification of SUN proteins in *S. mediterranea* and the localization of Smed-SUN1
(A) CLUSTALW alignment of the SUN domains of mouse SUN1 and the three *S. mediterranea* SUN proteins. **(B)** UPGMA neighbor-joining tree of the SUN domains of SUN proteins from several species. Sc = *Saccharomyces cerevisiae*, Sp = *Schizosaccharomyces pombe*, Ce = *C. elegans*, Mm = *Mus musculus*, Sm = *Schmidtea mediterranea*. **(C)** Smed-SUN1 localizes throughout the nuclear envelope in mesenchymal and epidermal cells. **(D)** SUN1 localizes to the bouquet in spermatocytes. Yellow, telomere FISH; pink, α-SUN1; blue, DAPI.

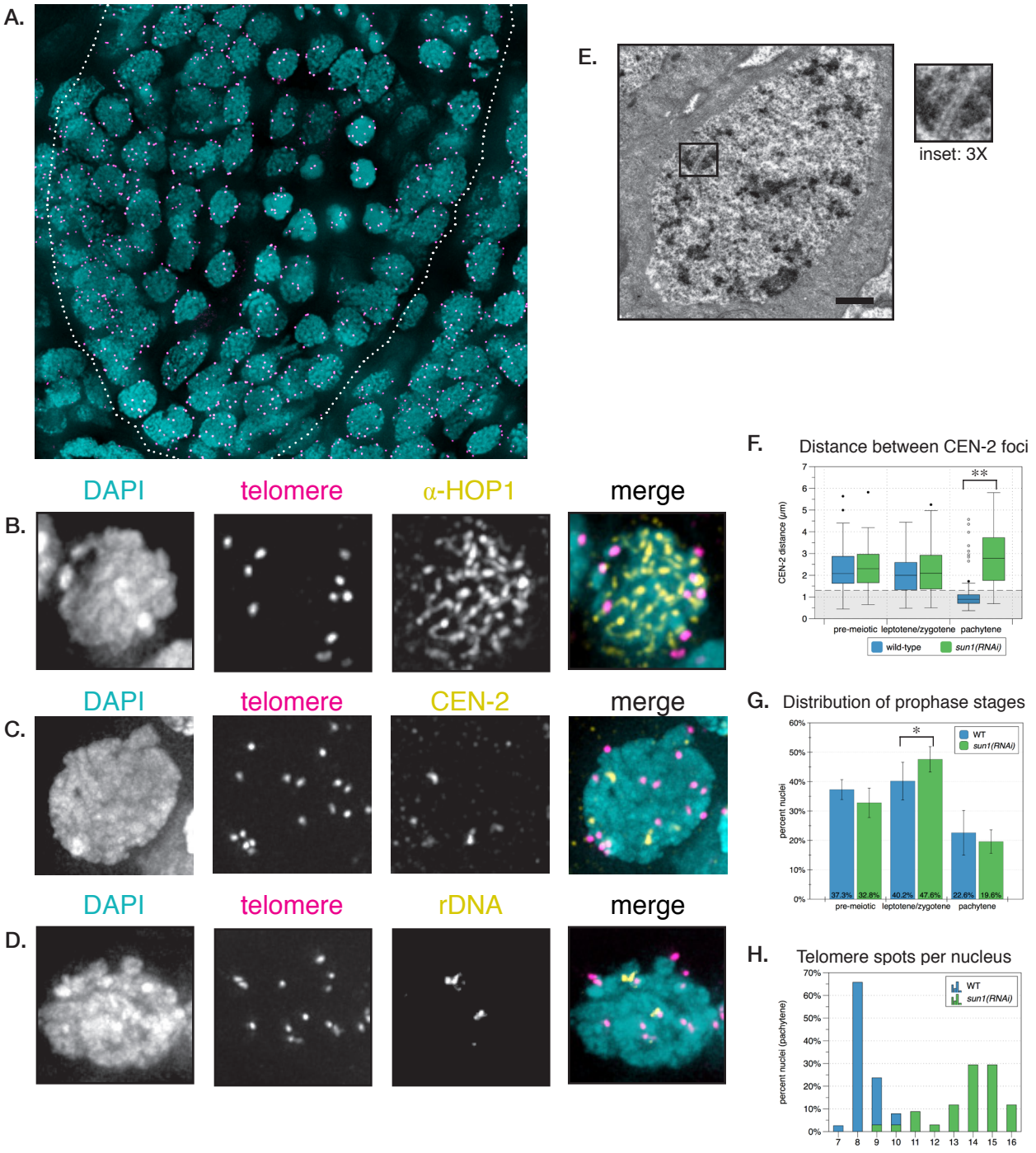

Figure 2. RNAi of *Smed-sun1* disrupts bouquet formation and pairing, causing non-homologous synapsis. **(A)** Testis section showing the absence of bouquet formation and presence of pachytene-stage nuclei in *sun1(RNAi)* testes. Scale bar = 5μm. **(B)** HOP1 loads normally in *sun1(RNAi)*. **(C,D)** Homologs do not pair in *sun1(RNAi)*. CEN-2 loci remain well-separated in pachytene nuclei (C). Homologous rDNA foci are also well-separated in pachytene (D). **(E)** Transmission electron microscopy reveals normal SC morphology in *sun1(RNAi)*. Scale bar = 1μm. **(F)** Measurement of the distances between CEN-2 foci shows that these loci are significantly further apart in *sun1(RNAi)* than in WT in pachytene. **p<0.001. **(G)** Distribution of prophase stages in WT vs. *sun1(RNAi)*, suggesting a slight delay of pachytene entry. n=561 nuclei from two animals. *p<0.05. **(H)** More distinct telomere spots are oberved in *sun1(RNAi)* than in WT, indicating that synapsed chromosomes are not aligned from end to end. n=34 nuclei.

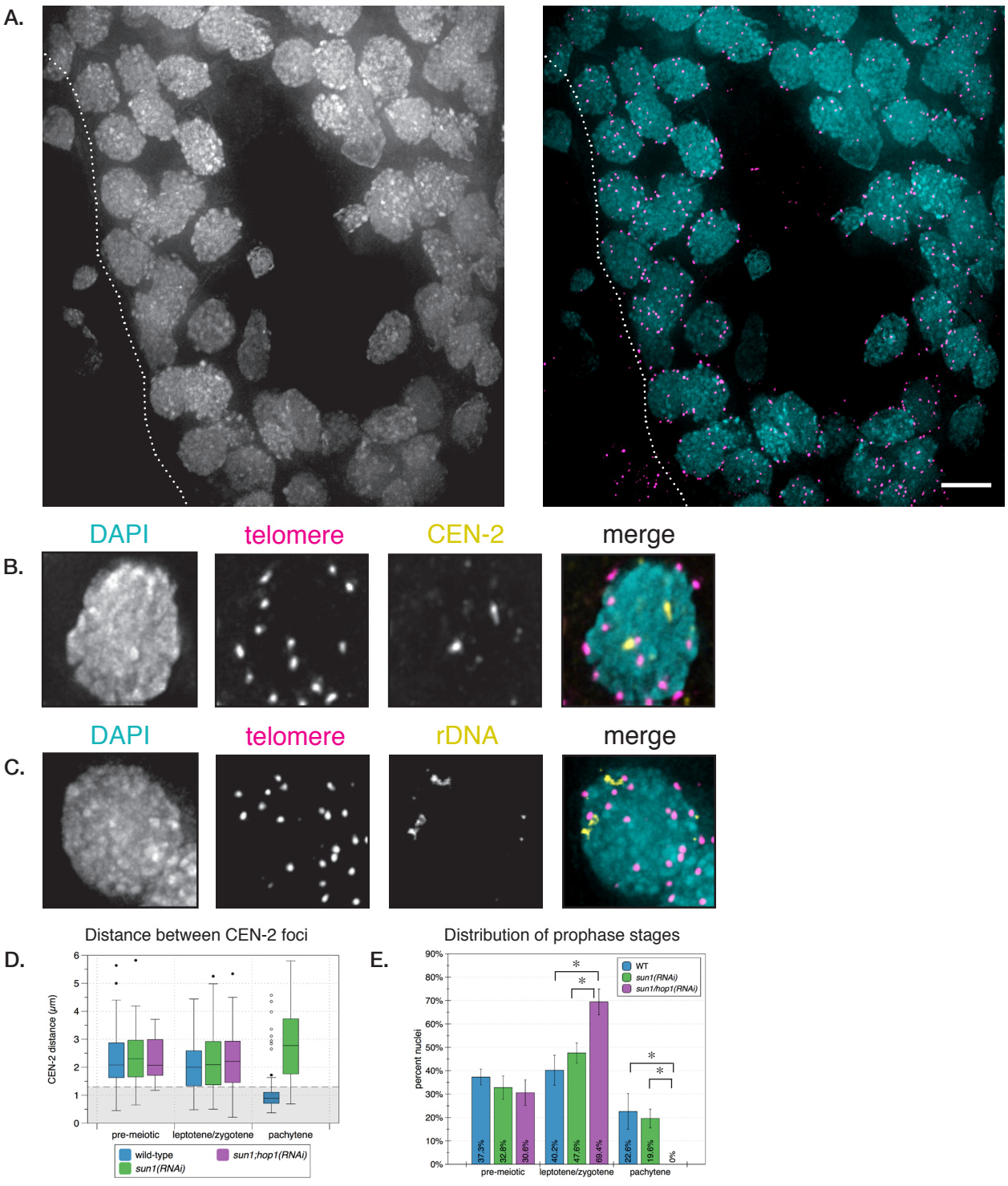

Figure 3. Co-depletion of SUN1 and HOP1 inhibits SC formation, bouquet formation, and pairing.
(A) Testis section showing the absence of bouquet formation and pachytene-stage nuclei in *sun1;hop1(RNAi)* testes. Pink, telomere FISH; blue, DAPI. Scale bar = 5μm. **(B,C)** Neither bouquet formation nor homolog pairing occur in *sun1;hop1(RNAi)* spermatocytes. Homologous CEN-2 foci (B) and rDNA foci (C) remain well separated, and telomeres are distributed throughout the nuclear envelope. **(D)** Measurement of the distances between CEN-2 foci shows a similar distribution to *sun1(RNAi)* in leptotene/zygotene. **(E)** Distribution of prophase stages in WT, *sun1(RNAi)*, and *sun1;hop1(RNAi),* showing a failure to enter pachytene (i.e., synapse) in *sun1;hop1(RNAi).* *p<0.001.

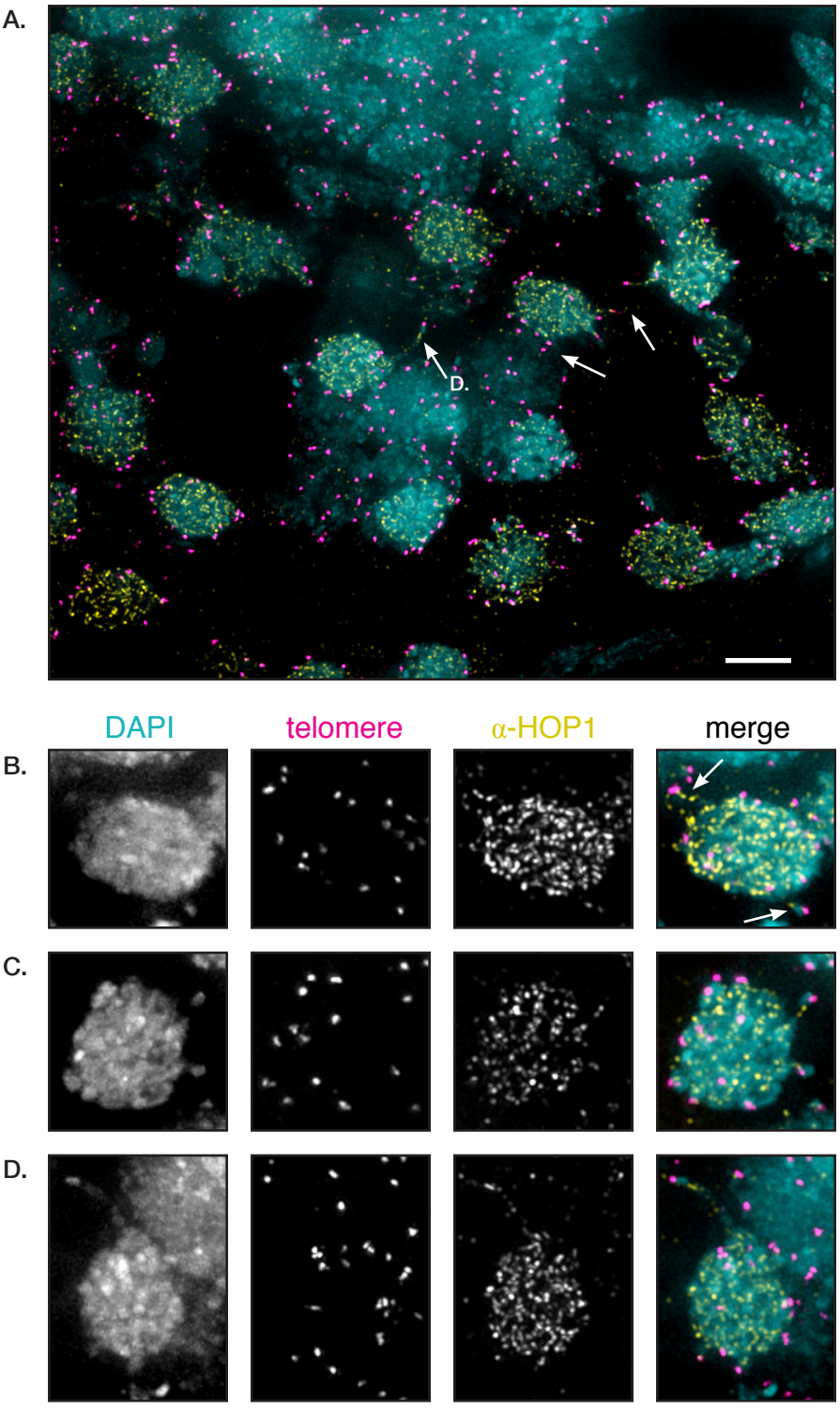

Figure 4. "Maverick" chromosomes are observed in some *sun1(RNAi)* spermatocytes after short feedings. **(A)** Testis section showing multiple nuclei with maverick chromosomes in a single *sun1(RNAi)* testis. α-HOP1 staining is included to facilitate the identification of chromosome tracks. Pink, telomere FISH; yellow, α-HOP1; blue, DAPI. Scale bar = 5μm. **(B-D)** Examples of individual spermatocytes with maverick chromosomes in *sun1(RNAi)*. Mavericks can be of variable length, are always telomere led, and can even involve two chromosome ends (B).

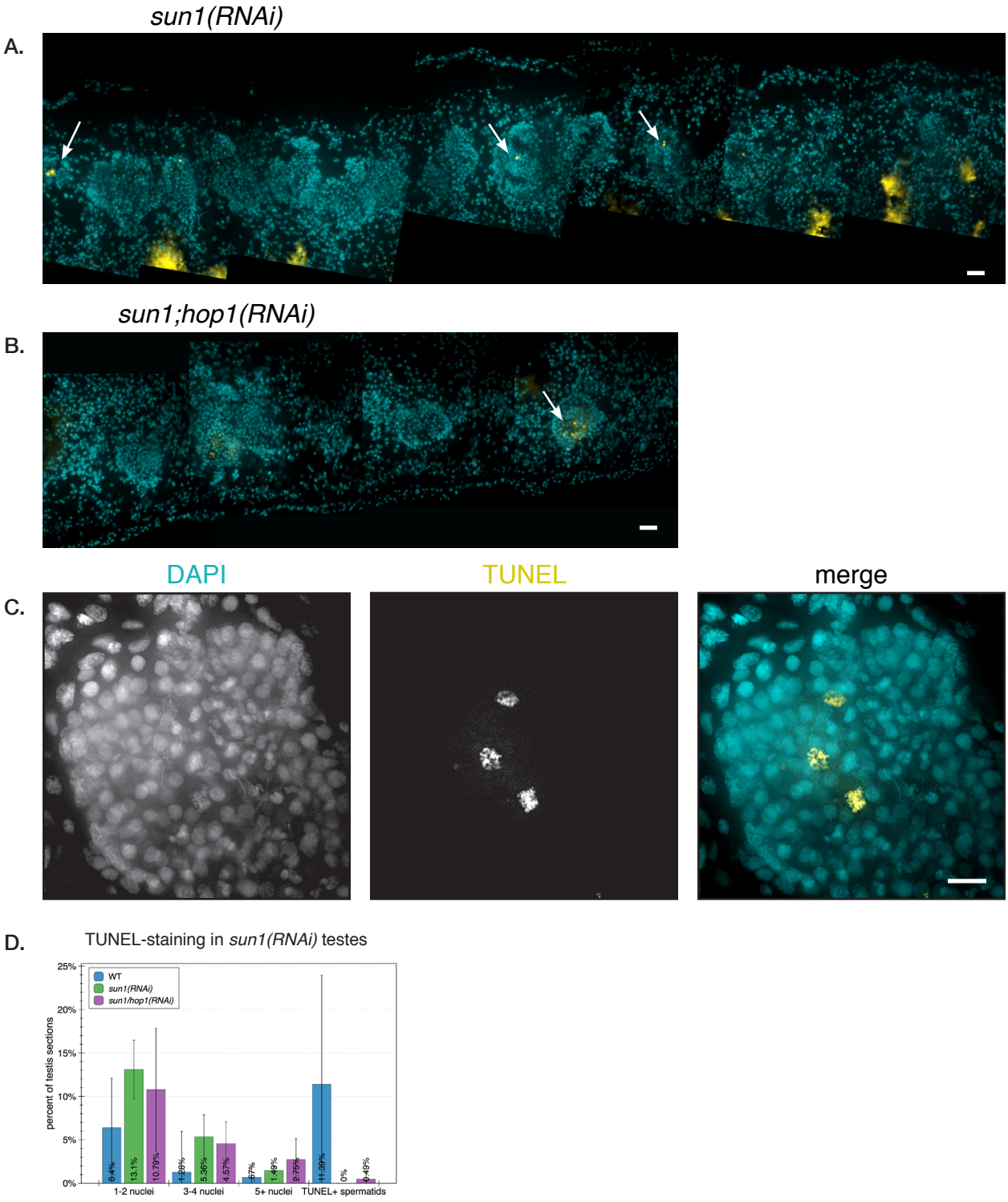

Figure 5. TUNEL staining of apoptosis in *sun1(RNAi)* and *sun1;hop1(RNAi)* testes.
(A) TUNEL staining of a longitudinal section of a *sun1(RNAi)* animal. Blue, DAPI; yellow, TUNEL. Scale bar = 50µm. **(B)** TUNEL staining of a longitudinal section of a *sun1;hop1(RNAi)* animal. Scale bar = 50µm. **(C)** Clusters of TUNEL-positive spermatocytes can be observed in some testes. Scale bar = 10µm. **(D)** Quantification of TUNEL staining in wild-type demonstrates variability from animal to animal and a potential elevation of programmed cell death in *sun1(RNAi)* and *sun1;hop1(RNAi)*. n=140 testes in 2 animals and 355 testes in 4 animals, respectively.

References

Bhalla, N., and Dernburg, A. F. (2008). Prelude to a division. Annu Rev Cell Dev Biol *24*, 397-424.

Chikashige, Y., Tsutsumi, C., Yamane, M., Okamasa, K., Haraguchi, T., and Hiraoka, Y. (2006). Meiotic proteins bqt1 and bqt2 tether telomeres to form the bouquet arrangement of chromosomes. Cell *125*, 59-69.

Conrad, M. N., Lee, C., Wilkerson, J. L., and Dresser, M. E. (2007). MPS3 mediates meiotic bouquet formation in Saccharomyces cerevisiae. Proc Natl Acad Sci USA *104*, 8863-8868.

Davis, L., and Smith, G. R. (2006). The meiotic bouquet promotes homolog interactions and restricts ectopic recombination in Schizosaccharomyces pombe. Genetics *174*, 167-177.

Ding, X., Xu, R., Yu, J., Xu, T., Zhuang, Y., and Han, M. (2007). SUN1 Is Required for Telomere Attachment to Nuclear Envelope and Gametogenesis in Mice. Dev Cell *12*, 863-872.

Hiraoka, Y., and Dernburg, A. F. (2009). The SUN rises on meiotic chromosome dynamics. Dev Cell *17*, 598-605.

Koszul, R., Kim, K. P., Prentiss, M., Kleckner, N., and Kameoka, S. (2008). Meiotic chromosomes move by linkage to dynamic actin cables with transduction of force through the nuclear envelope. Cell *133*, 1188-1201.

Koszul, R., and Kleckner, N. (2009). Dynamic chromosome movements during meiosis: a way to eliminate unwanted connections? Trends Cell Biol *19*, 716-724.

Penkner, A., Tang, L., Novatchkova, M., Ladurner, M., Fridkin, A., Gruenbaum, Y., Schweizer, D., Loidl, J., and Jantsch, V. (2007). The Nuclear Envelope Protein Matefin/SUN-1 Is Required for Homologous Pairing in C. elegans Meiosis. Dev Cell *12*, 873-885.

Penkner, A. M., Fridkin, A., Gloggnitzer, J., Baudrimont, A., Machacek, T., Woglar, A., Csaszar, E., Pasierbek, P., Ammerer, G., Gruenbaum, Y., et al. (2009). Meiotic chromosome homology search involves modifications of the nuclear envelope protein Matefin/SUN-1. Cell *139*, 920-933.

Sato, A., Isaac, B., Phillips, C. M., Rillo, R., Carlton, P. M., Wynne, D. J., Kasad, R. A., and Dernburg, A. F. (2009). Cytoskeletal forces span the nuclear envelope to coordinate meiotic chromosome pairing and synapsis. Cell *139*, 907-919.

Scherthan, H. (2007). Telomere attachment and clustering during meiosis. Cell Mol Life Sci *64*, 117-124.

Schmitt, J., Benavente, R., Hodzic, D., Höög, C., Stewart, C. L., and Alsheimer, M. (2007). Transmembrane protein Sun2 is involved in tethering mammalian meiotic telomeres to the nuclear envelope. Proc Natl Acad Sci USA *104*, 7426-7431.

Sheehan, M. J., and Pawlowski, W. P. (2009). Live imaging of rapid chromosome movements in meiotic prophase I in maize. Proceedings of the National Academy of Sciences *106*, 20989-20994.

Tang, X., Jin, Y., and Cande, W. Z. (2006). Bqt2p is essential for initiating telomere clustering upon pheromone sensing in fission yeast. J Cell Biol 173, 845-851.

Wang, Y., Stary, J. M., Wilhelm, J. E., and Newmark, P. A. (2010). A functional genomic screen in planarians identifies novel regulators of germ cell development. Genes Dev *24*, 2081-2092.

Zayas, R. M., Hernández, A., Habermann, B., Wang, Y., Stary, J. M., and Newmark, P. A. (2005). The planarian Schmidtea mediterranea as a model for epigenetic germ cell specification: analysis of ESTs from the hermaphroditic strain. Proc Natl Acad Sci USA *102*, 18491-18496.

Chapter V. Preliminary characterization of other *S. mediterranea* genes with possible roles in meiosis

In addition to the two genes described in detail in Chapters II and III, I also conducted preliminary investigations of other genes with potential or likely roles in meiosis.

At the outset of these studies, we were particularly interested in identifying genes that might affect bouquet dynamics, synaptonemal complex (SC) formation, or control double strand DNA break (DSB) and crossover/recombination dynamics. Because so little was known about the molecular basis of meiosis in *S. mediterranea*, and because many aspects of planarian biology preclude an unbiased screening for meiotic components, I instead took advantage of the available genome sequence to identify homologs of conserved genes that are known to be involved in meiosis in other organisms. After an extensive literature search, I compiled a list of genes that are known to be involved in sister chromatid cohesion, DSB formation and repair, crossover formation, axial element and synaptonemal complex formation, telomere function, and nuclear envelope dynamics, and retrieved the associated protein sequences from NCBI. Then, I performed simple tblastn searches of the *S. mediterranea* genome, initially using an in-house BLAST server set up and kindly shared by the Newmark lab, and later using the public SmedGD (Robb et al., 2007). This list was updated periodically and every time I was made aware of changes to the *S. mediterranea* genome assembly. The top results of these BLAST searches are shown in Table 1.

In addition to these homology searches, I took advantage of several comparative studies that have been conducted by other labs to identify genes that are specifically expressed or highly enriched in adult sexual animals relative to animals without developed germlines (asexual clones (Zayas et al., 2005) or *nanos(RNAi)* animals (Wang et al., 2010)). Though these studies mainly identified genes involved in germ cell identity or spermatid development, several interesting potential meiotic genes were also highlighted in these analyses (Table 2) and added to my list of candidate genes to investigate.

After identifying these candidate sequences, I designed primers to amplify RNAi targets of 500-700 bp in length. In some cases, primers could not be designed because the candidate mRNAs were too short or poorly annotated; these candidates were discarded. RNAi target sequences were amplified from cDNA, cloned into an RNA feeding vector and verified by DNA sequencing. The resulting RNAi vectors were transformed into HT115 cells and dsRNA expression was induced; dsRNA-expressing bacteria were pelleted and mixed with calf liver paste and fed to planarians to induce knockdown. (This protocol, along with all primer sequences used to amplify RNAi target sequences, are described in more detail in Chapter VI).

The candidate genes for which knockdown was conducted are highlighted in Table 1. Two of these genes (*hop1* and *sun1*) had particularly interesting knockdown phenotypes and were characterized in depth (see Chapters III and IV). Several other genes seemed to have subtle, pleiotropic, or surprisingly absent knockdown phenotypes and were characterized in more limited fashion. The results of these studies are presented in this chapter.

The ubiquitous cohesin subunit Smc3 is required for homolog pairing, progression through meiosis, and normal telomere dynamics

Smc3 is a ubiquitous subunit of the cohesin complex, which is essential for maintaining sister chromatid cohesion in both mitosis and meiosis. Smc3 binds to Smc1, and the resulting heterodimer associates with a kleisin protein and often a non-SMC subunit of the cohesin complex (Fig. 1A). In meiosis, cohesin complexes associate with the chromosome axis and are important for the normal recruitment of axial element proteins, SC formation, and recombination, though not usually DSB formation (Klein et al., 1999; Eijpe et al., 2000; Pelttari et al., 2001). While a meiosis-specific isoform of Smc1 has been identified in some organisms (e.g., Smc1β in mice) and meiosis-specific kleisins have been well characterized in a number of organisms (e.g., Rec8 in *S. cerevisiae* and *C. elegans*, Rec11 in *S. pombe*, *afd1* in maize, and Rec8 or the recently identified Rad21L in mice), a single isoform of Smc3 is thought to be present in all mitotic and meiotic cohesin complexes (Wood et al., 2010; Lee and Hirano, 2011; Ishiguro et al., 2011). In *S. cerevisiae*, a temperature-sensitive allele of *smc3* causes premature separation of sister chromatids and usually results in arrest before the first meiotic division, and cells that do undergo division usually mis-segregate at least one pair of sister chromatids (Klein et al., 1999).

Smed-smc3 was identified as being upregulated in the sexual strain of *S. mediterranea* as compared to the asexual strain, and was shown to be expressed strongly in the testes, ovaries and central nervous system (Zayas et al., 2005). A BLAST search of the *S. mediterranea* genome database reveals three regions with homology to the mouse *smc3* gene. However, this is likely to represent the misannotation of a single *smc3* gene, as these three regions map to the N-terminus, middle region and C-terminus of the *M. musculus* Smc3 protein, respectively (Fig. 1B).

RNAi targeting a 3' fragment of the gene (corresponding to the mRNA sequence that was shown to be upregulated in the sexual strain) appeared to have mild somatic effects in *S. mediterranea*. Animals began to exhibit tissue degeneration/lesions in the head region 2-3 weeks after the initiation of RNAi feeding, a phenotype that is frequently seen when there are defects in neoblast proliferation and tissue homeostasis (Reddien et al., 2005) and is consistent with a role for Smc3 in mitosis.

Based on the meiotic phenotypes of cohesin mutants or nulls in other organisms, I expected that depletion of SMC3 would likely lead to defects in sister chromatid cohesion, meiotic axis formation, and synapsis, as well as possible disruption of recombination and arrest before the first meiotic division. Testes in *smc3(RNAi)* animals displayed a clear defect in meiotic progression, with few/no pachytene nuclei and no mature spermatids (Fig. 1C).

Chromosome attachment to the nuclear envelope was not apparently disrupted in *smc3 (RNAi)* spermatocytes, and cells were able to form a telomere bouquet, although the bouquet morphology was sometimes abnormal. In wild-type, 8-16 distinct telomere foci can generally be counted in leptotene/zygotene nuclei, representing the telomeres at either end of the four pairs of homologous chromosomes ($2 \times 4 \times 2 = 16$). However, >16 FISH signals, some of which seemed roughly half as bright as others, could be observed in a significant proportion of *smc3(RNAi)* nuclei (Fig. 1D). This observation suggests that some loss of sister chromatid cohesion has occurred, at least at telomeres. An alternative possibility might be that these extra telomere signals actually reflect some polyploidy as a result of non-disjunction in pre-meiotic divisions, although this seems unlikely to account for the reduced brightness of the extra foci. In contrast to the well-separated telomeres observed in some nuclei, other nuclei exhibited a hyperclustered bouquet (Fig. 1E), with all telomeric FISH signals essentially merged into a single large focus. Similarly, SUN1 seemed to be more than usually enriched in the bouquet region in some nuclei (Fig. 1F). It is not clear whether this is a phenomenon that is unique to *smc3(RNAi),* or the extension of a stage that occurs transiently in wild-type. Anecdotally, I have occasionally observed a similar hyperclustered bouquet and SUN1 aggregation in *hop1(RNAi), rad51(RNAi),* and *mre11(RNAi)* spermatocytes, with variable penetrance. Based on these observations and data from other organisms, in which the bouquet stage is prolonged or more intense upon disruption of the recombination machinery, I have speculated that this hyperclustering may occur in response to unresolvable DNA damage. Unfortunately, it was not possible to assay double strand DNA break formation/resolution with RAD51 immunofluorescence in *smc3(RNAi)* sections for technical reasons (failure of antibody staining).

Pairing of homologous chromosomes was not evident in significant numbers of leptotene/ zygotene stage *smc3(RNAi)* nuclei. As shown in Figure 1G, the distribution of distances between CEN-2 foci was slightly wider than in wild-type (2.51 ± 1.26 vs. 2.0 ± 0.99; $p=0.06$), and essentially identical to that of *hop1(RNAi).* No obvious difference was observed in distances between CEN-2 foci in nuclei with hyperclustered vs. ‘normal’ bouquets in the limited number of nuclei analyzed (n=40 from two animals).

Chromosome morphology in leptotene/zygotene nuclei, as assayed by DAPI staining, appeared normal and was not suggestive of major defects in chromosome axis formation. HOP1 staining could also be seen in many nuclei, although long stretches were not usually present and unusually bright HOP1 foci were observed in some nuclei (Fig. 2). This is consistent with the phenotypes shown for disruption of cohesion during meiosis (usually via perturbation of Rec8

function) in other organisms; very frequently, axial element components can associate with chromosomes but do not mature fully (Klein et al., 1999; Bhatt et al., 1999; Colaiacovo et al., 2003; Golubovskaya et al. 2006; Wojtasz et al., 2009).

In general, these phenotypes are all consistent with what would be expected for a partial loss of sister chromatid cohesion during meiosis. Because this analysis was based upon RNAi knockdown, it is possible (or likely) that some residual SMC3 protein was present on chromosome axes in these spermatocytes, and that loss of cohesion was therefore incomplete. Longer or more complete knockdown might generate more severe phenotypes, although study of a more penetrant knockdown is likely to be complicated by the mitotic effects of SMC3 depletion.

Multiple genomic sites exhibit homology to *smc3*, and it is formally possible that multiple isoforms of *smc3* are expressed in *S. mediterranea.* However, I believe that this is unlikely based on the ubiquity of a single *smc3* isoform in other species that have been studied. The observed upregulation of *smc3* in sexual animals compared to asexual animals is probably due to the increased proportion of proliferating (both mitotic and meiotic) cells in the sexual line. Notably, BLAST searches of the *S. mediterranea* genome with other cohesin subunits reveals only one kleisin (Scc1/Rad21/Rec8) homolog, one Scc3/SA/STAG homolog, and two regions of the genome with homology to the N and C termini of Smc1, respectively (which, like Smc3, are likely to represent a single misannotated gene). Thus, it is not clear what factors, if any, distinguish the meiotic cohesin complex(es) from the mitotic cohesin(s). This may be an interesting area for investigation in the future.

Depletion of the DSB repair protein RAD51 *has pleiotropic effects and causes testis regression*

Rad51 is a well-conserved component of the machinery that catalyzes the strand invasion step of homologous recombination in response to DNA damage. In meiosis, Rad51 (and/or a meiosis-specific paralog, Dmc1) are required for the repair of programmed DSBs as crossovers or non-crossovers. The disruption of Rad51/Dmc1 precludes the normal formation of recombination intermediates, which has different effects in different organisms. In budding yeast, for example, deletion of *dmc1* or *rad51* perturbs homolog pairing and alignment, delaying meiotic progression; homologous synapsis is eventually able to occur, but crossovers fail to form (Bishop et al., 1992; Rockmill et al., 1995). *Dmc1-/-* spermatocytes in mice do not undergo synapsis and arrest in meiotic prophase, demonstrating that in mammals, Dmc1-dependent intermediates are important to mediate homolog alignment and SC initiation (Pittman et al., 1998; Yoshida et al., 1998). In contrast, deletion of *rad51* in maize induces almost complete nonhomologous synapsis (Li et al., 2007).

The *S. mediterranea* genome database shows two predicted genes with significant homology to the DNA repair protein Rad51 (and a lesser degree of homology to the meiosis-specific homolog Dmc1). The annotated gene products differ in length, but are likely to represent a single gene[1]; the longer gene is homologous to the entire *M. musculus* Rad51. The RNAi here targeted a 3' fragment of the gene with homology to both predicted gene products (Fig. 3A) and also corresponds to a cDNA fragment that was predicted to be upregulated in the sexual strain of *S. mediterranea* (Zayas et al., 2005).

RNAi of *Smed-rad51* had pleiotropic effects with variable penetrance. Some animals showed signs of lysis or lesions, others decreased in size, and one animal exhibited a pinched head and pinched tail phenotype, all of which are consistent with defects in neoblast function (Reddien et al., 2005), although the basis of the variable penetrance of this phenotype is not clear. Among animals that maintained their size and did not display other significant somatic defects during a month of RNAi feeding (n=6, two independent feeding trials), most exhibited a shrunken testis phenotype. Normally-sized testes lobes were not found in these animals, but testis remnants including spermatogonia, spermatocytes and some spermatids at varying stages of maturity could be found in some sections (Fig. 3B).

The small number of spermatocytes per testis section obviously complicate the analysis of this knockdown, and these remaining spermatocytes might have some residual RAD51 activity that allowed their escape. Nevertheless, a few observations are worth noting. Most interestingly, a few nuclei with a pachytene morphology can be observed in *rad51(RNAi)* testes. The CEN-2 foci in these nuclei appear to be unpaired and >8 telomere spots are observed, leaving open the possibility that *rad51(RNAi)* causes non-homologous synapsis (Fig. 3E,F). If so, this would imply that recombination intermediates are important for homolog pairing and alignment, but not required to initiate SC loading, in *S. mediterranea*. CEN-2 foci are occasionally closely juxtaposed in leptotene/zygotene spermatocytes (e.g., Fig. 3D) but most are well-separated (Fig. 3C), as is true of wild-type. Telomere attachment and bouquet formation appear grossly normal, although some nuclei could be considered to have hyperclustered bouquets (e.g., Fig. 3D). HOP1 also appeared to load normally (Fig. 3G).

RNAi targeting the DSB repair protein MRE11 *has no obvious effects on spermatogenesis*

Mre11 is a member of the MRN (Mre11, Rad50, Nbs1/Xrs2) complex, which is required for DSB formation and processing and is conserved from *S. cerevisiae* to mammals (Assenmacher and Hopfner, 2004; Cherry et al., 2007). The MRN complex also participates in checkpoint signaling. BLAST search of the *S. mediterranea* genome revealed two Mre11

[1] Alignment of these two genomic regions reveals 99% nucleotide identity within the longer gene sequence and >97% nucleotide identity in ~5 kB of 3' and 5' bordering regions.

homologs with 99% homology in the shared region (Fig. 4A). RNAi targeting both isoforms (i.e., the overlapping sequence) did not have any apparent effects on meiosis in several attempts at feeding. Testes were normal in size and contained mature spermatids, and bouquet formation appeared to be similar to that in wild-type (Fig. 4B,C). Significant numbers of pachytene nuclei were observed, indicating that synapsis probably occurs normally, and CEN-2 foci were paired in the vast majority of synapsed nuclei. If anything, there may have been a slight increase in the proportion of pachytene cells, compared to wild-type, which could be consistent with a weak defect in late DNA repair. However, I did not quantify pairing or nuclear stages in this background due to the absence of gross defects.

Based on the requirement for Mre11 for completion of meiosis in most other organisms, the enzymatic nature of MRE11 and the potential presence of multiple *mre11* paralogs in the genome, the lack of phenotype seen here is likely to reflect unsuccessful or incomplete knockdown. It is unlikely that MRE11 is dispensable for meiosis in *S. mediterranea*.

Depletion of a possible MER3 homolog in S. mediterranea is lethal

The DNA helicase Mer3 is one of the so-called ZMM proteins that is required for normal completion of crossovers and crossover control in budding yeast (Nakagawa and Ogawa, 1999; Mazina et al., 2004; Lynn et al., 2007). Mer3 function is important for SC loading in yeast (Börner et al., 2004) and *Coprinus cinerus* (Sugawara et al., 2009). Similarly, *mer3* is required for crossover formation, but not initial homolog alignment, in rice (Wang et al., 2009). Mer3 appears to be conserved in humans, where it is called Hfm1 (Tanaka et al., 2006), although its function in mammalian meiosis has not been described.

Because I was interested in examining the effects of disrupting crossovers in *S. cerevisiae*, I looked for Mer3 as a potential target. One homolog of *mer3* is present in the *S. mediterranea* genome (mk4.002244.00.01), and RNAi targeting this gene was always lethal within several weeks of feeding. Given the lack of somatic phenotypes for *mer3* disruption in other organisms, it is likely that this RNAi affected a different gene, or that the gene I assumed to be *mer3* has a different function. BLAST of the predicted protein to the NCBI database retrieves several other helicases, including the U5 small nuclear ribonucleoprotein 200 kDa helicase; the lethal phenotype may be mediated by defects in RNA processing or other critical processes.

Depletion of polo kinase homologs is lethal or has no meiotic phenotype

Polo kinases are a diverse family of protein kinases with multiple roles in mitotic and meiotic cell cycle regulation. In *C. elegans*, PLK-2 promotes homolog pairing and synapsis by acting at Pairing Centers to phosphorylate SUN-1 (Harper et al., in press). Simultaneous

disruption of *plk-2* and *plk-1* (which does not normally play a critical role in meiosis but can partially compensate for lost *plk-2* function) prevents chromosome clustering at the nuclear envelope (i.e., "bouquet" formation), leading to complete loss of homolog pairing and some SC loading between non-homologous chromosomes. Because I was especially interested in identifying factors that might disrupt bouquet formation in *S. mediterranea*, these seemed like good candidates for RNAi. I searched the genome for potential PLK homologs that could be depleted via RNAi. Five distinct genomic regions were found to have homology to *C. elegans* PLK-2 (Fig. 5A), though the gene annotation in several of these regions was poor. I designed several sets of primers to amplify RNAi target sequences from cDNA for all five regions. Plkc3 (de_novo.18895.1, v31.003234:18435..24058) could not be amplified with the primers used. Plkc1 (mk4.001509.00.01) was successfully amplified from cDNA but could not be cloned into an RNAi feeding vector for technical reasons. Plkc2 (v31.007361:12834..15539), Plkc4 (v31.002811:7575..8527), and Plkc5 (de_novo.17941.1, v31.003052:16515..19047) were successfully amplified and cloned into the RNAi feeding vector.

All *plkc2(RNAi)* animals died due to tissue lysis within three weeks from the first RNAi feeding, suggesting that PLKC2 may have roles in neoblast function.

After two months of feeding, two *plkc4(RNAi)* and three *plkc5(RNAi)* animals were cryosectioned and FISH/IF was used to evaluate bouquet formation, homolog pairing, and axial element formation (Fig. 5B-E). No obvious defects in spermatogenesis were observed in any of these animals. Testis size seemed normal and abundant mature spermatids were observed, indicating that there were no gross defects in spermatogenesis. Pachytene nuclei were observed at normal levels in all testes (though this was not quantified carefully). HOP1 staining in one *plkc-4(RNAi)* testis appeared somewhat more polarized than normal (Fig. 5C), but it was unclear whether this phenomenon is widespread. Together, these results do not indicate a role for either Plkc4 or Plkc5 in meiosis, but given the many Plk paralogs in *S. mediterranea* it is possible that co-depletion of these or other Plk paralogs would yield a meiotic phenotype.

The conserved double strand break protein Spo11 has not been found in S. mediterranea

Among the meiotic genes that have not been identified in *S. mediterranea*, one of the most notable is the meiosis-specific endonuclease Spo11. This protein generates the programmed double strand breaks that are required for recombination and has been found in essentially all sexually reproducing organisms to date (Malik et al., 2007), but has thus far proven elusive in the *S. mediterranea* genome. A genome search identified one sequence with limited homology over 33aa to *spo-11* (v31.002904:17270..19571), but mRNA-seq (whole transcriptome sequencing) and attempts to PCR this transcript from purified cDNA showed no sign that this region is expressed. It is formally possible that these animals rely on a different enzyme or other alternative mechanism to generate DSBs. With that said, it would be extremely surprising if no

spo-11 homolog is present in *Schmidtea*, given that it is conserved in species from *Giardia* to humans and that a putative homolog can be found in the relatively closely related parasitic flatworm *Schistosoma mansoni* (XP_002573205). Whatever the case, it will be especially interesting to identify the components of the DSB formation machinery in *S. mediterranea*, and determine how they interact with *hop1* to create breaks.

Attempts to identify central element components

The proteins that make up the central region of the synaptonemal complex are among the meiotic proteins that are least amenable to identification by computational means. Transverse filaments, or TFs, make up the whole central region and are well-conserved at the level of secondary structure, but not at the level of primary sequence and are thus notoriously difficult to identify by computational means. Other proteins, which localize to the central element, have been recently identified and characterized in mouse (Syce1, Syce2, Tex12) and *Drosophila* (Corona) but also do not appear to have clear primary sequence-level homologs in other organisms (Hamer et al., 2006; Costa et al., 2005; Page et al., 2008; Bolcun-Filas et al., 2007; 2009). Most known central region components have been identified through forward genetic screens, which is not currently possible in *S. mediterranea*.

Despite these challenges, I wanted to attempt to find TF proteins in *S. mediterranea* for several reasons. First, an analysis of TF knockdowns will be required to determine whether stable homolog pairing and/or completion of recombination are dependent on synapsis in *S. mediterranea*. Secondly, from a cytological standpoint, immunofluorescence to TFs would provide a simpler and more reliable assay for synapsis than does chromosome morphology.

In 2003, Bogdanov and colleagues used a structure prediction-based search method to computationally identify (previously known) transverse filament candidates in *Drosophila* and *C. elegans* (Bogdanov et al., 2003). We asked this group to find candidate TF sequences in the *S. mediterranea* genome; their analysis yielded five candidate proteins with a globular-coiled coil-globular structure and of the appropriate length, dubbed TFC1-5 (TFC1: mk4.000440.02.01, TFC2: mk4.000675.02.01, TFC3: mk4.001379.07.01, TFC4: mk4.002345.03.01, TFC5: mk4.018982.00.01). Unfortunately, TFC2, TFC4, and TFC5 were not good candidates for RNAi because they shared so much homology with many other regions of the genome, which prevented both specific knockdown and also specific cloning from cDNA. TFC3 was discarded as a candidate because it was clearly a lamin protein. A fragment specific to the top candidate, *tfc1*, was successfully amplified and cloned, but feeding RNAi did not have any apparent effect on synapsis (i.e., many spermatocytes with normal pachytene morphology were still observed after RNAi), indicating that it is unlikely to be a true TF. Cross-referencing this sequence against microarray data comparing the sexual strain to asexual or *nanos(RNAi)* also indicated that this gene is not upregulated in the sexual strain, supporting this conclusion.

An in vitro biochemical approach was also pursued briefly. Because Sycp1 can be co-immunoprecipitated with Hormad1 from mouse testis extracts (Fukuda et al., 2010), I believed it might be feasible to use co-immunoprecipitation from *S. mediterranea* protein extracts with anti-HOP1 antibody, followed by mass spectrometric analysis, to identify transverse filament proteins and other components of the synaptonemal complex. However, initial western blot analyses of whole animal protein extracts were not encouraging; no HOP1 band was identified in the soluble fraction of the extracts and the bands that appeared in the protein pellet were not of the expected size, suggesting that HOP1 might be challenging to immunoprecipitate with this antibody. Additional investigation suggested that mass spectrometric analysis would require more input material than could be produced in the time available for the experiment (i.e., more animals than I could rear in a few months time) and might also require more anti-HOP1 antibody than was available, so I did not pursue this further. However, this could still be a useful approach for identifying SC components in the future. Alternatively, yeast 2-hybrid or other affinity-based approaches might be more feasible.

Materials and methods - see Chapter VI.

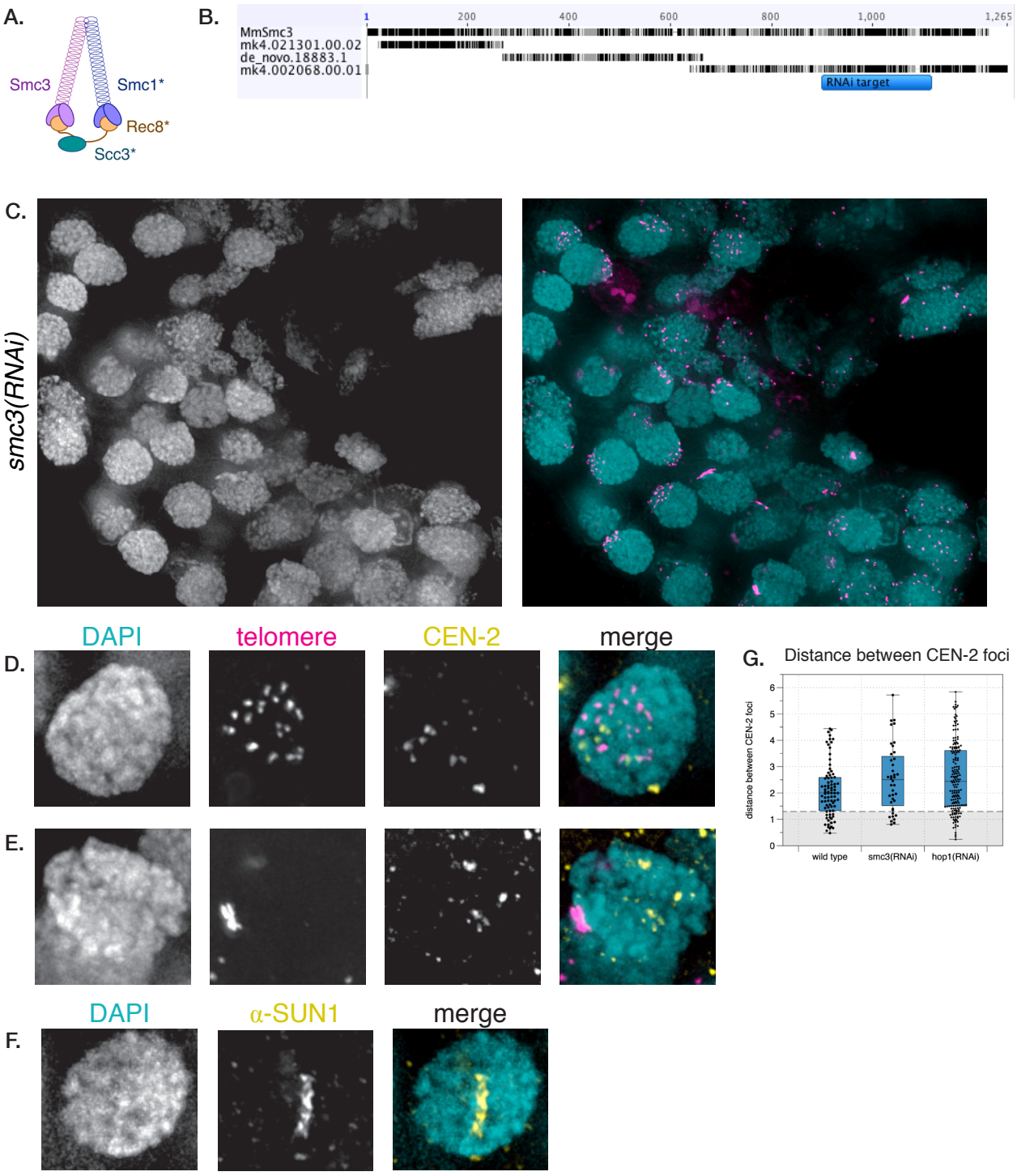

Figure 1. Smc3 is required for normal bouquet dynamics, pairing, and progression through meiosis.
(A) Cartoon depiction of the cohesin complex. Asterisks denote subunits with one or more meiosis-specific paralogs in some organisms. **(B)** Alignment of the three *S. mediterranea* genome regions with homology to mouse Smc3. **(C)** Testis section showing the absence of pachytene-stage nuclei and mature spermatids in *smc3(RNAi)* testes. Pink, telomere FISH; blue, DAPI. Scale bar = 5µm. **(D)** Some telomeres appear to have cohesion loss, evidenced by >16 telomere FISH foci (D). **(E,F)** Aberrant bouquet forms in *smc3(RNAi)*. Hyperclustered bouquets are observed in some nuclei (E); similarly, hyperaggregated SUN1 is also observed in some nuclei (F). **(G)** Pairing is disrupted in *smc3(RNAi)*, similar to the phenotype seen in *hop1(RNAi)*. n=40 nuclei from 2 animals.

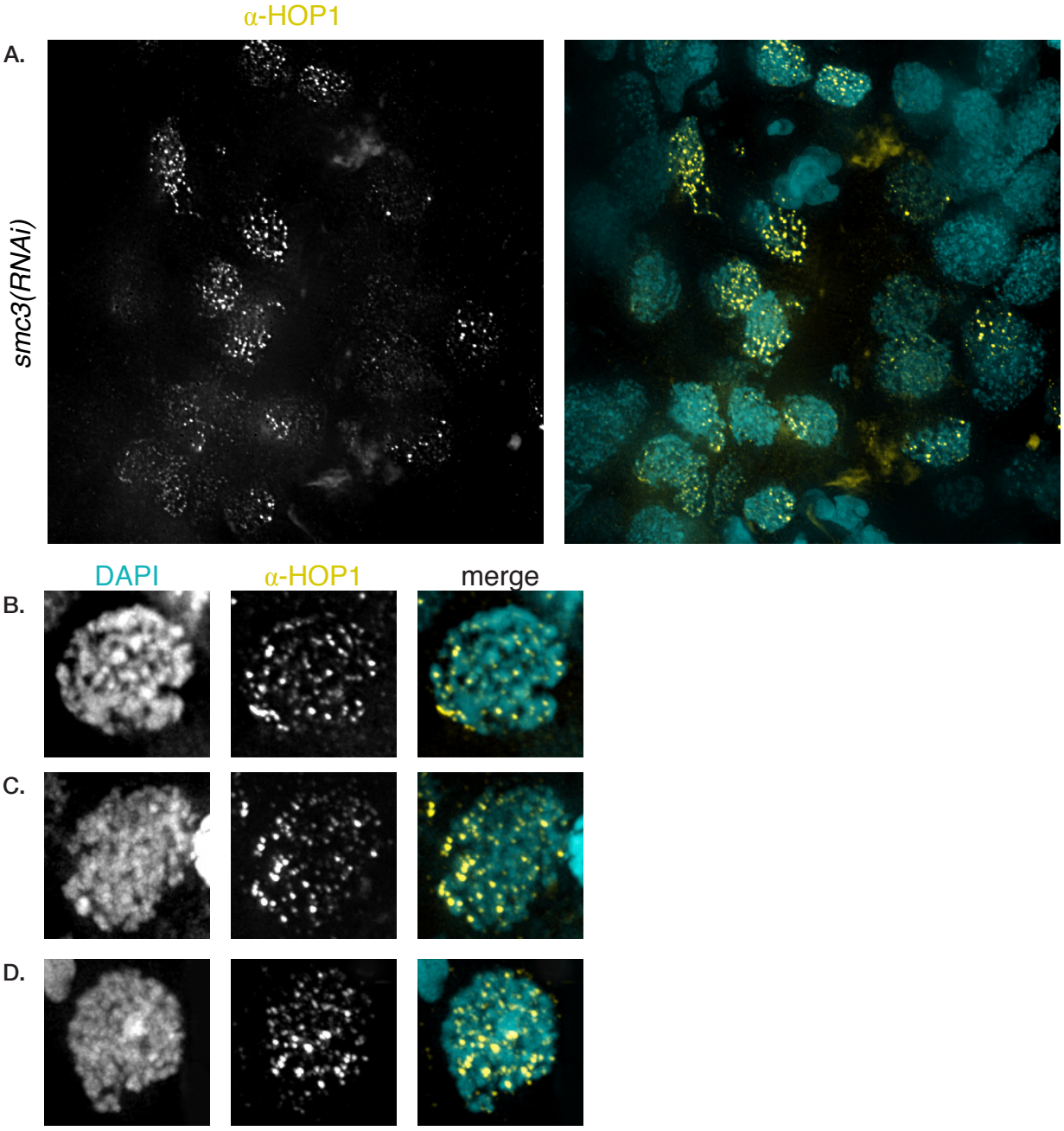

Figure 2. HOP1 loads, but may not localize fully normally, in *smc3(RNAi)*.
(A) α-HOP1 staining of a testis section from an *smc3(RNAi)* animal. Foci of HOP1 can be observed along chromosomes throughout the nucleus, but stretches of HOP1 are seen much more rarely. **(B-D)** More examples of α-HOP1 staining in individual *smc3(RNAi)* spermatocytes. Thin stretches of HOP1 can be appreciated in some nuclei, and bright foci are frequently observed throughout the nucleus.

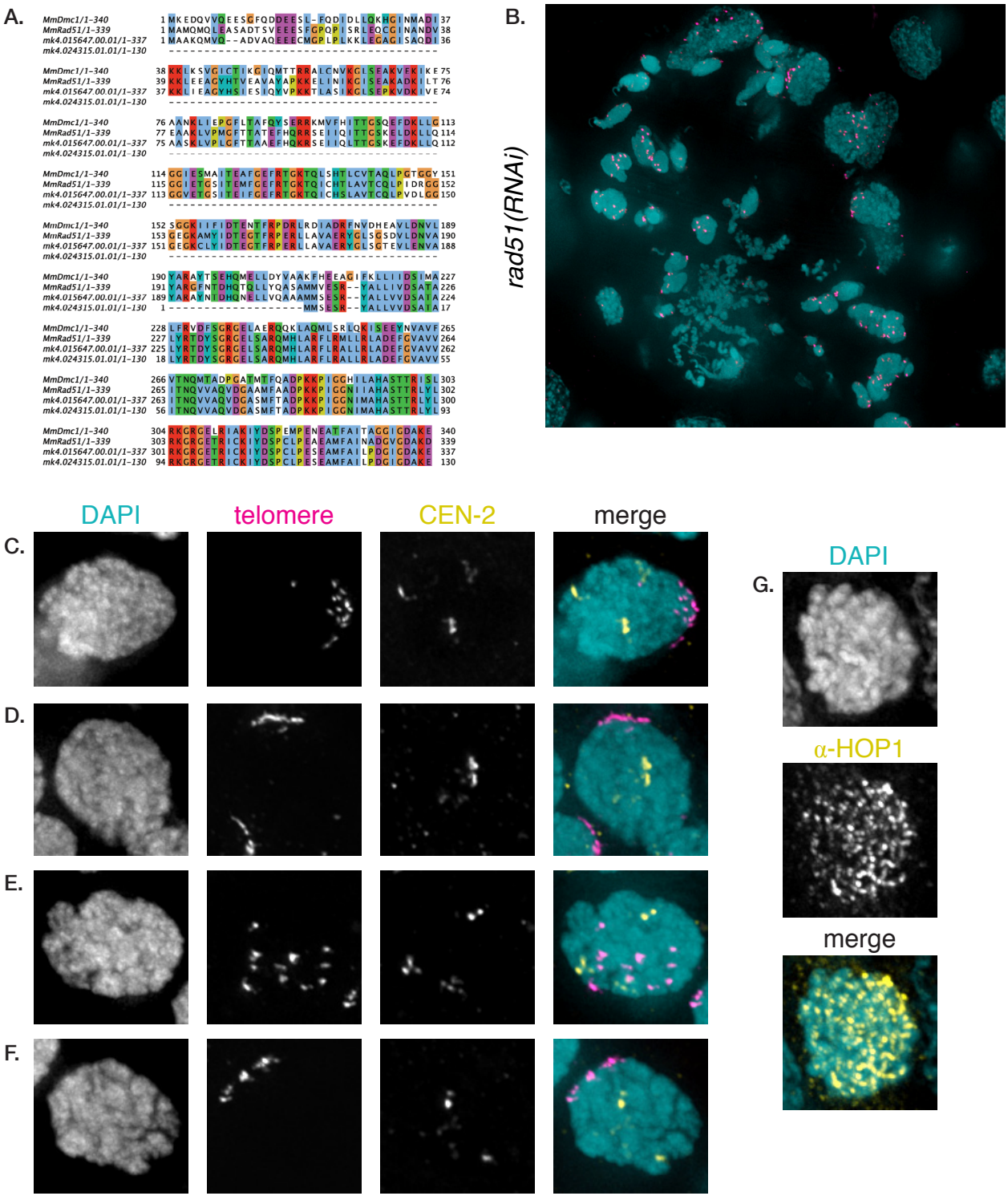

Figure 3. Meiotic phenotypes of *rad51(RNAi)*.
(A) Alignment of the two Rad51-like proteins predicted in *S. mediterranea* with the mouse Dmc1 and Rad51 protein sequences, showing greater homology to Rad51. **(B)** Cryosection showing the small testis phenotype of *rad51(RNAi)*. Pink, telomere FISH; blue, DAPI. Scale bar = 5µm. **(C-F)** Pairing and synapsis may be disturbed in *rad51(RNAi)*. Well-separated CEN-2 foci can be seen in some of the few pachytene-like nuclei that appear to have polymerized SC (E, F). **(G)** HOP1 seems to load normally in *rad51(RNAi)* spermatocytes.

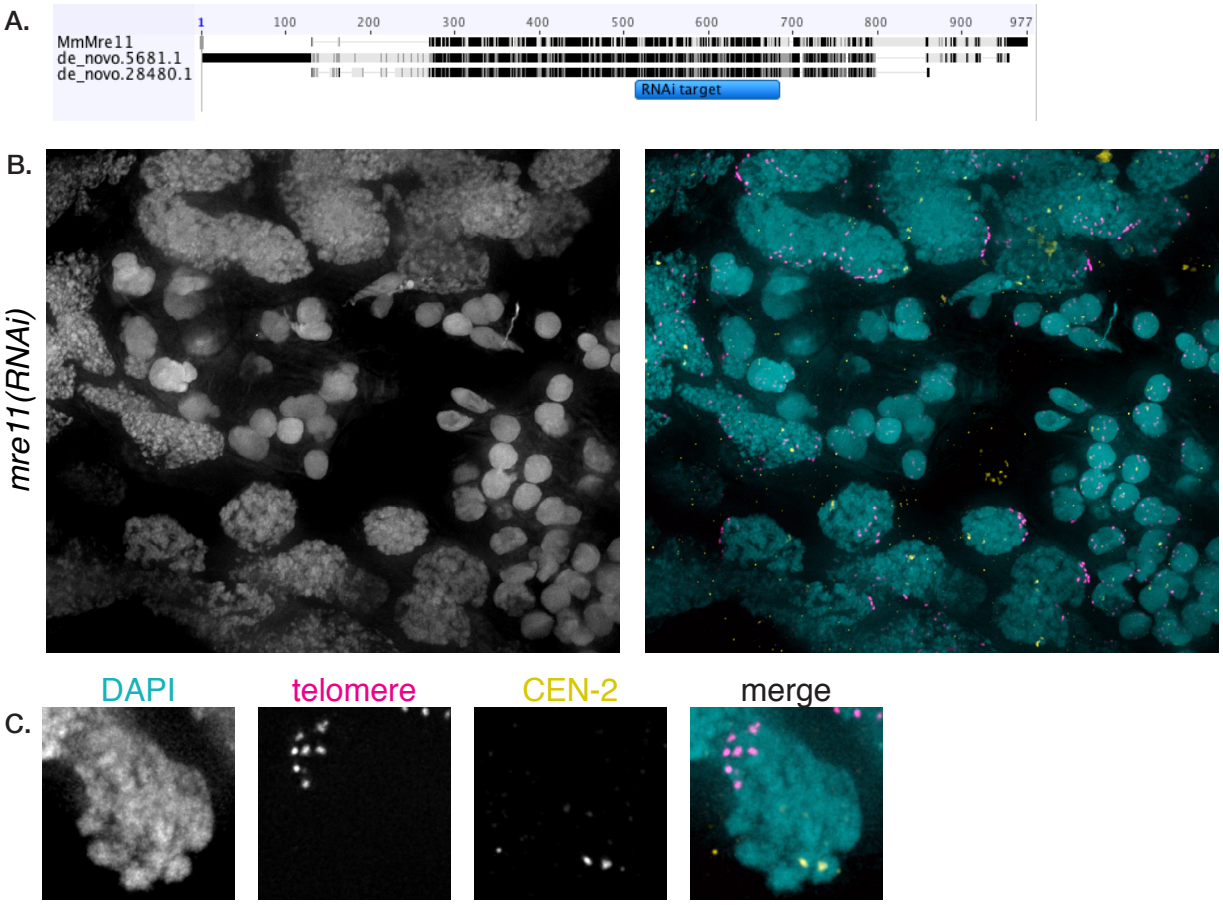

Figure 4. Absence of meiotic phenotypes in *mre11(RNAi)*.
(A) Alignment of the two Mre11-like genes predicted in *S. mediterranea* with the mouse Mre11 sequence. **(B)** Section showing the normal testis phenotype of *rad51(RNAi)*. Pink, telomere FISH; yellow, CEN-2 FISH; blue, DAPI. Scale bar = 5µm. **(C)** A single spermatocyte nucleus demonstrating that pairing and synapsis appear to be normal in *mre11(RNAi)*.

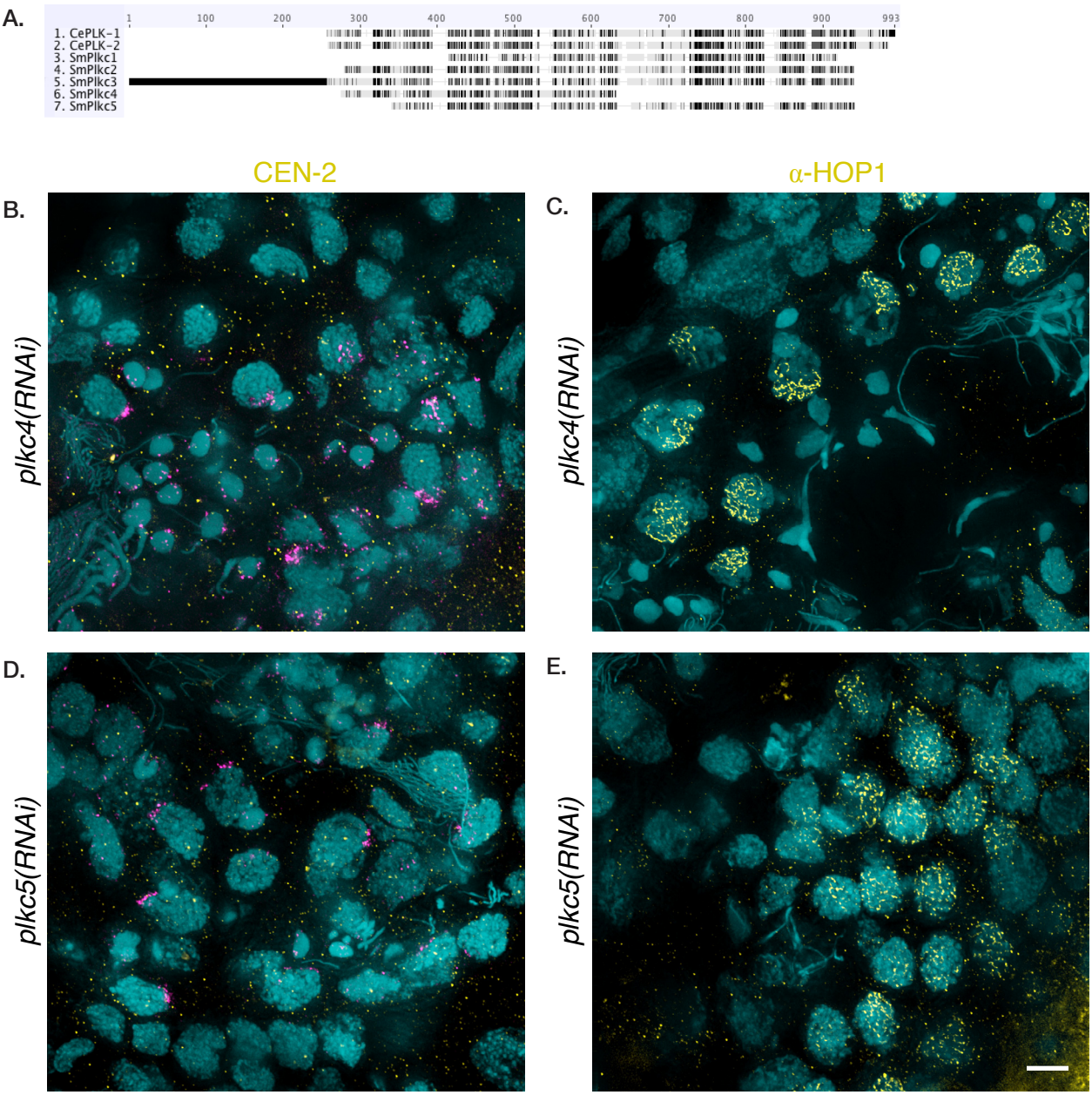

Figure 5. Absence of obvious meiotic phenotypes in *plkc4(RNAi)* and *plkc5(RNAi)*.
(A) Alignment of the five PLK-like regions predicted in *S. mediterranea* with the *C. elegans* PLK-1 and PLK-2 protein sequences. RNAi targets for SmPlkc1 and SmPlkc3 could not be amplified from cDNA, and RNAi targeting SmPlkc2 was lethal. **(B)** Section showing normal bouquet formation and homolog pairing in *plkc4(RNAi)*. Pink, telomere FISH; yellow, CEN-2 FISH; blue, DAPI. **(C)** Section showing α-HOP1 staining in *plkc4(RNAi)*. The polarization of α-HOP1 is particularly pronounced in some nuclei. **(D)** Section showing the normal bouquet and pairing in *plkc5(RNAi)*. Pink, telomere FISH; yellow, CEN-2 FISH; blue, DAPI. **(E)** Section showing apparently normal α-HOP1 staining in *plkc5(RNAi)*. Scale bars = 5µm.

Table 1-1. BLAST search results of meiotic genes against the *S. mediterranea* genome (v.3.1)

category	protein name	accession #	organism	Smed homolog	bit score	E value	notes
bouquet/NE	bqt-1	XP_001713078	*S. pombe*	no hits			
	bqt-2	NP_593493	*S. pombe*	no hits			
	bqt-3	SPCC594.07c	*S. pombe*	no hits			
	bqt-4	SPBC19C7.10	*S. pombe*	no hits			
	Nuclear LIM interactor-interacting factor 2	NP_666124	*M. musculus*	mk4.000028.05.01	161	5.00E-41	confirmed by bi-directional BLAST
		NP_666124	*M. musculus*	mk4.003785.04.01	113	2.00E-26	NLI interacting family member
	sad-1	NP_595947	*S. pombe*	mk4.001469.07.01	87	1.00E-17	SmSun1
		NP_595947	*S. pombe*	mk4.001275.01.01	82	5.00E-16	SmSun2 (testis expressed; Y. Wang pers. comm. and Wang et al. 2010)
		NP_595947	*S. pombe*	mk4.003039.01.01	68	5.00E-12	SmSun3
	Unc-84 homolog A	NP_077771	*M. musculus*	mk4.001469.07.01	180	1.00E-45	SmSun1
		NP_077771	*M. musculus*	mk4.003039.01.01	120	2.00E-27	SmSun3
		NP_077771	*M. musculus*	mk4.001275.01.01	102	4.00E-22	SmSun2
	ZYG-12	CE39461	*C. elegans*	mk4.009102.01.01	69	6.00E-12	several other hits with similarly good bitscores; all homology is in C terminus
centromeres	**CENP-E**			mk4.021405.00.01			centromere protein E or SPB. Came up in C(3)G search.
	SPB/kendrin			mk4.075285.00.01			SPB/kendrin, inner plaque. Came up in C(3)G search.
checkpoint and signaling	**ATM1**	NP_000042	*H. sapiens*	mk4.002177.01.01	197	4.00E-50	only matches very c-term of protein. Splice variant 1
		NP_000042	*H. sapiens*	mk4.002177.02.01	153	8.00E-37	only matches very c-term of protein. Splice variant 2
		NP_000042	*H. sapiens*	mk4.008791.03.01	138	2.00E-32	only matches very c-term of protein (bridges splice variants above?)
	Cdk2	NP_955795	*R. norvegicus*	mk4.008987.01.01	260	3.00E-70	lots of good hits (many cdks, apparently). See HTML file.
	Chk2	NP_057890	*M. musculus*	mk4.000295.03.01	146	1.00E-35	several similarly good hits; best BLAST to NCBI is Dmel CaM kinases.
	Hus1	NP_032342	*M. musculus*	mk4.000210.16.01	81	4.00E-16	confirmed by bi-directional BLAST
	MRT-2	NP_499521	*C. elegans*	mk4.000218.01.01	65	2.00E-11	see Rad1
	Plk2	NP_006613.2	*H. sapiens*	mk4.001509.00.01	119	8.00E-52	SmPlkc1
		NP_006613.2	*H. sapiens*	v31.007361	223	1.00E-56	SmPlkc2, poor annotation.
		NP_006613.2	*H. sapiens*	de_novo.18895.1	130	7.00E-29	SmPlkc3
		NP_006613.2	*H. sapiens*	v31.002811	159	2.00E-48	SmPlkc4, poor annotation.
		NP_006613.2	*H. sapiens*	de_novo.17941.1	180	8.00E-44	SmPlkc5
	Rad1	NP_035362	*M. musculus*	mk4.000218.01.01	102	1.00E-22	confirmed by bi-directional BLAST (also detects MRT-2)
	Rad9	NP_035367	*M. musculus*	mk4.008617.00.01	56	2.00E-08	confirmed by bi-directional BLAST
	Trip13/PCH-2	NP_081458.1	*M. musculus*	mk4.000527.02.01	239	6.00E-82	confirmed by bi-directional BLAST. Expressed (EST: DN315530) in juv. hermaphrodites

Table 1-2. BLAST search results of meiotic genes against the *S. mediterranea* genome (v.3.1)

category	protein name	accession #	organism	Smed homolog	bit score	E value	notes
cohesin	Rec8	NP_064386	*M. musculus*	no hits			
	SCC-1	NP_494836	*C. elegans*	mk4.000085.12.01	179	2.00E-45	same as Rad21
		NP_494836	*C. elegans*	mk4.000085.17.01	168	4.00E-42	mostly identical to mk4.000085.12.01 but with N-terminal extension. May be misannotated or a separate isoform
	Rad21	NP_033035.3	*M. musculus*	mk4.000085.12.01	202	1.00E-50	confirmed by bi-directional BLAST
	Scc3/Irr1	NP_012238	*S. cerevisiae*	mk4.005291.03.01	98	1.00E-20	BLAST to NCBI finds STAG3, Scc3
	Sgo1	NP_014716	*S. cerevisiae*	no hits			
	Smc1a	NP_062684.2	*M. musculus*	mk4.004021.04.01	164	3.00E-58	Smc1 (C-terminus) confirmed by bi-directional BLAST
		NP_062684.2	*M. musculus*	mk4.009253.01.01	80	2.00E-26	Smc1 (N-terminus) confirmed by bi-directional BLAST
		NP_062684.2	*M. musculus*	mk4.000285.05.01	126	3.00E-27	SMC-4 (condensin)
	Smc1b	NP_536718.1	*M. musculus*	mk4.004021.04.01	151	8.00E-41	Smc1 (C-terminus) confirmed by bi-directional BLAST
		NP_536718.1	*M. musculus*	mk4.009253.01.01	79	2.00E-23	Smc1 (N-terminus) confirmed by bi-directional BLAST
		NP_536718.1	*M. musculus*	mk4.000285.05.01	125	6.00E-27	SMC-4 (condensin)
	Smc3	NP_005436	*H. sapiens*	mk4.002068.00.01	442	1.00E-124	Smc3 (C-terminus) confirmed by bi-directional BLAST. Germline-enriched/expressed (Zayas et al. 2005)
		NP_005436	*H. sapiens*	mk4.021301.00.02	318	8.00E-87	Smc3 (N-terminus) confirmed by bi-directional BLAST
	Smc3	NP_005436	*H. sapiens*	mk4.003369.02.01	236	3.00E-62	Smc2 (condensin)/MIX-1(DCC)
		NP_005436	*H. sapiens*	mk4.032314.00.01	222	4.00E-58	Smc3 (central region) confirmed by bi-directional BLAST
	STAG3	NP_058660	*M. musculus*	mk4.005291.03.01	624	1.00E-179	no homology to very termini of protein. BLAST to NCBI also pulls up STAG1
DSB formation and repair	**CtIP/RBBP8**	Q99708.2	*H. sapiens*	EE281868	52	4.00E-05	confirmed by bi-directional BLAST
	DMC-1	NP_034189	*M. musculus*	mk4.015647.00.01	333	3.00E-92	Rad51, matches germline enriched/expressed Rad51 (Zayas et al. 2005)
		NP_034189	*M. musculus*	mk4.024315.01.01	153	8.00E-38	Rad51-like? or short? matches germline enriched/expressed Rad51 (Zayas et al. 2005)
	Mei4	NP_010963	*S. cerevisiae*	no hits			
	Mer2/Rec107	NP_012555.1	*S. cerevisiae*	no hits			
	Mre11	NP_071615	*R. norvegicus*	mk4.014816.00.01	461	1.00E-130	Mre-11A
		NP_071615	*R. norvegicus*	mk4.006709.01.01	458	1.00E-129	Mre-11
	Rad50	NP_033038.2	*M. musculus*	mk4.010022.01.01	184	1.00E-55	Rad50
	Rad51	NP_035364	*M. musculus*	mk4.015647.00.01	522	1.00E-149	Rad51, matches germline enriched/expressed Rad51 (Zayas et al. 2005)
		NP_035364	*M. musculus*	mk4.024315.01.01	216	1.00E-56	Rad51-like? or short? matches germline enriched/expressed Rad51 (Zayas et al. 2005)
	Rec102	NP_013433.2	*S. cerevisiae*	no hits			
	Rec104	NP_012027	*S. cerevisiae*	no hits			

Table 1-3. BLAST search results of meiotic genes against the *S. mediterranea* genome (v.3.1)

category	protein name	accession #	organism	Smed homolog	bit score	E value	notes
DSB formation and repair, contd.	Rec114	NP_013852.1	*S. cerevisiae*	no hits			
	Sae2	O74986.2	*S. pombe*	no hits			
	Ski8	NP_011302.1	*S. cerevisiae*	no hits			
	Spo11	NP_036176	*M. musculus*	v31.002904	49	2.00E-04	does not appear to be expressed
	Xrs2	NP_010657.1	*S. cerevisiae*	no hits			
heterochromatin	Clr4	NP_595186	*S. pombe*	mk4.001291.04.01	97	1.00E-20	
	Clr4	NP_595186	*S. pombe*	mk4.001106.07.01	94	9.00E-20	
	Rik1	NP_588204	*S. pombe*	no hits			
pairing	HIM-8	NP_501954	*C. elegans*	no hits			
	teflon	NP_523766	*D. melanogaster*	no hits			
recombination	**Hop2**	NP_011482	*S. cerevisiae*	mk4.002840.00.01	46	7.00E-06	poor homology, but BLAST to NCBI finds Hop2. Very small protein (just over 100aa, vs ~200aa Hop2), sequence may be incomplete
	Mer3/Hfm1	NP_011263	*S. cerevisiae*	mk4.002244.00.01	295	7.00E-80	several other proteins with >100 bitscores, all within first 3/4 (800aas) of the protein. Top BLAST to NCBI hits are all to “activating signal cointegrator 1 complex” ER translocators (?)
	Mnd1	NP_001088280	*X. laevis*	mk4.000603.04.01	147	2.00E-26	only homolog in the genome, bi-directional BLAST brings up all Mnd1 proteins. Smed protein seems to have a long C-terminal extension; may be incorrectly annotated
	Mlh1	NP_081086.2	*M. musculus*	v31.004482	229	2.00E-58	confirmed by bi-directional BLAST
	Mlh1	NP_081086.2	*M. musculus*	v31.066030	184	8.00E-45	Pms1/2 (?)
	MSH-5	NP_010127	*S. cerevisiae*	mk4.003196.04.01	115	4.00E-26	probably Msh2? Also top hit for mouse Msh5 (120, 1e-27)
	MSH-5	NP_010127	*S. cerevisiae*	mk4.064554.00.01	112	6.00E-25	bi-directional BLAST finds mainly bacterial MutS homologs
	MSH-5	NP_010127	*S. cerevisiae*	mk4.000110.01.01	111	8.00E-25	probably Msh6?
	Msh4	NP_114076	*M. musculus*	mk4.013659.03.01	101	9.00E-22	confirmed by bi-directional BLAST, but top Smed hit for Msh4 is Msh2 (mk4.003196.04.01,188 5e-48); next best is Msh6 (mk4.000110.01.01 136 2e-32); then the MutS, then Msh4 (??).
	Msh5	NP_038628	*M. musculus*	ASA.00077.01	110	1.00E-24	Msh5
	Rad3	NP_011098	*S. cerevisiae*	mk4.006459.01.01	531	1.00E-151	ERCC2 (nucleotide excision repair helicase)
	Rad3	NP_011098	*S. cerevisiae*	mk4.010255.00.01	365	1.00E-101	ERCC2
	Rad3	NP_011098	*S. cerevisiae*	mk4.009546.00.01	303	9.00E-83	ERCC2/XPD
synaptonemal complex (AEs and SCs)	**Hop1**	NP_012193	*S. cerevisiae*	mk4.001053.00.01. P20050		3.00E-09	mainly N-terminal (HORMA domain). Best hit for bi-directional BLAST is Hormad1 in mouse.
	HIM-3	NP_501078.1	*C. elegans*	no hits			
	HTP-1	NP_500799.2	*C. elegans*	no hits			
	HTP-2	NP_500981.3	*C. elegans*	no hits			
	HTP-3	NP_491458	*C. elegans*	mk4.001053.00.01	55	2.00E-08	same as Hop1 homolog.

Table 1-4. BLAST search results of meiotic genes against the *S. mediterranea* genome (v.3.1)

category	protein name	accession #	organism	Smed homolog	bit score	E value	notes
synaptonemal complex (AEs and SCs), cont'd.	Red1	NP_013365	*S. cerevisiae*	no hits			
	Sycp1 (central)	NP_003167	*H. sapiens*				lots of weak hits (myosins)
	Sycp2 (axial)	NP_055073	*H. sapiens*				a few weak hits
	Sycp3 (axial)	NP_035647	*M. musculus*	no hits			
	Syce1 (central)	Q9D495.1	*M. musculus*				lots of weak hits (myosins etc.)
	Syce2 (central)	Q505B8.1	*M. musculus*	no hits			
	SYP-1 (central)	NP_507145	*C. elegans*	mk4.002231.04.01	64	7.00E-11	several ok matches but bi-directional BLAST does not bring up SYP-1
	SYP-2 (central)	NP_504462	*C. elegans*	no hits			
	SYP-3 (central)	NP_492345	*C. elegans*	no hits			
	Tex12 (central)	NP_079963	*M. musculus*	no hits			
	Zip1	NP_010571	*S. cerevisiae*	mk4.075285.00.01	103	3.00E-22	best hit for BLAST to NCBI is Spc110p (NP_010643.1 Inner plaque spindle pole body (SPB) component)
	Zip2	NP_011265	*S. cerevisiae*	mk4.006638.00.01	44	2.00E-04	best hit for BLAST to NCBI is NP_055023.1, dentin sialophosphoprotein preproprotein [Homo sapiens]
telomeres	ccp1	NP_012992	*S. cerevisiae*	no hits			
	ccq1 (smc)	NP_588210	*S. pombe*	mk4.016111.00.01	49	5.00E-06	four other similarly poor hits, all to C-terminus. Best BLAST to NCBI is Dmel "zipper" myosin-like protein.
	EST1A	NP_001002764	*M. musculus*	mk4.006651.00.01	135	1.00E-31	
	Kms1	NP_594198	*S. pombe*	no hits			several poor hits, all have better homology to myosin heavy chain
	menin	NP_062081	*R. norvegicus*	mk4.002429.02.01	145	2.00E-35	SmedGD splits into two isoforms, but assume just one protein.
	mlp1	NP_013021	*S. cerevisiae*	mk4.025889.00.01	127	4.00E-29	smooth muscle myosin?
	mlp1	NP_013021	*S. cerevisiae*	ASA.00038.01 (mk4.001750.02.01 ,mk4.001750.01.01)	123	4.00E-28	regular myosin?
	mlp1	NP_013021	*S. cerevisiae*	ASA.00034.01 (mk4.002240.06.01 ,mk4.002240.07.01)	199	8.00E-51	several others with bitscores >100. Bi-Directional Blast comes up with "chromsome segregating ATPases" (SMC domain) ?
	mlp2	NP_012117	*S. cerevisiae*	ASA.00034.01	162	1.00E-39	see mlp1
	mlp2	NP_012117	*S. cerevisiae*	mk4.001035.01.01	159	8.00E-39	see mlp1
	mlp2	NP_012117	*S. cerevisiae*	ASA.00038.01	155	1.00E-37	see mlp1
	ndj1	NP_014537	*S. cerevisiae*	no hits			
	Rap1	NP_061848	*H. sapiens*	no hits			
	Rif1	NP_780447.4	*M. musculus*	mk4.001959.00.01	68	3.00E-11	bi-directional BLAST does not support Rif1 homology (hits nucleolar and coiled body protein)

Table 1-5. BLAST search results of meiotic genes against the *S. mediterranea* genome (v.3.1)

category	protein name	accession #	organism	Smed homolog	bit score	E value	notes
telomeres (contd.)	tankyrase-binding protein	NP_203754	*H. sapiens*	no hits			
	tankyrase1	NP_780300	*M. musculus*	mk4.000820.07.01	437	1.00E-123	good homology across whole protein, confirmed by bi-directional BLAST
	tankyrase1	NP_780300	*M. musculus*	mk4.000820.04.01	224	1.00E-58	splice isoform?
	telomerase associated protein 1	NP_033377	*M. musculus*	mk4.022086.00.01	161	3.00E-39	confirmed by bi-directional BLAST
	telomerase associated protein 1	NP_033377	*M. musculus*	mk4.001386.00.01	123	8.00E-28	confirmed by bi-directional BLAST
	telomerase associated protein 1	NP_033377	*M. musculus*	mk4.027082.00.01	119	9.00E-27	confirmed by bi-directional BLAST
	TERT	NP_033380	*M. musculus*	no hits			
	TRF1	NP_033378	*M. musculus*	no hits			
	TRF1-interacting factor 2	NP_663751	*M. musculus*	no hits			
	TRF1-interacting protein PIN2	NP_082504	*M. musculus*	no hits			
	TRF2	NP_033379	*M. musculus*	no hits			
other	**MEI-1/katanin**	NP_492257	*C. elegans*	mk4.002295.02.01	235	2.00E-62	confirmed by bi-directional BLAST. Lots of other good matches (AAA ATPases) all to C-terminus.
	MEI-2	NP_491894	*C. elegans*	no hits			
	Spo13	NP_011878	*S. cerevisiae*	no hits			
	Spo22	NP_012192	*S. cerevisiae*	no hits			
	UBC-9	CE09784	*C. elegans*	mk4.001799.00.01	248	6.00E-67	
	UBC-9	CE09784	*C. elegans*	mk4.028470.00.01	246	2.00E-66	
	UBC-9	CE09784	*C. elegans*	mk4.014363.03.01	191	1.00E-49	splice variant 1
	UBC-9	CE09784	*C. elegans*	mk4.014363.03.02	156	2.00E-39	splice variant 2
	ZYG-9	CE20707	*C. elegans*	mk4.019504.00.01	180	3.00E-45	

Table 2-1. Candidate germline enriched genes identified by comparative studies

predicted function	mRNA/cDNA	Homolog description	GenBank no.	notes	in testes	in ovaries
AE/SC		Spermatogenesis associated 1 [Rattus norvegicus]	AAH79224	* could not find in genome		
AE/SC	mk4.018041.00.01	spermatogenesis associated 18 homolog [Homo sapiens]	NP_660306.1			
cell cycle	mk4.029895.00.01	Cyclin B1 interacting protein 1 [Homo sapiens]	AAH01218.1	weak homology to Cst9p (sumo E3 required for SC assembly)		
cell cycle	mk4.008575.01.01	Cyclin B1 interacting protein 1 [Homo sapiens]	AAH01218.1	weak homology to Cst9p (sumo E3 required for SC assembly)		
cell division (?)	DN301795	bridging integrator 3 [Rattus norvegicus]	NP_001013204.1			
chromatin mod	mk4.007164.02.01	chromosome condensation protein G [Homo sapiens]	NP_071741.2	C-terminus		
chromatin mod	mk4.007164.01.01	chromosome condensation protein G [Homo sapiens]	NP_071741.2	N-terminus		
chromatin mod	DN296566	DPY30 domain containing 1 [Homo sapiens]	NP_620167.1			
chromatin mod	DN305359	DPY30 domain containing 1 [Homo sapiens]	NP_620167.1			
chromatin mod	DN315009	FtsJ methyltransferase domain containing 2 [Danio rerio]	NP_956427			
chromatin mod	DN306647	H2A histone family, member Y isoform 1 [Homo sapiens]	NP_613075.1			
cytoskeleton	de_novo.20267.1	ankyrin and armadillo repeat containing [Mus musculus]	NP_795954.1			
cytoskeleton	DN295423	ankyrin repeat and MYND domain containing 1 isoform 1 [Homo sapiens]	NP_057636.2			
cytoskeleton	mk4.008324.00.01	ankyrin repeat and MYND domain containing 1 isoform 1 [Homo sapiens]	NP_057636.2			
DNA repair		MORC family CW-type zinc finger 2 [Homo sapiens]	NP_055756.1			
MTs (kinesin)	DN315360	spermatogenesis associated 6 precursor [Homo sapiens]	NP_061946.1			
MTs (kinesin)	DN313586	spermatogenesis associated 6 precursor [Homo sapiens]	NP_061946.1			
NE	**de_novo.28457.1**	**LEM domain containing 3 [Homo sapiens]**	**NP_055134.2**	**yes**		
pachytene		spermatogenesis associated, serine-rich 1 [Homo sapiens]	NP_659463.1	* could not find in genome		
recombination/ checkpoint	AY068379	DnaJ homolog (Subfamily A Member 1)				
recombination/ checkpoint	AY067277	DnaJ/spermatogenesis apoptosis protein (Subfamily B Member 4)	NP_705842.2	axoneme related		
recombination/ checkpoint	DN301846	spermatogenesis associated 4 [Ciona intestinalis]	NP_001029005.1|			
spindle/MTs	DN315777	inscuteable [Mus musculus]	NP_776128.2			
spindle/MTs	**mk4.004247.01.01**	**multiple asters 1 [Homo sapiens]**	**AAQ15051**			
spindle/MTs	**mk4.000165.13.02**	**multiple asters 1 [Homo sapiens]**	**AAQ15051**			
spindle/MTs	DN308206	Spag8 protein [Rattus norvegicus]	AAH79031			
spindle/MTs	DN309411	spindle assembly 6 [Danio rerio]	NP_998603			
spindle/MTs	mk4.008627.02.01	Tekt2 protein [Xenopus tropicalis]	AAH80153			
spindle/MTs	mk4.000010.08.01	Tekt2 protein [Xenopus tropicalis]	AAH80153			
TM	DN300963	transmembrane protein 106A [Rattus norvegicus]	NP_001020138			
TM	DN304449	transmembrane protein 106A [Rattus norvegicus]	NP_001020138			
TM	DN302196	Transmembrane protein 45b [Xenopus tropicalis]	AAH84505			
TM	EC616064	Transmembrane protein 45b [Xenopus tropicalis]	AAH84505			

Table 2-2. Candidate germline enriched genes identified by comparative studies

predicted function	mRNA/cDNA	Homolog description	GenBank no.	notes	in testes	in ovaries
	DN315266	bromo domain containing 2 (M. musculus)	NP_034368		y	n
		Itpk1 (inositol kinase) [Xenopus laevis]	AAH54977.1			
	DN294441	KIAA0953 protein (H. sapiens)	AAH49384		y	n
	DN311405	lymphocyte cytosolic protein 1 (M. musculus)	NP_032905		y	n
	DN315261	plastin 1 (H. sapiens)	NP_002661		y	n
	DN295646	potassium channel modulatory factor 1 (H. sapiens)	NP_064507		y	y
	DN304366	**Rad51 (C. pyrrhogaster)**	**BAA78377**		**y**	**y**
	DN312988	RANGAP1 protein (H. sapiens)	AAH41396		y	y
	DN304066	similar to germinal histone H4 gene (R. norvegicus)	XP_225391		y	y
	DN311193	T-plastin (R. norvegicus)	CAA50037		y	n
	DN298167	transcription factor Dp-2 (E2F dimerization partner 2) (H. sapiens)	AAR89905		y	n
	de_novo.29745.1	zinc finger, matrin type 4 isoform a [Homo sapiens]	NP_078921.1			

References

Assenmacher, N., and Hopfner, K. (2004). MRE11/RAD50/NBS1: complex activities. Chromosoma *113*, 157-166.

Bhatt, A. M., Lister, C., Page, T., Fransz, P., Findlay, K., Jones, G. H., Dickinson, H. G., and Dean, C. (1999). The DIF1 gene of Arabidopsis is required for meiotic chromosome segregation and belongs to the REC8/RAD21 cohesin gene family. Plant J *19*, 463-472.

Bishop, D. K., Park, D., Xu, L., and Kleckner, N. (1992). DMC1: a meiosis-specific yeast homolog of E. coli recA required for recombination, synaptonemal complex formation, and cell cycle progression. Cell *69*, 439-456.

Bogdanov, Y. F., Dadashev, S. Y., and Grishaeva, T. M. (2003). In silico search for functionally similar proteins involved in meiosis and recombination in evolutionarily distant organisms. In Silico Biol. (Gedrukt) 3, 173-185.

Bolcun-Filas, E., Hall, E., Speed, R., Taggart, M., Grey, C., de Massy, B., Benavente, R., and Cooke, H. J. (2009). Mutation of the mouse Syce1 gene disrupts synapsis and suggests a link between synaptonemal complex structural components and DNA repair. PLoS Genet 5, e1000393.

Bolcun-Filas, E., Costa, Y., Speed, R., Taggart, M., Benavente, R., de Rooij, D. G., and Cooke, H. J. (2007). SYCE2 is required for synaptonemal complex assembly, double strand break repair, and homologous recombination. J Cell Biol 176, 741-747.

Börner, G. V., Kleckner, N., and Hunter, N. (2004). Crossover/noncrossover differentiation, synaptonemal complex formation, and regulatory surveillance at the leptotene/zygotene transition of meiosis. Cell *117*, 29-45.

Cherry, S. M., Adelman, C. A., Theunissen, J. W., Hassold, T. J., Hunt, P. A., and Petrini, J. H. J. (2007). The Mre11 complex influences DNA repair, synapsis, and crossing over in murine meiosis. Curr Biol *17*, 373-378.

Colaiacovo, M. P., MacQueen, A. J., Martinez-Perez, E., McDonald, K., Adamo, A., La Volpe, A., and Villeneuve, A. M. (2003). Synaptonemal complex assembly in C. elegans is dispensable for loading strand-exchange proteins but critical for proper completion of recombination. Dev Cell *5*, 463-474.

Costa, Y., Speed, R., Ollinger, R., Alsheimer, M., Semple, C. A., Gautier, P., Maratou, K., Novak, I., Höög, C., Benavente, R., et al. (2005). Two novel proteins recruited by synaptonemal complex protein 1 (SYCP1) are at the centre of meiosis. J Cell Sci 118, 2755-2762.

Eijpe, M., Heyting, C., Gross, B., and Jessberger, R. (2000). Association of mammalian SMC1 and SMC3 proteins with meiotic chromosomes and synaptonemal complexes. J Cell Sci *113 (Pt 4)*, 673-682.

Fukuda, T., Daniel, K., Wojtasz, L., Toth, A., and Höög, C. (2010). A novel mammalian HORMA domain-containing protein, HORMAD1, preferentially associates with unsynapsed meiotic chromosomes. Exp Cell Res 316, 158-171.

Golubovskaya, I. N., Hamant, O., Timofejeva, L., Wang, C. R., Braun, D., Meeley, R., and Cande, W. Z. (2006). Alleles of afd1 dissect REC8 functions during meiotic prophase I. J Cell Sci *119*, 3306-3315.

Harper, N.C., Jover Gil, S., Rillo, R., Assaf, Z.J., Bhalla, N., and Dernburg, A. F. (2011). A Polo-like kinase orchestrates meiotic chromosome dynamics in C. elegans. Nature Cell Biology, in press.

Hamer, G., Gell, K., Kouznetsova, A., Novak, I., Benavente, R., and Höög, C. (2006). Characterization of a novel meiosis-specific protein within the central element of the synaptonemal complex. J Cell Sci 119, 4025-4032.

Ishiguro, K., Kim, J., Fujiyama-Nakamura, S., Kato, S., and Watanabe, Y. (2011). A new meiosis-specific cohesin complex implicated in the cohesin code for homologous pairing. EMBO Rep *12*, 267-275.

Klein, F., Mahr, P., Galova, M., Buonomo, S. B., Michaelis, C., Nairz, K., and Nasmyth, K. (1999). A central role for cohesins in sister chromatid cohesion, formation of axial elements, and recombination during yeast meiosis. Cell *98*, 91-103.

Lee, J., and Hirano, T. (2011). RAD21L, a novel cohesin subunit implicated in linking homologous chromosomes in mammalian meiosis. J Cell Biol *192*, 263-276.

Li, J., Harper, L. C., Golubovskaya, I., Wang, C. R., Weber, D., Meeley, R. B., McElver, J., Bowen, B., Cande, W. Z., and Schnable, P. S. (2007). Functional analysis of maize RAD51 in meiosis and double-strand break repair. Genetics *176*, 1469-1482.

Lynn, A., Soucek, R., and Börner, G. V. (2007). ZMM proteins during meiosis: crossover artists at work. Chromosome Res *15*, 591-605.

Malik, S., Ramesh, M. A., Hulstrand, A. M., and Logsdon, J. M. (2007). Protist homologs of the meiotic Spo11 gene and topoisomerase VI reveal an evolutionary history of gene duplication and lineage-specific loss. Mol Biol Evol *24*, 2827-2841.

Mazina, O. M., Mazin, A. V., Nakagawa, T., Kolodner, R. D., and Kowalczykowski, S. C. (2004). Saccharomyces cerevisiae Mer3 helicase stimulates 3"-5" heteroduplex extension by Rad51; implications for crossover control in meiotic recombination. Cell *117*, 47-56.

Nakagawa, T., and Ogawa, H. (1999). The Saccharomyces cerevisiae MER3 gene, encoding a novel helicase-like protein, is required for crossover control in meiosis. EMBO J *18*, 5714-5723.

Page, S. L., Khetani, R. S., Lake, C. M., Nielsen, R. J., Jeffress, J. K., Warren, W. D., Bickel, S. E., and Hawley, R. S. (2008). Corona is required for higher-order assembly of transverse filaments into full-length synaptonemal complex in Drosophila oocytes. PLoS Genet 4, e1000194.

Pelttari, J., Hoja, M. R., Yuan, L., Liu, J. G., Brundell, E., Moens, P., Santucci-Darmanin, S., Jessberger, R., Barbero, J. L., Heyting, C., et al. (2001). A meiotic chromosomal core consisting of cohesin complex proteins recruits DNA recombination proteins and promotes synapsis in the absence of an axial element in mammalian meiotic cells. Mol Cell Biol *21*, 5667-5677.

Pittman, D. L., Cobb, J., Schimenti, K. J., Wilson, L. A., Cooper, D. M., Brignull, E., Handel, M. A., and Schimenti, J. C. (1998). Meiotic prophase arrest with failure of chromosome synapsis in mice deficient for Dmc1, a germline-specific RecA homolog. Mol Cell *1*, 697-705.

Reddien, P. W., Bermange, A. L., Murfitt, K. J., Jennings, J. R., and Sánchez Alvarado, A. (2005). Identification of genes needed for regeneration, stem cell function, and tissue homeostasis by systematic gene perturbation in planaria. Dev Cell *8*, 635-649.

Robb, S. M., Ross, and Sánchez Alvarado, A. (2007). SmedGD: the Schmidtea mediterranea genome database. Nucleic Acids Res.

Rockmill, B., Sym, M., Scherthan, H., and Roeder, G. S. (1995). Roles for two RecA homologs in promoting meiotic chromosome synapsis. Genes Dev *9*, 2684-2695.

Sugawara, H., Iwabata, K., Koshiyama, A., Yanai, T., Daikuhara, Y., Namekawa, S. H., Hamada, F. N., and Sakaguchi, K. (2009). Coprinus cinereus Mer3 is required for synaptonemal complex formation during meiosis. Chromosoma *118*, 127-139.

Tanaka, K., Miyamoto, N., Shouguchi-Miyata, J., and Ikeda, J. (2006). HFM1, the human homologue of yeast Mer3, encodes a putative DNA helicase expressed specifically in germ-line cells. DNA Seq. *17*, 242-246.

Wang, K., Tang, D., Wang, M., Lu, J., Yu, H., Liu, J., Qian, B., Gong, Z., Wang, X., Chen, J., et al. (2009). MER3 is required for normal meiotic crossover formation, but not for presynaptic alignment in rice. J Cell Sci *122*, 2055-2063.

Wang, Y., Stary, J. M., Wilhelm, J. E., and Newmark, P. A. (2010). A functional genomic screen in planarians identifies novel regulators of germ cell development. Genes Dev *24*, 2081-2092.

Wojtasz, L., Daniel, K., Roig, I., Bolcun-Filas, E., Xu, H., Boonsanay, V., Eckmann, C. R., Cooke, H. J., Jasin, M., Keeney, S., et al. (2009). Mouse HORMAD1 and HORMAD2, two conserved meiotic chromosomal proteins, are depleted from synapsed chromosome axes with the help of TRIP13 AAA-ATPase. PLoS Genet *5*, e1000702.

Wood, A. J., Severson, A. F., and Meyer, B. J. (2010). Condensin and cohesin complexity: the expanding repertoire of functions. Nat Rev Genet *11*, 391-404.

Yoshida, K., Kondoh, G., Matsuda, Y., Habu, T., Nishimune, Y., and Morita, T. (1998). The mouse RecA-like gene Dmc1 is required for homologous chromosome synapsis during meiosis. Mol Cell *1*, 707-718.

Zayas, R. M., Hernández, A., Habermann, B., Wang, Y., Stary, J. M., and Newmark, P. A. (2005). The planarian Schmidtea mediterranea as a model for epigenetic germ cell specification: analysis of ESTs from the hermaphroditic strain. Proc Natl Acad Sci USA *102*, 18491-18496.

Chapter VI. Materials and methods development for *S. mediterranea*

At the outset of these studies, limited tools were available for cytological analyses in *S. mediterranea*. Both *in situ* and immunofluorescence approaches had been used to examine whole animals, and a number of antibodies with useful localization had been described (Robb and Sánchez Alvarado, 2002; Sánchez Alvarado et al., 2002). However, the methods used for immunostaining in whole mount animals were generally unsuitable for preserving morphology at the level of detail and magnification required for a close analysis of meiotic events. Furthermore, DNA FISH approaches, which were necessary to examine homolog pairing, had never been attempted in whole tissue from planarians, although some FISH studies in chromosome spreads and spermatid nuclei from *Polycelis tenuis* had been published (Joffe et al., 1996; 1998).

In this section, I will discuss the various methods that I have tried and give the protocols that I have found yield the best results for chromosome FISH and immunofluorescence for the analysis of spermatogenesis in tissue cryosections (which are ideal as they allow multiple instances of FISH/IF analysis in tissue from the same animal). I will also describe the generation of antibodies and FISH probes used as tools throughout this study, and the TUNEL protocol used. Finally, I will describe the methods I have used for planarian culture and molecular biology, electron microscopy, and other procedures referenced in the previous chapters.

Killing and fixation methods

The first step of cytological analysis in *S. mediterranea* is to kill the worms. This step is not trivial, as the worms are very flexible tend to curl or hyperextend due to muscle spasms while they are dying, both of which complicate whole animal staining or cryosectioning. The planaria also curl upon direct freezing, making a preliminary killing step necessary. Curling can be reduced somewhat by chilling the animals on ice (in 0.75 X Montjuic culture medium) for 3-5 minutes prior to killing, which seems to relax the muscles.

I have primarily used either shaking for 5 minutes in ice cold 2% HCl or rocking for 5-10 minutes in 5-10% N-acetyl cysteine in PBS, to kill the animals. N-acetyl cysteine has the advantage of removing the mucus layer that surrounds the planarian. I have not found that this improves immunofluorescence staining of cryosections, although it significantly improves RNA in situ hybridization in whole animals (Pearson et al., 2009). Other modifications for staining presented in that paper, including solubilization with SDS and NP-40, and reduction with DTT, did not consistently improve immunofluorescence in sections.

Fixation of the animals can be carried out immediately after killing, or the animal can be frozen and sectioned prior to fixation. I prefer to use the latter method because I feel that it

reduces the variability introduced by differences in animal size and conformation upon death (i.e., degree of extension/stretching), which are a major complication — in larger animals, the percent formaldehyde and length of fixation required for preservation of interior tissues may cause overfixation of tissue closer to the epidermal surface. It is preferable to rinse the animal a few times in cold PBS, transfer to cryosectioning medium, and then flash-freeze. The animals can be stored frozen in cryosectioning medium at -20°C or -80°C for at least several months, with the block stored in an Eppendorf tube to prevent dehydration of the cryosectioning medium. If animals are fixed prior to cryosectioning (4% formaldehyde in PBS, 30 minutes), a clearing step with 100% ethanol or methanol (≥2 hours at -20°C) may be used to reduce background fluorescence. The bleaching step used in most whole mount methods (8% H_2O_2 in methanol or PBS, overnight at RT under light; Sánchez Alvarado and Newmark, 1999) does not improve imaging in sections. It should also be noted that even when controlling for animal size and performing fixation after sectioning, differences in animal thickness, and probably other factors that are more difficult to control (e.g., amount last eaten, age, mucus content of the epidermis), can generate variable results with the same fixation protocol in different animals. This has been a significant challenge to working with these animals.

Sectioning at 30 µm offers good antibody/probe penetration and imageability and ensures that each section will have a sufficient number of whole spermatocyte nuclei to allow quantitative analysis. I typically begin collecting sections 500-700 µm from the first tail section and take 6-10 sections per slide. The number of total slides per animal depends on animal size, but generally a mature animal will yield 10-15 slides. Slides should be kept frozen after sections are collected and until ready for fixation, although some melting/drying during section collection is unavoidable.

Fixation for 20 minutes in 4% formaldehyde is preferable for FISH (either alone or in combination with IF) as it offers superior preservation of chromosome morphology. FISH treatment seems to improve IF in some cases, although this has not been observed consistently. Antigen retrieval after fixation, either with sodium citrate or Trilogy reagent (Cell Marque), typically improves immunofluorescence results but can be destructive to chromosome morphology. Trilogy should not be used in conjunction with FISH as it creates very diffuse signals. Alternatively, a lighter fixation (as low as 10 minutes in 1% formaldehyde) without antigen retrieval can be used. Optimal fixation methods may differ for different antigens. The best protocol I have used is reproduced on the following page.

Protocol for planarian fixation, sectioning, and FISH/IF

1. Collect planaria (starved for 1 week) in a glass vial. Chill on ice 3-5 minutes.
2. Remove planaria water and replace with ice-cold 2% HCl. Shake 2 minutes, ice 1 minute, shake 1 minute, ice 1 minute. (Alternatively, kill in 5-10% N-acetyl cysteine freshly dissolved in PBS, with rocking).
3. Remove HCl and rinse several times briefly with PBS.
4. Remove PBS and add OCT cryosectioning medium. Transfer worms to freezing mold in OCT and flash freeze. Remove frozen block from mold (can store at -80°C in Eppendorf tube).
5. Cryosection at 20-30 µm. Keep slides at -20°C or colder.
6. Fix slides in 4% formaldehyde (in PBS), 20 minutes.
7. Wash slides in PBS, 2 x 5 minutes.
8. (Optional, but recommended if no FISH) Antigen retrieval: 7 minutes at 60°C in Trilogy reagent (Cell Marque) or 20 minutes at 95°C in sodium citrate buffer (10mM trisodium citrate, 0.5% Tween-20, pH 6.0). Cool ~15 minutes, and rinse slides in PBS + 0.5% Triton X for 5-10 minutes.
9. Continue with FISH protocol, or begin IF protocol directly.

FISH protocol

1. Wash slides 2 x 5 minutes in 2X SSC.
2. Apply 100 ng/µl RNAse A in 2X SSC (50 µl on Parafilm) and incubate at 37°C, 1 hour.
3. Incubate 3 minutes at 80-91°C with FISH probe mixture: 200-400 pg/µl probe, 1:10 *C. elegans* genomic DNA or other generic DNA in hybridization buffer (10% dextran sulfate, 50% formamide, 2X SSCT) on a coverslip.
4. Incubate overnight at 37°C in humid chamber.
5. Remove coverslips from slides with a razor under 2X SSC.
6. Fill two coplin jars with 50% formamide/2X SSCT. Transfer slides to one jar, and place both jars at 37°C, 10 minutes.
7. Transfer slides to the other jar and incubate at 37°C another 10 minutes.
8. Rinse 5 minutes with 2X SSCT. Continue with IF protocol if desired, or stain with DAPI (500 ng/ml in 2X SSCT), wash, and mount.

Immunofluorescence protocol

1. Block 1.5 hours with 0.5% IgG-free BSA + 0.45% fish gelatin in PBSTx (PBS + 0.5% Triton X).
2. Apply primary antibody diluted in block, incubate overnight at 4°C (or >1 hour at room temperature).
3. Wash 30 minutes with PBSTx.
4. Wash 10 minutes with PBST.
5. Apply secondary antibody (1:500, Jackson Immunoresearch) diluted in block, incubate 1 hour at room temperature.
6. Wash 3 x 10 minutes (alternating PBSTx and PBST).
7. Stain 10 minutes with DAPI, 500 ng/ml in PBSTx.
8. Wash 2 x 10 minutes (or longer) with PBST.
9. Mount in NPG glycerol mounting media, seal coverslip with nailpolish and view under microscope.

FISH probe synthesis

All probes for FISH were synthesized from unlabeled oligonucleotides or digested PCR products by amino-allyl end labeling and subsequent reaction with Alexa 488, 555, or 647 NHS esters, as described in (Dernburg et al., 1996).

The planarian telomere repeat sequence TTAGGG was identified previously (Joffe et al., 1996). Telomere probes were generated from an LNA oligonucleotide (5'-G+GT +TAG +GG+T TAG +GG+T TAG +GG-3') that was synthesized by IDT (Coralville, IA). Hybridization to metaphase spreads and cryosections confirmed that this probe recognizes the ends of all four chromosomes (Fig. 1A).

The rDNA probe was generated from a PCR product amplified from genomic DNA with the 18STIF and 28SR primers described in (Carranza et al., 1996) and digested with a mixture of restriction enzymes (AluI, HaeIII, MseI, MspI, RsaI, and MboI; New England Biosciences). Hybridization to metaphase spreads and cryosections showed that this probe recognizes a locus at one end of Chromosome II (Fig. 1B,C).

The CEN-2 probe sequence (5'-GCT ATC ATG TAG AGA ATC AAA-3') was selected randomly from a pair of highly abundant 158 and 159 bp genomic repeats that were identified and kindly shared by Jarrod Chapman. Tests in metaphase chromosome spreads revealed that this sequence hybridized strongly with the centromere of Chromosome II and weakly with the centromere of Chromosome III (Fig. 1D); the signals from Chr. III are weak in spermatocytes, however, and easily distinguishable from the brighter Chr. II foci (Fig. 1E). Several other random sequences were selected from the longer centromeric repeats and tested, but hybridized with too many loci in testis sections to be useful for assaying homolog pairing (e.g., Fig. 1G). The full sequences of these repeats is shown in Figure 3, and probe sequences that were tested are highlighted. All candidate CEN probe sequences are given in Table 1.

I also took several other approaches in efforts to identify chromosome-specific FISH probes, which were unsuccessful. These attempts are summarized below:

(A) **Simple repeat probes**. A subset of all possible 5- and 6-mer sequences were chosen based on their representation in the *S. mediterranea* genome according to RepBase (http://www.girinst.org/repbase). Oligonucleotides of varying lengths were designed for a target Tm of >60°C, ordered from IDT, and labeled as for other FISH probes. These sequences are given in Table 2. Only the sequence corresponding to the telomere repeat was successful.

(B) **Complex repeat probes.** Candidate regions were identified computationally (by Dustin Cartwright) based on the following criteria: 1) repeat region at least 2000 bases in total length; 2) repeat present in at least 2.5 copies; 3) repeat size under 2000; and 4) repeat not present at significant copy number outside of the identified region. Oligonucleotide sequences corresponding to the top nine candidates were designed in order to achieve a

target T_m of >60°C, ordered from IDT, and labeled as for other FISH probes. These sequences are given in Table 3. None of these sequences yielded successful probes.

(C) **Single copy probes.** Target regions with low repeat content were identified computationally by Dustin Cartwright. I designed primers to amplify these regions in 2-3 kb fragments by tiled PCR. I initially chose three regions to target (v31.000238:22664..77888, 20 kb targeted; v31.000308:101536..158100, 30 kb targeted; v31.000234:149942..192280, 38 kb targeted). Unfortunately, I was unable to amplify more than 10 kb cumulative product for any of them, possibly due to errors in the genome assembly or to failure of genomic PCR due to the high repeat content of the genome. This strategy was therefore not pursued further.

(D) **Fosmid probes**. Fosmids were selected after BLASTing forward and reverse paired end sequences (downloaded from GenBank) to the *S. mediterranea* genome sequence (v3.1). Sequences were deemed usable if the start and end points mapped to the same contig and were sufficiently far apart (>20 kB; 40 kB target) and if the primary sequence from SmedGD did not have significant gaps (>100 bp missing sequence). The fosmids selected are given in Table 4 and were kindly provided by Pietr de Jong.

Fosmid DNA was amplified with CopyControl Fosmid Induction Solution and purified using the FosmidMax purification kit as indicated by the manufacturer protocol (Epicentre Biotechnologies, Inc.). Purified fosmid DNA was digested as for other FISH probes, followed by an extra digestion step with Taqα1 to fragment A/T rich sequences, and aa-dUTP labeled and dye conjugated as for other FISH probes. When this was unsuccessful, I attempted to amplify the fosmids using DOP-PCR with 0.2 µg/µl BsmI long primer (5'-TAT CCC AAC GAT GCG AAT GCN NNN NCA GG-3') in a 50 µl reaction volume containing 10 mm Tris-Cl pH 8.9, 50 mM KCl, 1.5 mM $MgCl_2$, 0.1% Tx-100, 0.01% gelatin, 0.2 mM each dNTP, 5 ng fosmid template and 5 U NEB Taq 2000 and the following PCR program: 4 minutes at 93°C, 3 cycles (30 seconds at 94°C, 1 minute at 30°C, ramp to 72°C at 0.2˚C/second, and hold 90 seconds), 3 cycles (30 seconds at 94°C, 1 minute at 30°C, 2 minutes at 72°C), 36 cycles (20 seconds at 94°C, 1 minute at 56°C, 2 minutes at 72°C), 10 minute extension at 72°C. The resulting product was digested and labeled as for other FISH probes. I also tried direct-labeling DOP-PCR to amplify the fosmids, following the protocol of Backx and colleagues (Backx et al., 2008). None of these approaches yielded a reliable single-copy probe.

All FISH probes were initially tested in cryosections to determine their likely utility in homolog pairing and then validated by FISH to chromosome spreads. The protocol for chromosome spreading (reproduced on the following page) was adapted from S. Carranza and kindly translated by Sara Jover-Gil.

Protocol for FISH to metaphase spreads of planarian chromosomes

1. Cut 1 mm tail fragments from 5-10 planaria.
2. Regenerate the tails under normal growth conditions (0.75X montjuic buffer, 18°C) for 2-4 days
3. Place tails in a 0.15% colchcine/0.75X montjuic solution for 8-12 hours (10 µM nocodozole works too)
4. Transfer pieces to 1% sodium citrate at 37°C for 20 minutes.
5. Remove sodium citrate and replace with 3:1 MeOH:glacial acetic acid.
6. Store at -20°C for at least 2 hours, up to several months.
7. Remove tail pieces from fix and place them in 1 ml 60% glacial acetic acid until the tails are degraded, approximately 20 minutes. Pipetting up and down at ~10 minutes facilitates this process.
8. Drop this solution onto clean slides (3-4 drops per slide) and allow to air dry. Slides may be stored dry at -20°C for several months.
9. Treat slides for 1 hour at 37°C with 100 ng/µl RNAse in 2X SSC. Add 50 µl per slide, via parafilm.
10. Rinse 2 x 5 minutes in 2X SSC solution at RT.
11. (optional) Treat slides with a solution of 2 mg pepsin in 500 ml 10 mM HCl, 10 minutes at RT. (I did not find that this step appreciably improved FISH for my probes, but it might be useful for other sequences).
12. Rinse 5 minutes in 2X SSC.
13. Incubate 3 minutes at 80-91°C with FISH probe mixture: 200-400 pg/µl probe, 1:10 *C. elegans* genomic DNA or other generic DNA in hybridization buffer (10% dextran sulfate, 50% formamide, 2X SSCT) on a coverslip.
14. Incubate overnight at 37°C in humid chamber.
15. Remove coverslips from slides with a razor under 2X SSC.
16. Fill two coplin jars with 50% formamide/2X SSCT. Transfer slides to one jar, and place both jars at 37°C, 10 minutes.
17. Transfer slides to the other jar and incubate at 37°C another 10 minutes.

18. Rinse 5 minutes with 2X SSCT.
19. Stain 10 minutes with DAPI, 500 ng/ml in 2X SSCT.
20. Wash 2 x 10 minutes (or longer) with 2X SSCT.
21. Mount in NPG glycerol mounting media, seal coverslip with nailpolish and view under microscope.

Antibody Generation and Testing

Another key step for assaying meiosis in *S. mediterranea* was to generate antibodies to allow the detection of key meiotic structures (e.g., chromosome axes, DSBs, synaptonemal complex, the nuclear envelope, crossovers) by immunofluorescence.

As shown in previous sections, we generated rabbit antibodies specific to fragments of SMED-HOP1 (aa 298-397) and SMED-SUN1 (aa 92-191) by synthetic genetic immunization through the company SDI (Newark, DE). We also generated an antibody specific to SMED-RAD51 (aa 1-100), which failed to recognize DSBs in my hands. The SMED-RAD51 immunofluorescence shown throughout this work was performed by Youbin Xiang, using a guinea pig antibody against full-length RAD51 protein generated by Cocalico Biologicals (Reamstown, PA).

We also generated a rabbit antibody specific to SMED-LAMINB2 (mk4.001379.07.01; aa 298-397) by synthetic genetic immunization through SDI in an attempt to generate a nuclear envelope marker. Immunostaining with this antibody showed good localization to the nuclear envelope in somatic cells, but none to the nuclear envelope of spermatocytes (Fig. 3A).

A number of publically available antibodies are useful markers in *S. mediterranea* (Robb and Sánchez Alvarado, 2002); among these, the tubulin antibody stains testes nicely, though only under ideal fixation conditions (Fig. 3). Several other commercially available antibodies are also useful for staining testes, including phospho-histone H3(pSer10) and anti-Sm monoclonal antibody Y12 (Pisetsky and Lerner, 1982), which label neoblasts and spermatogonia (Wang et al., 2007).

Methods for investigating germline apoptosis (TUNEL)

As discussed in Chapter II, germline apoptosis can be induced by a variety of errors in meiosis, and I was interested in examining this phenomenon in wild type and RNAi animals. Attempts to recognize apoptotic cells by immunofluorescence to cleaved caspase 3 were

unsuccessful, and homologs to other typical markers of apoptosis (e.g., Annexin V, CED-4) could not be found in the *S. mediterranea* genome.

In 2009, Pellettieri and colleagues published a technique for examining apoptosis in whole asexual worms using TUNEL staining with the commercially available Chemicon ApopTag kit (Pellettieri et al., 2009). The larger sexual worms proved somewhat recalcitrant to this method in whole mounts, but staining of cryosections was frequently successful (see Chapter II, Fig. 5). Conveniently, the elevated apoptosis at amputation sites reported by Pellettieri et al. can be used as an internal control for the success of the staining. However, it should be noted that bright TUNEL staining of maturing spermatids (described in Chapter II) was not observed in all animals where TUNEL was observed at the cut site, although it was not clear whether this is a biological phenomenon or due to variability in the protocol. Furthermore, the same caveats for variability in results based on animal size, etc. discussed above for FISH and IF apply here. The TUNEL protocol that I have used is reproduced on the next page.

TUNEL to detect apoptosis in *S. mediterranea* cryosections

1. Cut large (mature) planaria 1-2 mm from the head and allow to regenerate 4-5 hours in 0.75X montjuic buffer.
2. Kill animals 10 minute in 10% N-acetyl cysteine **in PBS** on nutator.
3. Rinse briefly 2-3 times with PBS.
4. Remove PBS and replace with OCT medium as quickly as possible.
5. Freeze animals in OCT in molds as quickly as possible. Store at -80°C.
6. Cut longitudinal cryosections at 20-30 µm. May store at -20°C for several days before proceeding.
7. Rinse away OCT in 2-3 brief changes of PBS.
   (note: at this point, proceed as indicated in Chemicon ApopTag Red Kit protocol for cryosections)
8. Fix 10 minutes in 1% formaldehyde in PBS.
9. Wash 2 x 5 minutes in PBS.
10. Post-fix 5 minutes in cold 2:1 EtOH:glacial acetic acid (pre-chilled to -20°C).
11. Wash 2 x 5 minutes in PBS.

12. Aspirate PBS and apply equilibration buffer (100 µl per 22 x 40mm parafilm). Incubate for at least 10 seconds at RT.

13. Aspirate equilibration buffer and apply working strength TdT enzyme mix (7:3 reaction buffer:TdT enzyme mix; 50 µl per 22 x 40mm parafilm).

14. Incubate 1 hour at 37°C in humid chamber.

15. Remove parafilms and transfer to coplin jar containing working strength stop/wash buffer (1 ml stop/wash concentrate + 34 ml MilliQ water). Agitate 15 seconds and incubate 10 minute at RT.

16. Rinse 3 x 1 minute in PBS.

17. Aspirate PBS and apply working strength anti-dig conjugate (68 µl block : 62 µl anti-dig concentrate; 50 µl per 22 x 40mm parafilm). Incubate for 30 minute in humid chamber at RT, shielded from light.

18. Wash 4 x 2 minutes in PBS.

22. Stain 10 minutes with DAPI, 500 ng/ml in PBSTx.

23. Wash 2 x 10 minutes (or longer) with PBST.

24. Mount in NPG glycerol mounting media, seal coverslip with nailpolish and view under microscope.

General molecular biology and planarian culture

Planarian culture

Animals were kept in 0.75X Montjuic buffer (1.2 mM NaCl, 0.75 mM $CaCl_2$, 0.75 mM $MgSO_4$, 0.075 mM $MgCl_2$, 0.075 mM KCl, 0.9 mM $NaHCO_3$) at 18°C in the dark, in plastic Tupperware containers, as indicated by Phil Newmark (personal communication). I occasionally experimented with different light/dark cycles (12:12 and 18:6) in an effort to increase mating and fertility but this did not have any obvious effect. Different culture densities also did not produce obvious effects on mating habits or fertility. Animals were fed organic, free-range calf liver paste (stored frozen at -80°C) 2-3 times per week and water was changed after each feeding. Containers were cleaned once per week or as necessary. Cultures were perpetuated by amputating animals into 2-3 mm lateral fragments; amputated animals were allowed to regenerate 10 days under normal conditions before feeding was resumed. Animals were always starved for one week before proceeding with other experiments.

Genomic DNA purification

Genomic DNA for PCR and other applications was prepared from whole worms using a standard phenol chloroform extraction. I generally used small or sick animals for efficiency. One small animal (4 mm when stretched) weighs about 10 mg and yields about 1 µg genomic DNA. Prior to phenol chloroform extraction, worms are cut in half to break the epidermis, homogenized with a plastic pestle in an Eppendorf tube in DNA isolation buffer (100 mM NaCl, 10 mM Tris pH 8, 25 mm EDTA, 0.5% SDS, 0.1 mg/ml proteinase K), and incubated at 50°C overnight (12-16 hours). Extraction with an equivalent volume of phenol chloroform is followed by a basic ethanol precipitation with 1/10 volume 3 M NaOAc and 2.5-3 volumes 95% ethanol. For some applications, subsequent treatment with RNase was desirable; genomic DNA frequently co-purifies with a band of RNA that runs around 900 bp.

RNAi plasmid construction and feeding

Bulk cDNA was prepared from sexually mature animals with an RNeasy kit (Qiagen) and RETROscript kit (Ambion) according to the manufacturers' instructions. One large, sexually mature animal (~1 cm when stretched) weighs about 20 mg and yields between 5-10 µg RNA. RNAi target fragments of 500-700 bp were amplified from the cDNA with transcript-specific primers (described in Table 5) in a 50 µl reaction volume with NH_4 PCR buffer (final concentration: 16 mM ammonium sulfate, 67 mM Tris HCl pH 8.8, 0.01% Tween-20), 0.2 mM

each dNTP, 2 mM $MgCl_2$, 1 µl RT product template, 2 µm each primer, and 5 U Taq polymerase using the following touch-down PCR program: 1:30 minutes at 93°C, 10 cycles (20 seconds at 94°C, 30 seconds at 56°C, decrease by 0.3˚C/cycle, 72°C for 1 minute), 20 cycles (20 seconds at 94°C, 30 seconds at 53°C, 1 minute + 3 seconds/cycle at 72°C), 5 minute extension at 72°C. The target fragments were checked on a 2% agarose gel and isolated by gel purification (Qiagen) or ethanol precipitation (described above), as appropriate. Purified fragments were cloned into the pPR244 plasmid using the Gateway system, transformed into HT115 cells, and confirmed by DNA sequencing.

Cells were grown overnight at 37°C in LB medium containing kanamycin and tetracycline (50 µg/ml each), then diluted 1:10 in LB medium without antibiotics and allowed to grow another 1.5 hours. Expression of double-stranded RNA was induced for 4 hours with 0.4 mm IPTG in liquid culture and cells were pelleted in 1.5 ml aliquots and frozen for future use. For RNAi feeding, a bacterial pellet equivalent to 1.5 ml of cells was mixed with ~40 mg of calf liver paste and 2 µl of red food coloring (adapted from Gurley et al., 2007); this paste was fed to the planarians three times in the first week of knockdown and 1-2 times per week thereafter. Animals were fixed four weeks from the date of the first feeding unless otherwise noted. An empty pPR244 vector was used as a negative control.

Other materials and methods

Electron microscopy

Sexually mature planaria were cut in half under fixative (2% glutaraldehyde, 4% paraformaldehyde in 100 mM Na cacodylate buffer) and exposed to microwaves at low power under vacuum (1 minute microwave with 22 Hg vacuum, 1 minute vacuum only, 1 minute microwave) to allow infiltration of the fixative. The fixative was exchanged for 3% glutaraldehyde and the sample was stored at 4°C overnight. The glutaraldehyde was washed out with three five minute washes with 0.1 M sodium cacodylate and stained with 1% osmium tetraoxide for 1 hour. After two 10 minute washes with 0.1 M sodium cacodylate and three 10 minute washes with MilliQ water, the animals were stained with 0.5% uranyl acetate overnight at 4°C. Stained samples were dehydrated in a cold ethanol series (15 minutes each in 30%, 50, 75, 80, 95, 95, 100, 100, 100%) and washed twice for 5 minutes with 100% acetone. Resin infiltration with an acetone/epon araldite series (10, 25, 40, 60, 60, 80, 80, 100, 100, 100%) was performed in a microwave under vacuum and samples were embedded in 100% epon araldite resin. Thin sections were cut at 70 nm (approximately 1-2 mm from the tail tip), post-stained with uranyl acetate and lead citrate, and imaged with an FEI Tecnai 12 transmission electron microscope at 100 kV.

X-ray irradiation

X-ray irradiation experiments were performed by Youbin Xiang. Animals (regenerated for at least 4 months) were exposed to a dose of 10 Gy at a rate of 1.0 Gy/minute and allowed to recover under normal conditions (0.75 X Montjuic at 18°C, in the dark) for 5 hours before processing for immunofluorescence.

Statistical analyses

Weighted averages (per section) and standard deviation of meiotic stage distribution and bouquet formation were calculated in Apple Numbers. Between-group differences were calculated from these values with unpaired t-tests using GraphPad online tools (http://graphpad.com/quickcalcs/ttest2.cfm). For CEN-2 pairing distances, within-group (section-to-section and animal-to-animal) statistical similarity was confirmed with Kruskal-Wallis tests in Kaleidagraph. Between-group differences were analyzed with Kolgorov-Smirnov tests to detect differences in mean/median and distribution shape (http://www.physics.csbsju.edu/stats/KS-test.html).

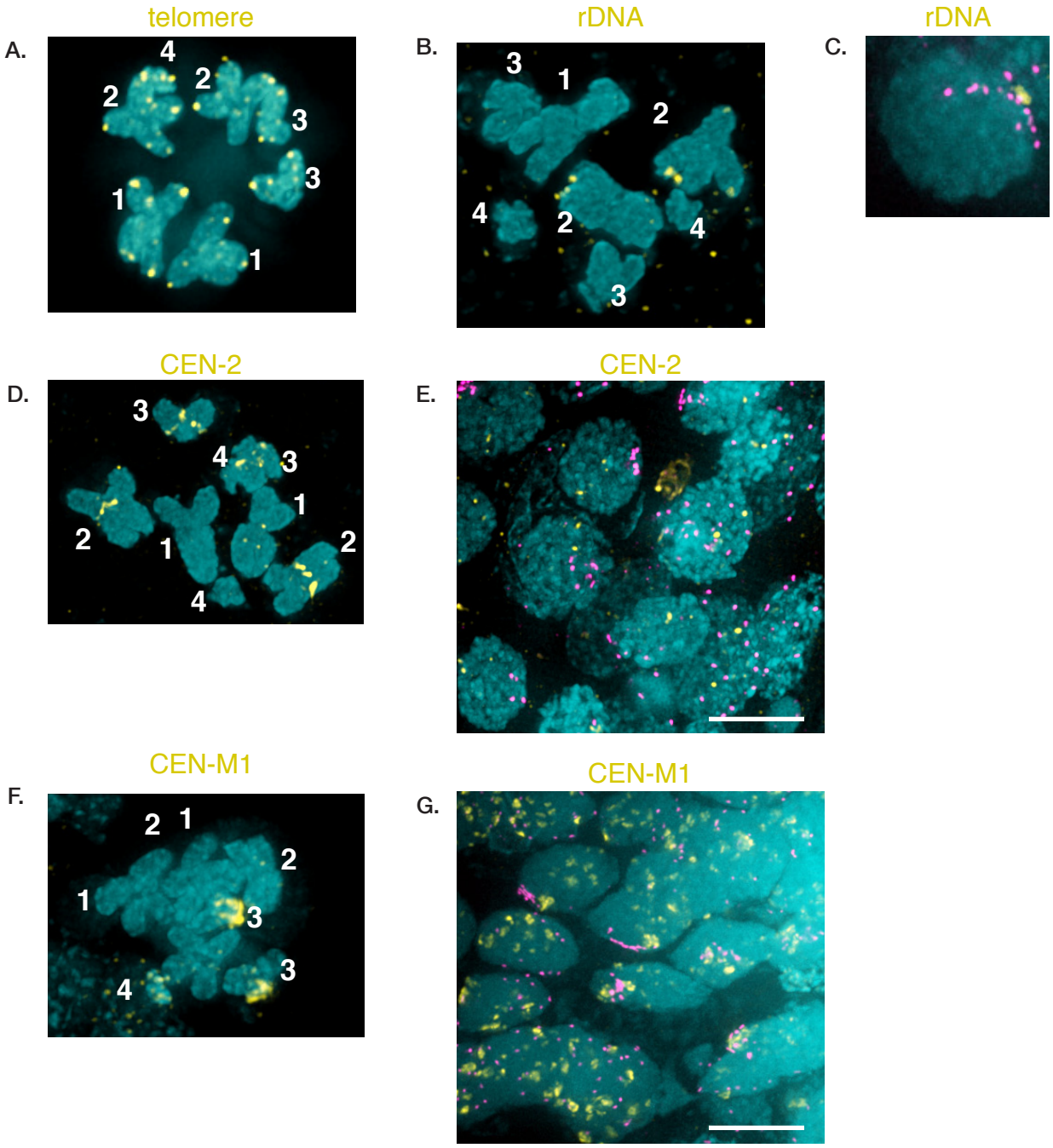

Figure 1. FISH probe validation.
(A) Telomere FISH to spread metaphase chromosomes. **(B)** rDNA FISH to spread metaphase chromosomes. **(C)** rDNA FISH to a spermatocyte nucleus. Pink, telomere FISH; yellow, rDNA FISH; blue, DAPI. **(D)** CEN-2 FISH to spread metaphase chromosomes. **(E)** Testis section showing CEN-2 FISH in spermatocyte nuclei. Pink, telomere FISH; yellow, CEN-2 FISH; blue, DAPI. Scale bar = 5µm. **(F)** CEN-M1 FISH to spread metaphase chromosomes. **(G)** Testis section showing CEN-M1 FISH in spermatocyte nuclei. Pink, telomere FISH; yellow, CEN-M1 FISH; blue, DAPI. Scale bar = 5µm.

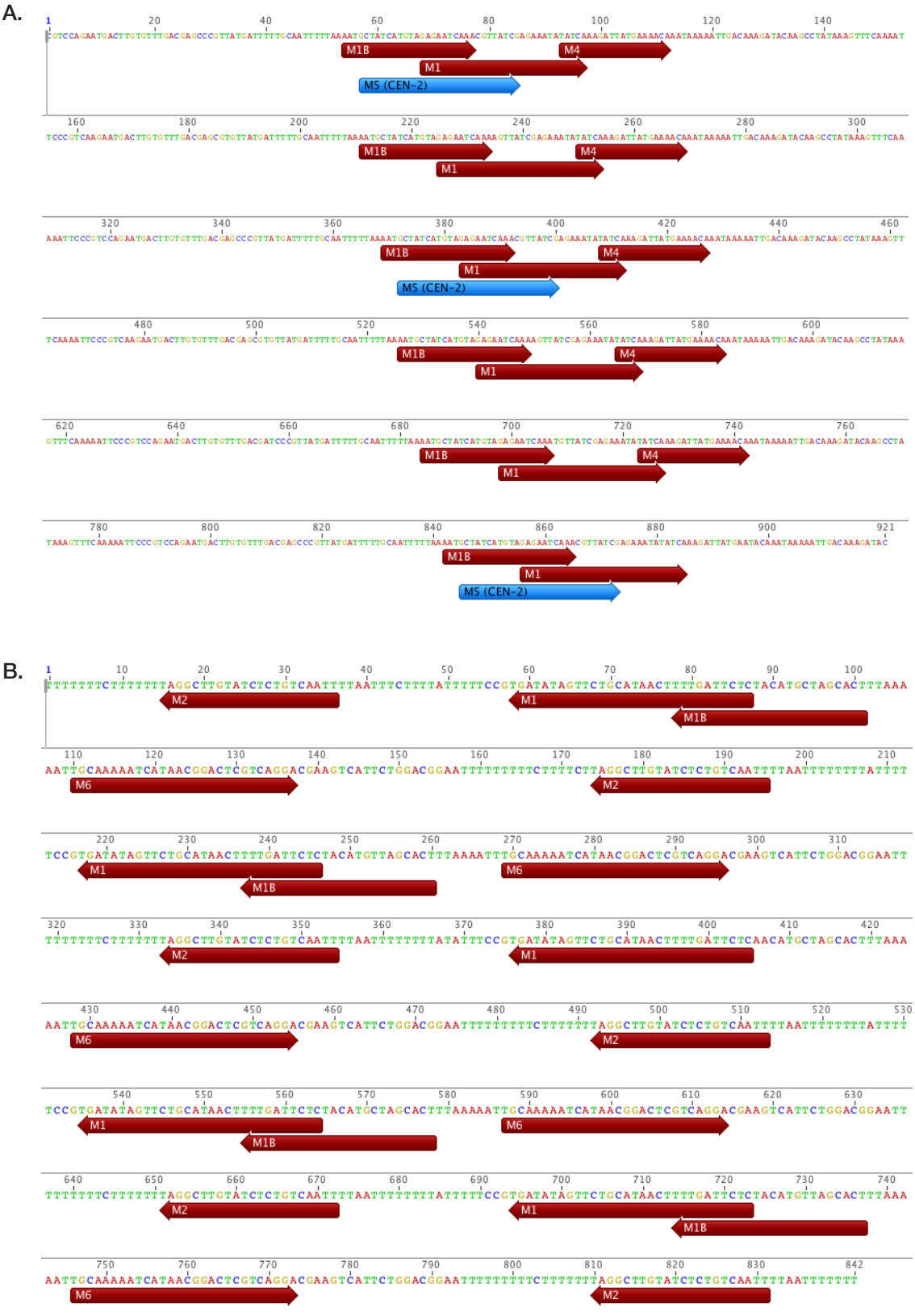

Figure 2. CEN repeat sequences
(A) 158 bp repeat. (B) 159 bp repeat. Probe sequences that were tested with FISH are highlighted.

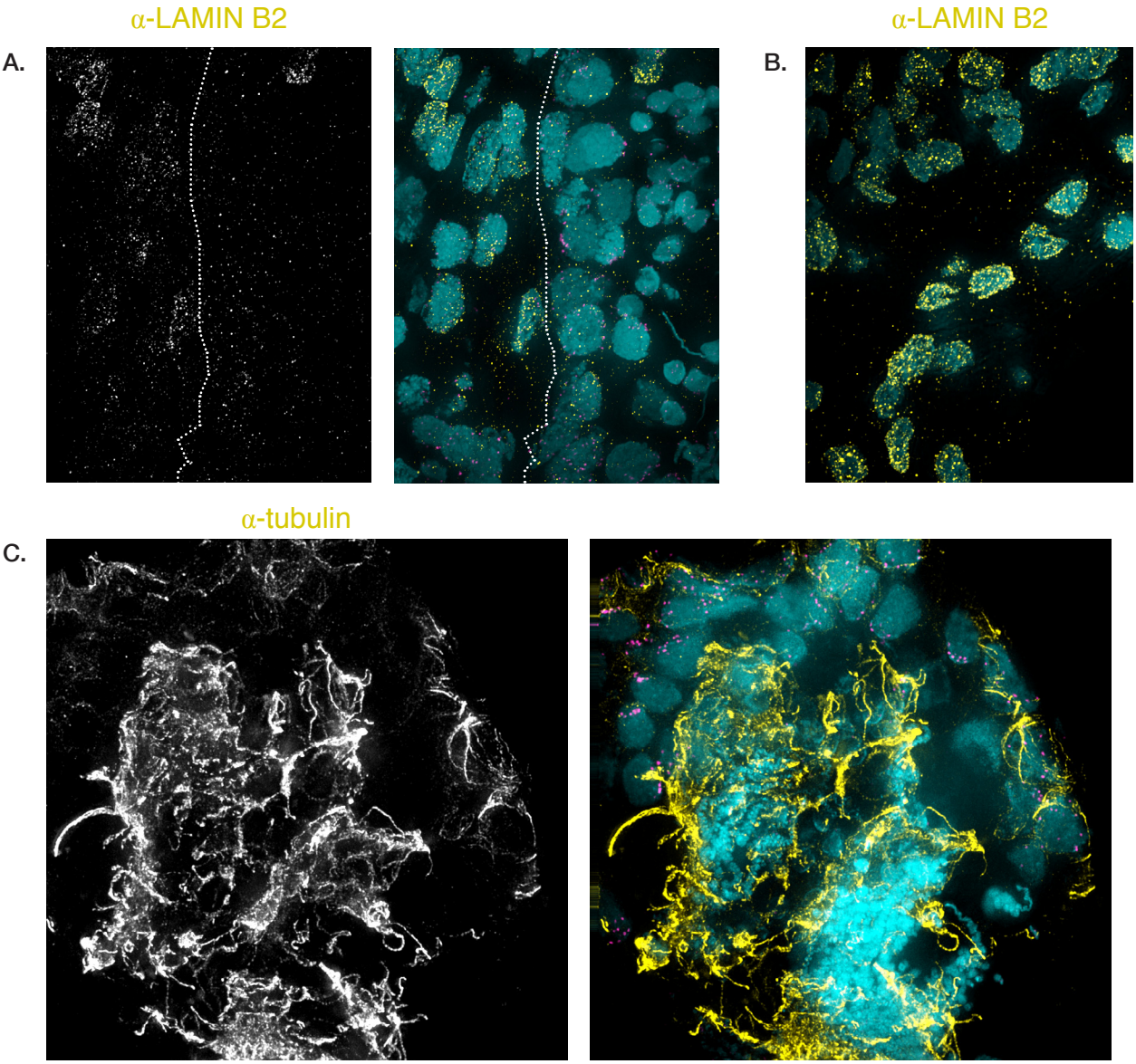

Figure 3. Other antibodies for use in *S. mediterranea*.
(A, B) LaminB2 staining of testes and adjacent tissues (A) and the epidermis (B) demonstrating the absence of LaminB2 in spermatocyte nuclear envelopes. **(C)** Tubulin staining of testis cross section. Yellow, α-tubulin; pink, telomere FISH; blue, DAPI.

Table 1. CEN candidate sequence probes

sequence name	sequence	# in 158bp	# in 159bp	results
CEN/alt cen M1	GAGAATCAAAHGTTATSSAGAAMTATATCA			localizes to short arm of Chr. III, maybe also Chr. IV in spreads. Widespread staining in spermatocytes.
CEN/alt cen M1B	ARTGCTADCATGTAGAGAATCAAA			same as M1
CEN/alt cen M2	AATTGACAGARATACAAGCCTA			same as M1
CEN M4	TATCAAAGATTATGAAAACA			no staining
CEN M5	**GCTATCATGTAGAGAATCAAACGTTATCG**			**CEN-2**
CEN M6	TGCAAAAATCATAACGGACTCGTCAGGA			no staining
Seq96	CCATTAAGATACATACGAGTAAATTCAAC	n/a	n/a	no staining
Seq96b	AAATACTCCGGATGGTCATCTTAAAA	n/a	n/a	no staining

Table 2. Simple repeat probes

Repeat	oligo	length	%GC	abundance (RepBase)	date tested	results
TAAAAA	AATAAAAATAAAAATAAAAATAAAAATAAAAATAAAAATA	40	0%	0.46%	2/5/10	no
TATACA	CATATACATATACATATACATATACATATACATATACA	38	18%	0.33%	2/5/10	no
TCACCA	TCACCATCACCATCACCATCACCATCACCA	30	50%	0.24%	2/5/10	no
TGGCCC	TGGCCCTGGCCCTGGCCCTGGCCT	24	79%		2/5/10	no
CAAAAA	CAAAAACAAAAACAAAAACAAAAACAAAAACAAAAAC	37	19%	0.99%	2/5/10	no
CCCCAA	CCAACCCCAACCCCAACCCCAACC	24	67%	0.23%	2/5/10	no
CCCCCA	CCACCCCCACCCCCACCCCCACCC	24	83%	0.44%	2/5/10	no
CCCGAA	CCGAACCCGAACCCGAACCCGAAC	24	67%	0.25%	2/5/10	no
CCCTAA	CCTAACCCTAACCCTAACCCTAACCCTAAC	30	50%	1.51%	2/5/10	telomere
CCCTCA	CCTCACCCTCACCCTCACCCTCAC	24	67%	0.10%	2/5/10	no
GAAAAA	GAAAAAGAAAAAGAAAAAGAAAAAGAAAAAGAAAAAG	37	19%	0.60%	2/5/10	no
GAGACA	GAGACAGAGACAGAGACAGAGACAGAGACA	30	50%	0.06%	2/5/10	no
GCCCCA	CCCAGCCCCAGCCCCAGCCCCAGC	24	83%	0.12%	2/5/10	no
GCCCCC	GCCCCCGCCCCCGCCCCCGCCCCC	24	100%	0.33%	2/5/10	no
GGAGAA	GAGAAGGAGAAGGAGAAGGAGAAGGAGAAG	30	50%	0.18%	2/5/10	no
GGGAGA	GGAGAGGGAGAGGGAGAGGGAGAG	24	67%	0.15%	2/5/10	no
GGGGGA	GGGGAGGGGGAGGGGGAGGGGGAG	24	83%	0.09%	2/5/10	no
CAAAA	CAAAACAAAACAAAACAAAACAAAAC	26	23%	2.34%	2/23/10	no
CAAA	CAAACAAACAAACAAACAAACAAAC	25	28%	1.98%	2/23/10	no
AC	CACACACACACACACACACACAC	23	52%	17.94%	2/23/10	no
AG	GAGAGAGAGAGAGAGAGAGAGAG	23	52%	5.38%	2/23/10	no
GAAA	GAAAGAAAGAAAGAAAGAAAGAAAG	25	28%	2.74%	2/23/10	no
GCCCA	CAGCCCAGCCCAGCCCAGCCCAG	23	78%	1.94%	2/23/10	no

Table 3. Complex repeat probes

Repeat name	oligo	length	%GC	size of repeat region	date tested	results
Contig18998	AATGAAATGAAATGAAATGAAATGA	25	20%	8,999	8/11/09	no
Contig3692a	TAATTACACAATCGACATCGGAAAGTACTC	30	36%	11,648	8/11/09	no
Contig3692b	CAACTGGAACAGCAACTACTTCACCAATAA	30	40%	11,648	8/11/09	no
Contig200	TAGTTGCAGACCGAAGTAGTTGCAGACCGAAG	32	50%	7,478	8/11/09	no
Contig8466a	TTTTAATTTTAAACAAAGACCATGACTCATTCAAGGT	37	27%	19,013	8/11/09	no
Contig24668	TGGAATGGAATGAAATGGAATGGAATGAAA	30	33%	5,190	8/11/09	no
Contig23367	GACGTAGTTGTAGTAGACGTAGTTGTAGTA	30	40%	5,115	8/11/09	no
Contig27402	ATTCCATTCCATTCCATTCCATTCC	25	40%	5,108	8/11/09	no
Contig31919	CATTTCATTTCATTTCATTTCATTTCATTT	30	20%	5,060	8/11/09	no

Table 4. Fosmid probes

Plate	fwd read	rev read	contig #	start	end	length (bp)
18A02	1314586544	1314590888	v31.000923	74724	116420	41696
18A14	1314586550	1314587013	v31.000272	88276	148998	60722
18C22	1314586565	1314587025	v31.001662	35945	78111	42166
18G04	1314586575	1314587032	V31.001609	36444	72316	35872
18I22	1314586589	1314587042	v31.002694	47401	88149	40748
18K02	1314586591	1314587043	v31.000795	52244	93695	41451
18K18	1314586599	1314587049	v31.000609	80628	118950	38322
18M12	1314586607	1314587055	v31.000577	39551	68856	29305
18M22	1314586612	1314587060	v31.001546	24785	66708	41923
18O20	1314586620	1314587068	v31.001479	50351	82442	32091

Table 5-1. Primers used to amplify cDNA sequences (for RNAi)

gene name	Smed accession #	fwd primer	reverse primer	amplicon size (bp)
a-tubulin	mk4.001685.05.01	GAACTGGTTCGGGATTTCAA	TGCGGTTGAGTTGGTAATCA	718
Atm1A	mk4.002177.01.01	TGCCAAGTTCCCTTGGTTTA	CACTCAAAATTCCAAGGGTGA	520
Atm1B	mk4.008791.03.01	CAGCAAAAATCGACATTGGA	CAATCGACAATTGGGTCAAA	490
BLM	mk4.002999.00	GTCGAGACCAAGAAACAGCAC	AGATGGTGGAAAAATCGCTCT	507
Cyclin B1 interacting protein 1	mk4.029895.00.01	TTGACTTCGTTGAGGTGGAA	CCGAAAGTCGAATCAGGAGA	499
DnaJ/apoptosis protein	AY067277	TTGGAGAAAAATCAGGCAATG	GGGTCTTTCCCTCACACTCA	586
Dpy-30 homolog 1	DN305359	GGGAAGCTTTCCGTCTTCAT	TCGCGATCAGCTACGTCTTA	504
Dpy-30 homolog 2	DN296566	TCGGCCAAAAGATCCAATAG	GGGTCCTCAAGATTCTCAGC	501
Est1A	mk4.006651.00.01	CCTCTTCAATTACCGGCTGA	TACCGCACAAGAAATCACCA	485
FtsJ	DN315009	TATGTTGTGGAAACGCCAGA	TCAATGCGATTCGTGTCACT	504
Hop1	mk4.001053.00.01	GCAGTTGTGATTGGATTTTATACAG	CAGTTTCAACATGACCTAATTTA	511
inscuteable	DN315777.1	TGCGATACGGTGAAAATTGA	TGCCGCTTCGAAAAGAATAG	594
LEM domain containing 1	de_novo.28457.1	AAAAACCGGTTCTGACGTTG	GTAACCGGCGATGTTCAGTT	481
Mer3/Hfm1	mk4.002244.00	CGGCAGTGGATTTAATTCAGA	TTCTAACAACACGCGAACCTT	500
Mnd1	mk4.000603.04.01	AATTCGAATGCTTGAATTTTTC	CATGGTTCCAGTGTGTCCAG	481
Mre11	mk4.006709.01.01	GAATCGATCCCGAGTACAACA	GGCTAACAAAACCGTTGACAA	499
Msh4	mk4.013659.03	ACAACAATTCATCGCCGTTA	CCAAAAGACGGTTGCAAAAT	435
Msh5	ASA.00077.01	TTCGTCGTCAAAGAAGGAGTG	ATTGTGTTCACCCGCAATTAG	497
multiple asters 1	mk4.004247.01.01	CAAATTCCGCAGCCAGTTAT	CTTTGGGGCATTGTCTTTGT	571
nanos	mk4.008570.00	GGAAGCATGGCCTGAAAAGC	TTCGCAAAGAGAGTCATATTGAAC	
non-SMC condensin D2	mk4.003927.01	GAAAAAGTACACGGCGATGAA	AATTCTCCAAATGTGGGGTTC	488
Rad51	mk4.015647.00	GGGTCCTTTGCCTTTGAAAAAAT	CCTTCTCCACCACCCAAATCAAC	495
Rad51	mk4.015647.00	GGTATAAGTGCACAGGACATTAAAAAGTTG	CTGTTCCCGACAAACCGTACCGTTCAG	505
RTEH	mk4.000667.08.01	TCTGTGCAGCATTAGCTTGG	ATCGGCTGAATCGAACATTT	494
Smc1A	mk4.004021.04.01	AATTGCCAGTTCACAAAAACG	TTTTTGGGTATCGCACACAAT	496
Smc1C	mk4.000285.05.01	CGATGCTCAGAAGTGTGTTGA	TTGTTCTGTGGATTTCGGTTC	520
Smc3	mk4.002068.00.01	AAAGCGACGATTGGAAACAC	CGCCAGTGAAACTCACTTCA	605
SPAG-6 (1)	de_novo.20267.1	GGAAGCAATTGCGATTTTTG	GATGGACACCATTTCTGCAA	571
SPAG-6 (2)	de_novo.20267.1	TCGAGCAATTAGCGAGGAAT	CATAGAAAGCTGCGCAATGA	562
SPAG18	mk4.018041.00.01	GGTATTGGAAGACGCAGCAT	GGACATTTCCCATGCAATTC	532
Spag8	DN308206	TCACGGTAATCAAGCATTTGTT	ATTGGTTTGAGGAGCGAGAA	535
spermatogenesis associated 4	DN301846	TTCCAGAAAATTTGATTCATGG	GCATTTGTCAACTTGCTTCG	510
spermatogenesis associated 6	DN315360	AATCGATCTAGTGACGATGGTT	TTTTACCAGGTGATTGTCTTCG	403
spindle assembly 6	DN309411	TTGGTGCATTTGGACAAAAA	CTTGGTCGTGCTTTGATTTG	489
Sun1	mk4.001469.07	GGAGTATCTGTTGTAAGAAATG	CAGATTTTACCAAAAAAAACAACGC	509
Sun2	mk4.001275.01.01	TTATACAGCCAGGAAATCAGC	AAGGCGGTGTGGAGGACT	405
Sun3	mk4.003039.01.01	CCCAAGTGTGTTGTGTGGAC	TTGGATCTCCATGTTCGTCA	509
tankyrase	mk4.000820.07.01	TACGCCCGGAATGTAGGTAA	CACTTGTGCTCCCATTTCAA	532
Tap1B	mk4.001386.00.01	ATGCCATTTGAAAGGTTTCCT	AAGTTTAGCAACGTCCCCATT	484
Tekt2-a	mk4.008627.02.01	ATAATCACCAGCGAGCCAAC	CTCTGGCTTTTTCGCATTTC	513
Tekt2-b	mk4.000010.08.01	GTCGTGCAACGAGAATTGAA	CTTCCCATTCCTGAGGATCA	534
Trip13/PCH-2	mk4.000527.02.01	GATTTGTGGGATTCGCTTGT	GTCCAATGCACGCTGACTTA	723
XPF	mk4.000684.07	TTTGATCGAACGGTAATTTGG	ACGTTTCAAGCGGCTTTATTT	495
Plkc1	mk4.001509.00.01	ACGAAATCCTCCGTTTCAAG	TCACTCCTGTTGATCCGTCA	581
Plkc2	v31.007361:12834..15539	CCAGTGGTTTACCGACGAGT	AAGGCAACCTGATCATGGAC	666

Table 5-2. Primers used to amplify cDNA sequences (for RNAi)

gene name	Smed accession #	fwd primer	reverse primer	amplicon size (bp)
Plkc3	de_novo.18895.1	CAACAAAGCCAACCCAGAAT	GCATTTCCGGAGCCATATAA	530
Plkc4	v31.002811:7575..8527	TTATTAGGACGAGTAAAGCGTCA	AGGGAAGATTTCCGGTTGTT	684
Plkc5	de_novo.17941.1	TATCGTGTCCTCCTCGCTTT	AAACAAATGGCACTCGGTTC	553
Tfc1	mk4.000440.02.01	GGATGGAAGAAGCGAGACAG	CAATTTCTTCAGTGCGTTCG	609
Tfc2	mk4.000675.02.01	AAAGAATGCGCGCAAAATAC	CTGCTTCCAGCATTGTCGTA	699
Tfc4	mk4.002345.03.01	AAAGAACCGCGAGAAAGACA	TGGGCTTCGAGTTCTTTGTT	696
Tfc5	mk4.018982.00.01	AACCGCATACCATAGCGAAG	CTGCTCCCACATTTTCCAAT	700

* all forward primers include the sequence 5’-ggg gac aag ttt gta caa aaa agc agg ct-3’ and all reverse primers include the sequence 5‘-ggg gac cac ttt gta caa gaa agc tgg gt-3’ for Gateway cloning.

References

Backx, L., Thoelen, R., van Esch, H., and Vermeesch, J. R. (2008). Direct fluorescent labelling of clones by DOP PCR. Molecular Cytogenetics *1*, 3.

Carranza, S., Giribet, G., Ribera, C., Baguña, J., and Riutort, M. (1996). Evidence that two types of 18S rDNA coexist in the genome of Dugesia (Schmidtea) mediterranea (Platyhelminthes, Turbellaria, Tricladida). Mol Biol Evol *13*, 824-832.

Dernburg, A. F., Sedat, J. W., and Hawley, R. S. (1996). Direct evidence of a role for heterochromatin in meiotic chromosome segregation. Cell *86*, 135-146.

Gurley, K., Rink, J., and Sánchez Alvarado, A. (2007). {beta}-Catenin Defines Head Versus Tail Identity During Planarian Regeneration and Homeostasis. Science.

Joffe, B. I., Solovei, I. V., and Macgregor, H. C. (1996). Ends of Chromosomes in Polycelis tenuis (Platyhelminthes) have telomere repeat TTAGGG. Chromosome Res *4*, 323-324.

Joffe, B. I., Solovei, I. V., and Macgregor, H. C. (1998). Ordered arrangement and rearrangement of chromosomes during spermatogenesis in two species of planarians (Plathelminthes). Chromosoma *107*, 173-183.

Pearson, B. J., Eisenhoffer, G. T., Gurley, K. A., Rink, J. C., Miller, D. E., and Sánchez Alvarado, A. (2009). Formaldehyde-based whole-mount in situ hybridization method for planarians. Dev Dyn *238*, 443-450.

Pellettieri, J., Fitzgerald, P., Watanabe, S., Mancuso, J., Green, D., and Sánchez Alvarado (2009). Cell death and tissue remodeling in planarian regeneration. Dev Biol.

Pisetsky, D. S., and Lerner, E. A. (1982). Idiotypic analysis of a monoclonal anti-Sm antibody. J. Immunol. *129*, 1489-1492.

Robb, S. M., and Sánchez Alvarado, A. (2002). Identification of immunological reagents for use in the study of freshwater planarians by means of whole-mount immunofluorescence and confocal microscopy. Genesis *32*, 293-298.

Sánchez Alvarado, A., Newmark, P. A., Robb, S. M., and Juste, R. (2002). The Schmidtea mediterranea database as a molecular resource for studying platyhelminthes, stem cells and regeneration. Development *129*, 5659-5665.

Sánchez Alvarado, A., and Newmark, P. A. (1999). Double-stranded RNA specifically disrupts gene expression during planarian regeneration. Proc Natl Acad Sci USA *96*, 5049-5054.

Wang, Y., Zayas, R. M., Guo, T., and Newmark, P. A. (2007). nanos function is essential for development and regeneration of planarian germ cells. Proc Natl Acad Sci USA *104*, 5901-5906.